1 **Understanding the Role of Contrails and Contrail Cirrus in Climate Change: A Global**
2 **Perspective**

4 Dharmendra Kumar Singh, Swarnali Sanyal, Donald J. Wuebbles

5 Department of Climate, Meteorology & Atmospheric Sciences (CliMAS), University of Illinois
6 Urbana-Champaign, Urbana, IL 61802, Illinois, USA
7
8 *Correspondence to*: Dharmendra Kumar Singh (dksingh8@illinois.edu)

10 **Abstract**

11 Globally, emissions from aviation affect Earth's climate via complex processes. Contrail cirrus and
12 carbon dioxide emissions are the largest factors contributing to aviation's radiative forcing on
13 climate. Contrail cirrus, like natural cirrus clouds, impacts Earth's climate. Even with the extensive
14 ongoing research, the relative importance of the climate effects of contrails compared to other
15 aviation effects on climate still has major uncertainties requiring further research. Contrail cirrus
16 encompasses linear contrails and the associated cirrus clouds; these are characterized by ice
17 particle properties, e.g., size, concentration, mixing, extinction, ice water content, optical depth,
18 geometrical depth, and cloud coverage. The climate impact of contrails may intensify due to
19 projected increases in air traffic. The radiative forcing from global contrail cirrus has the potential
20 to triple and could reach as much as 160 mW m^{-2} by 2050. This projection is based on anticipated
21 growth in air traffic and a potential shift to higher altitudes. The future climate impact of contrail
22 cirrus is influenced by factors like the magnitude and geographical spread in air traffic,
23 advancements in fuel efficiency, the effects of the use of alternative fuels, and the effects of the
24 changing climate on the background atmosphere. This study reviews the microphysical processes
25 affecting contrail formation and the aging of contrails and contrail-cirrus. Furthermore, the study
26 explores global observational datasets for contrails, current analyses, and future projections and
27 will aid in evaluating the effectiveness and trade-offs associated with various mitigation strategies.
28 The research highlights gaps in knowledge and uncertainties while outlining research priorities for
29 the future.

31 Keywords: Aviation, contrails, contrail cirrus, radiative forcing, climate model, climate change

34
35
36
37
38
39
40

1 Introduction

The increase in the atmospheric carbon dioxide (CO_2) concentration has had the most substantial impact on human-induced climate change over recent decades (IPCC, 2021). Emissions from aviation are a minor but significant contributor to these changes in climate, especially because of emissions of CO_2 and the effects of contrail formation from emitted water vapor (H_2O). Aviation expansion is outpacing economic growth, with projections indicating that over the next two decades, the demand for aviation could grow to about 3 times its present level (Wuebbles et al., 2007), with the International Civil Aviation Organization having previously projected a 4.3% annual growth to 2050 (ICAO 2012). Recent analyses by Boeing and Airbus suggest slightly lower rates of increase of 3.6-3.8% (Boeing, 2022; Airbus, 2023). These analyses suggest that aviation could become an even more important contributor to climate change in the future. Taking both CO_2 and non-CO_2 effects into account, The global aviation industry comprises about 3.5-4% of the current human-made (anthropogenic) activities forcing on climate (Lee et al., 2020; Klöwer et al., 2021; Grewe et al., 2021).

Aviation-induced cirrus is one of the most significant radiative forcing contributors from the aviation sector. (IPCC, 1999; Lee et al., 2009, 2021; Brasseur et al., 2016). However, considerable ambiguities persist, stemming from various origins, such as our incomplete understanding of cirrus cloud characteristics, their geographical distribution, and their life span. (Kärcher 2018; Burkhardt et al., 2018; Schumann and Heymsfield 2017). With current aircraft largely burning fossil fuel, CO_2 emissions are the other major forcing. Additionally, NO_x (oxides of nitrogen) emission also has a notable impact through the production of tropospheric ozone, but this is partially counteracted by chemical feedback effects on concentrations of atmospheric methane (CH_4). Fig. 1 (Lee et al., 2021) provides the most current assessment of the climate-forcing effects resulting from different aviation emissions on a global scale, spanning from 1940 to 2018; these effects are shown in terms of radiative forcing (RF) and effective radiative forcing (ERF). Radiative forcing in the context of contrails is due to the net radiative energy flux at the top of the atmosphere (TOA) caused by the presence of contrails in the atmosphere (Fuglestvedt et al., 2010). A positive radiative forcing (RF) signifies an increase in atmospheric warming, as depicted by the red bars in Figure 1. ERF, on the other hand, adjusts the RF by accounting for rapid responses occurring within the Earth's climate system. While RF and ERF provide valuable insights, it's important to acknowledge that these are global metrics. Contrails primarily affect the upper troposphere and are short-lived, leading to potentially larger regional effects, particularly in densely populated areas with high air traffic.

In the scientific literature, contrail cirrus is defined as encompassing both linear contrails and the resulting formation of cirrus clouds. Figure 2 provides an overview of aviation exhaust plume emissions and factors influencing contrail formation. The characteristics of contrail cirrus include average ice particle sizes and concentrations, extinction, ice water content, optical depth, geometrical depth, and contrail coverage. Integral contrail properties involve parameters such as contrail cirrus volume, total number of ice particles, overall ice water content, and total extinction (area integral of extinction) per contrail length.

While significant progress has been made in recent years to incorporate contrail effects into global climate models, as evidenced by the pioneering work of Burkhardt and Kärcher (2011) and the continued advancements by others, like Bock and Burkhardt (2016), Bier and Burkhardt (2022), Chen and Gettelman (2013), and Schumann et al. (2015), uncertainties remain in how well these models capture the long-term influence of contrails on cirrus clouds. These uncertainties arise from

87 limitations in our understanding of how contrails age and spread (Bickel et al., 2020), the properties
88 of the tiny ice crystals that make them up, and the behavior of contrails in regions with high ice
89 content. Further research is crucial to address these uncertainties and improve the accuracy and
90 reliability of contrail modeling for future climate projections.

91 The generation of persistent contrails depends on coming across ice-supersaturated conditions
92 along a flight path, and these conditions show variability in both space and time within the
93 troposphere and tropopause region (Irvine et al., 2013; Lamquin et al., 2012; Bier et al., 2017).
94 Estimating the RF from contrail cirrus requires knowledge of complex microphysical processes,
95 radiative transfer, and the interaction of contrails with background cloudiness (Burkhardt et al.,
96 2010).
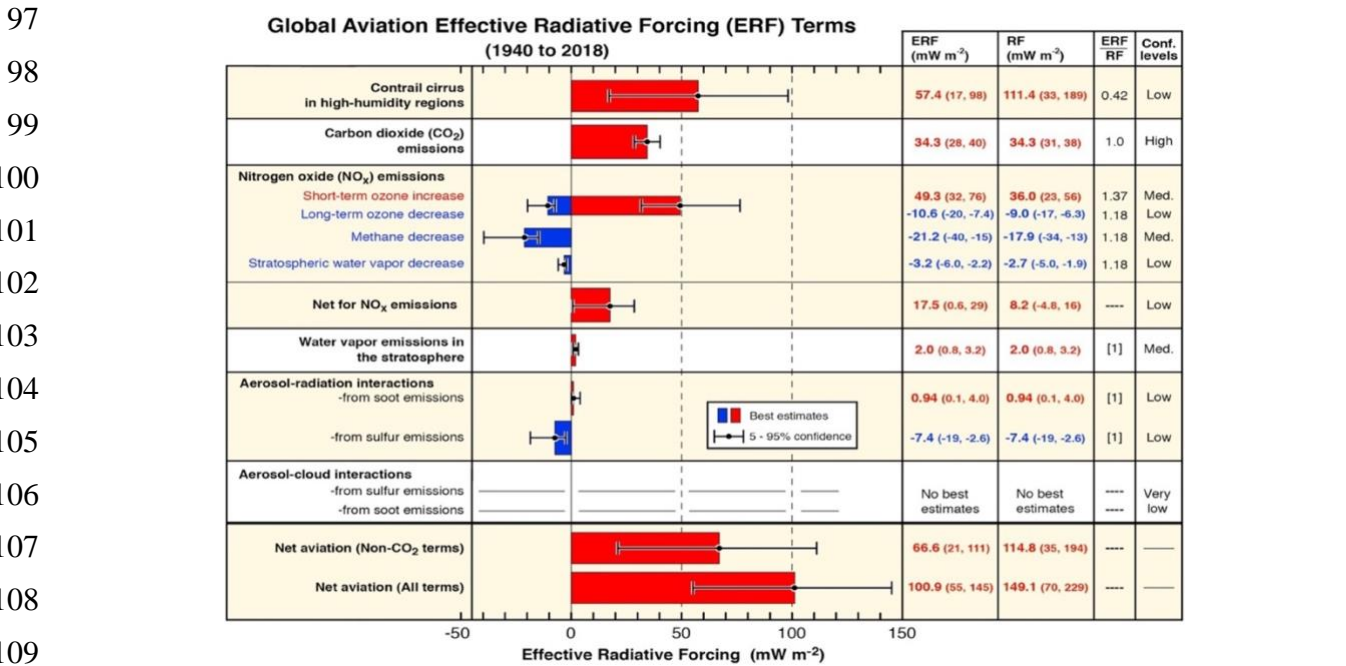
Figure 1. Current best evaluation of the climate forcing between 1940 and 2018 from commercial
aviation for different types of emissions. ERF accounts for short-term feedback in the climate
system not accounted for in the traditional RF evaluation. Adapted with permission from Lee et
al. (2021).
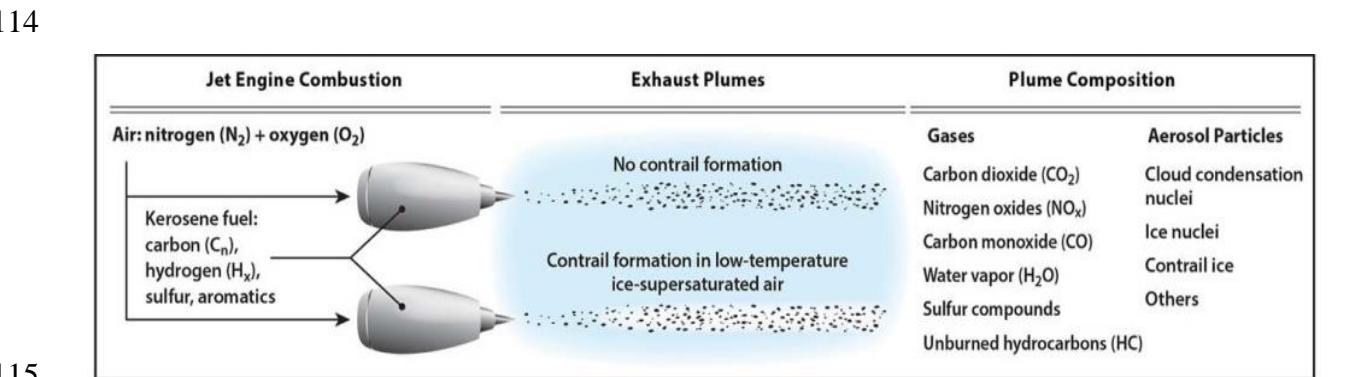
Figure 2. Schematic overview of exhaust plumes (contrail formation in low temperature) and their
composition. Adapted with permission from Lee et al. (2021).

118 This review article aims to provide a comprehensive overview of our understanding of contrails,
119 encompassing their formation, progression, and the consequent repercussions on Earth's climate
120 system. In the process, the microphysical processes underlying contrail formation are explored
121 along with their representation in the simulation of contrails in current climate-chemistry models
122 of the global atmosphere. Furthermore, we address the uncertainties surrounding this topic and
123 identify areas requiring further research in the future.

124 **2 Microphysics of Contrail Formation, Aging, And Transition to Contrail Cirrus**

125 Microphysical processes play a pivotal role in the formation of contrails and their evolution in the
126 atmosphere. This section is aimed at discussing these processes, their effects on the lifetime of
127 contrails, and the possible transition of contrails to contrail cirrus in the upper troposphere.

128 **2.1 The Physics of Contrail Formation and Aging**

129 The fundamental principles for determining the formation of contrails were independently
130 developed by E. Schmidt in 1941 and H. Appleman in 1953. Contrails appear when the hot and
131 moist exhaust from aircraft quickly mixes with the cold and humid surrounding air, causing the
132 humidity in the exhaust gases to exceed the saturation point for liquid water (Appleman, 1953;
133 Schmidt, 1941; Schumann, 1996). A schematic representation of the Schmidt-Appleman criterion
134 for contrail formation is shown in Figure 3. In this diagram, the two solid curves depict saturation
135 levels concerning liquid water (upper curve) and ice (lower curve). The phase trajectory of the
136 mixture, consisting of exhaust gases and ambient air, follows a straight line from the upper right
137 to the lower left in the e-T diagram, where 'e' represents the partial pressure of water vapor in the
138 mixture, and 'T' represents its absolute temperature (as denoted by the dashed lines). The path that
139 lines up with the water saturation curve (dotted) specifies the highest temperatures at which
140 contrail formation can take place. When the trajectory terminates in an ice-supersaturated state,
141 the persisting contrails have the potential to disperse and transform into contrail cirrus.

142 In cases where the conditions do not meet the criteria, the contrail formed will have a brief lifespan,
143 lasting only a few minutes. The mixing process is presumed to occur isobarically, resulting in a
144 straight-line mixing (phase) trajectory on an e-T diagram. The Schmidt–Appleman criterion
145 (SAC), which is primarily based on thermodynamics, establishes the threshold temperature for
146 contrail formation. This threshold is determined by several factors, such as ambient air pressure,
147 humidity, the amount of water and heat released by the aircraft per unit of fuel, and the overall
148 efficiency of the aircraft engine's propulsion system. (Jensen et al., 1998; Schumann, 1996).
149 Accurate assessments of contrails necessitate precise data on ambient meteorological conditions.
150 The persistence of contrails is contingent on meeting a specific humidity threshold, as defined
151 below.

152 The persistence of contrails hinges on the atmospheric-specific humidity. Temperature and vertical
153 motions within the atmosphere play key roles in determining this humidity. Additionally, the
154 optical characteristics and lifespan of contrails are key aspects of contrail formation and are
155 influenced by various meteorological factors. These factors include turbulence, vertical motions,
156 wind shear, and the presence of ambient cirrus clouds. The size and duration of the ice-
157 supersaturated region, the availability of water vapor for ice crystal growth, and consequently, the
158 sedimentation of these ice crystals within the contrail are also essential considerations (Bock and
159 Burkhardt, 2016). Crucially, the radiative forcing (RF) and the ensuing climate impacts depend on
160 a multitude of meteorological parameters. Additionally, factors such as the albedo and the

161 brightness temperature of the atmosphere in the absence of contrails play a significant role, as
162 outlined by Schumann et al. (2012).

163 Upon reaching the ambient temperature through the process of mixing with the surrounding air,
164 contrails undergo changes in size depending on the ambient humidity. When the ambient relative
165 humidity remains supersaturated concerning ice (RHice >100%), contrails experience growth in
166 ice water content and can remain detectable for up to 5 hours or even longer, as highlighted in
167 various studies (Gierens and Vázquez-Navarro, 2018; Schumann and Heymsfield, 2017; Bier et
168 al., 2017). This extended persistence contrasts with the mean lifetime of contrails, typically noted
169 to be around 2-3 hours (Schumann et al., 2015; Vázquez-Navarro et al., 2015; Tesche et al.,
170 2016; Sausen et al., 1998). Contrails, under such conditions, have the potential to disperse and
171 transform into thin cirrus layers. On the other hand, when the ambient relative humidity is not
172 supersaturated concerning ice, contrail ice particles sublimate and dissipate. The timescale of this
173 sublimation and dissipation process is contingent on the sizes of the contrail ice particles and the
174 ambient air RHice (Schumann, 2012).

175 Combinations of satellite information and ground-based lidar measurements, such as in the Atlas
176 et al. (2006) case study, showed a lifetime of more than 2 hours and a mean optical thickness
177 (integrated extinction coefficient over a vertical column of unit cross section) of 0.35. Duda et al.
178 (2004) studied the development of contrail clusters over the Great Lakes and derived optical
179 thickness (optical depth, τ) from 0.1 to 0.6 for contrails that lasted several hours (Kärcher et al.,
180 2009). Graf et al. (2012) studied the cirrus cover cycle and observed timescales between 2.3 to
181 4.1 hours for contrail cirrus and 1.4 to 2.4 hours for linear contrails.
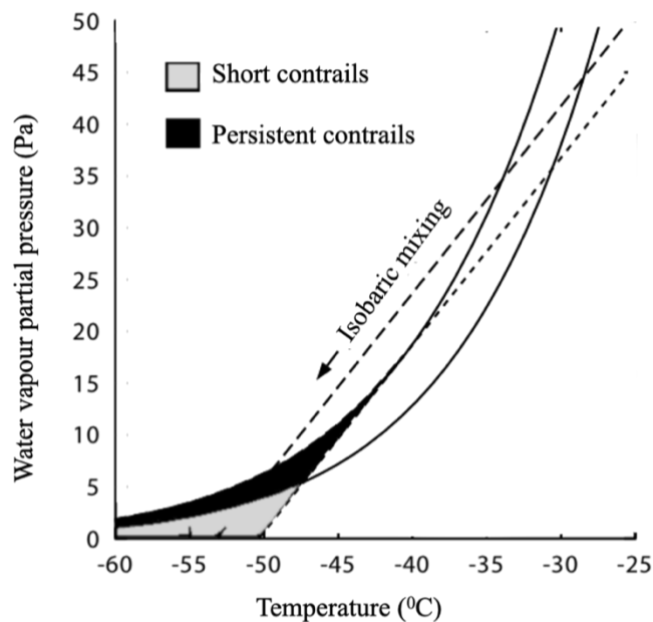
Figure 3. Phase diagram with mixing lines for aircraft exhaust Adapted from Gierens et al. (2008)
(Licensed under CC BY 4.0).

195 The critical factor influencing this contrasting behavior lies in the concept of ice supersaturation.
196 Ice supersaturation refers to conditions where the ambient humidity exceeds the saturation point

for ice, even at temperatures below freezing. These conditions are essential for the persistence and growth of contrails. While the initial formation process might occur at varying humidity levels, studies like Ovarlez et al. (2002) highlight the presence of ice supersaturation within cirrus clouds, which can significantly impact contrail persistence. Jensen et al. (2001) revealed a surprisingly high frequency of ice supersaturation in the upper troposphere, even in the absence of visible ice clouds. This finding highlights the importance of considering ice supersaturation for accurate assessments of contrail persistence and its potential transformation into cirrus clouds.

Upon reaching the ambient temperature through the process of mixing with the surrounding air, contrails undergo changes in size depending on the ambient humidity. When the ambient relative humidity remains supersaturated concerning ice (RHice >100%), contrails experience growth in ice water content and can remain detectable for up to 5 hours or even longer. The microphysical properties of contrails, including ice crystal size distribution and habit, significantly influence their radiative effects and persistence. These properties are determined by the initial conditions during contrail formation and subsequent processes. Ice crystal shapes in contrails are primarily randomly oriented, small ice crystals, with a possibility of some horizontally oriented plates existing as well. This finding is supported by Iwabuchi et al. (2012) who analyzed contrails using a combination of MODIS and CALIPSO satellite data. Their study showed that contrails have larger backscattering coefficients than neighboring cirrus clouds, indicative of smaller ice crystals. The analysis also suggested a tendency for stronger depolarization when ice crystals are small, with a mean linear depolarization ratio (LDR) of approximately 0.4-0.45 for young contrails and contrail cores (Iwabuchi et al., 2012).

There has been ongoing uncertainty regarding whether persistent contrails exclusively form in cloud-free supersaturated areas or if they can also develop within existing cirrus clouds (Burkhardt et al. 2008). Subsequent modeling work (Tesche et al. 2016) suggested that persistent contrails indeed have the potential to form within cirrus clouds. While the formation of contrails is commonly observed in clear skies, they also emerge in conditions where the sky is covered with thin or even subvisible cirrus clouds (Immler et al. 2008).

The temperature threshold for contrail formation, known as the SAC threshold, is slightly higher in cirrus clouds compared to clear air (Gierens, 2012). This difference is attributed to the additional humidity introduced by the ice water content (IWC) from cirrus clouds (Verma and Burkhardt 2022). In situ measurements have indicated high ice supersaturation both inside and outside cirrus clouds (Comstock et al. 2004). Moreover, observational evidence suggests that contrails embedded within cirrus clouds are not significantly thinner than contrails forming in clear air (Poellot et al. 1999).

A reliable estimation of the radiative effects stemming from contrail cirrus relies heavily on their optical properties, which are intricately linked to their microphysical properties and age, as well as their geographical distribution. The microphysical characteristics of contrail cirrus at various plume ages, as observed in diverse airborne campaigns, have been systematically compiled and detailed (Schröder et al. 2000; Schumann et al. 2017; Chauvigné et al. 2018). Fresh contrails, typically observed in plumes around 2 minutes old, exhibit distinct features, including an ice crystal number concentration reaching thousands per cubic centimeter and ice crystals measuring up to a few micrometers in diameter. This characterization is consistent with observations (Märkl et al., 2024, Bräuer et al., 2021a; Petzold et al., 1997). Contrails in their initial 2-5 minutes of existence have been frequently measured (Voigt et al., 2011; Gayet et al., 2012). The distinctive feature of these young contrails lies in their notably high ice crystal number concentration of small

ice particles, making them easily discernible from natural cirrus formations. However, contrails often coexist with natural cirrus and may be incorporated into thin or subvisible cirrus (Kübbeler et al., 2011; Gierens, 2012; Unterstrasser et al., 2017). This coexistence poses a challenge in distinguishing between aged contrails and natural cirrus, complicating efforts to clarify the contribution of contrail cirrus to the radiative balance. Contrail cirrus is characterized by a low ice water content (IWC) ranging from 0.1 to about 10 mg m^{-3}, a feature it shares with natural cirrus of in-situ origin, as observed by Schumann et al. (2017). Ice crystals within these clouds have formed and enlarged in an ice-cloud environment (Luebke et al., 2016; Krämer et al., 2020). In contrast to contrail cirrus and in situ-origin cirrus, cirrus clouds initiating from liquid often yield a higher IWC since their ice crystals originally form as liquid drops (Krämer et al., 2016, 2020) in a warmer atmosphere with an ambient temperature exceeding 235 K (-38°C), particles undergo freezing as they are lifted into the cirrus temperature region of the atmosphere.

Chauvigné et al. (2018) applied a method based on principal component analysis to differentiate between particles in contrail cirrus at various stages and those observed in natural cirrus during the CONCERT 2008 campaign (Voigt et al., 2010). The success of the campaign stemmed from the fact that contrails sampled during the CONCERT initiative were relatively young and exhibited greater distinctiveness compared to natural cirrus formations. Despite this success, the comprehensive acquisition of all necessary optical and microphysical parameters proved challenging during single aircraft campaigns, limiting the widespread application of this method. The CONCERT dataset is relatively small, encompassing approximately 4.0 hours of sampling time in total (Kübbeler et al., 2011). A commonly held assumption regarding the formation and evolution conditions of contrail cirrus is that it tends to persist particularly in ice-supersaturated regions (ISSRs) (Kärcher, 2018).

The collective presence of commercial, military, and other aircraft contributes to a global increase in cloudiness, primarily facilitated by the formation of persistent contrails when the surrounding atmosphere reaches supersaturation. Contrail cirrus exhibits both cooling and warming effects, with the nighttime impact being predominantly warming. Previous assessments of aviation's influence on climate (IPCC, 1999; Lee et al., 2009; Brasseur et al., 2016) were limited by the challenge of accurately quantifying the role of cloudiness arising from aging and spreading contrails (Minnis et al., 2013). The formation of a persistent contrail necessitates ice-supersaturated conditions along the aircraft's flight path. The life cycles of contrail cirrus are contingent upon the temporal and spatial scales of ice-supersaturated regions, which exhibit high variability in the troposphere and tropopause region (e.g., Lamquin et al., 2012; Irvine et al., 2013; Bier et al., 2017). Estimating the impact of contrail cirrus on upper tropospheric cloudiness requires the simulation of complex microphysical processes, contrail spreading, overlap with natural clouds, radiative transfer, and interaction with background cloudiness (Burkhardt et al., 2010).

Petzold et al. (2020) conducted a study investigating the frequency distribution of ice-supersaturated regions (ISSRs) through regular in-situ observations made by passenger aircraft across northern mid-latitude areas. Their research underscores the seasonal and geographical variability of ISSRs, indicating a higher likelihood of occurrence during winter and in specific geographic regions. This variability underscores the significance of considering the spatial and temporal distributions of ISSRs when assessing the potential for contrail formation.

Reutter et al. (2020) delved into the characteristics of ice-supersaturated regions using a combination of in-situ water vapor measurements obtained from the IAGOS research program and

data from ERA-Interim reanalysis. Their findings showcase the potential for validating reanalysis data with high-resolution aircraft observations. This validation process is critical for enhancing the accuracy of global models utilized in evaluating contrail formation and their subsequent climatic impacts.

The ERF of contrail cirrus was estimated for 2011 (relative to an atmosphere without contrails) as 50 mWm^{-2} by Boucher et al. (2013), with uncertainty ranging from 20-150 mWm-2. Lee et al. (2021) presented a new estimate derived from the outcomes of global climate models implementing process-based contrail cirrus parameterizations. Recent analyses by Lee et al. (2021) of the current aviation fleet emissions evaluate the ERF through 2018 as 57 mWm^{-2}, with an uncertainty range of 17-98 mWm^{-2}. Given the limited availability of independent estimates, assessing uncertainty becomes crucial. This necessitates analyzing the sensitivities of relevant processes and incorporating the uncertainties associated with the underlying parameters and fields.

Contrails form in the early exhaust plumes of airplanes during flight (Kärcher et al., 2015; aufm Kampe, 1943; Weickmann, 1945; Schumann and Wendling, 1990; Schumann, 1996). This happens when supercooled water droplets freeze into ice particles. At cruising altitudes, the atmospheric relative humidity (RH) is usually too low to sustain liquid water droplets but can support ice-phase particles (Gettelman et al., 2006; Lamquin et al., 2012). Consequently, freezing must occur soon after droplet formation within the moist exhaust plume to create persistent contrails. Appleman (1953) identified a key requirement for contrail formation, suggesting that many aerosol particles in the plume serve as centers for water condensation, known as the "water-saturation constraint." Another essential factor is the visibility constraint, which requires at least 10^4 cm^{-3} within a plume age of 0.3 seconds for small-scale research aircraft (Appleman, 1953; Kärcher et al., 1996). These are the main constraints for contrail formation.

2.2 Transition of contrails into contrail cirrus and contrail-cirrus-soot interaction

Contrail cirrus consists of elongated contrails trailing high-altitude aircraft and thin cirrus patches formed by the dispersion of persistent contrails. The morphology of contrails evolves based on factors such as humidity, shear, stratification, waves, turbulence, and radiative heating. Contrails, individually and collectively, interact with other cirrus formations, giving rise to what is termed "contrail cirrus" (Schumann and Wendling, 1990). The total extinction is less pronounced when contrails overlap due to humidity competition. Consequently, the climate impact does not always exhibit a linear correlation with air traffic density (Unterstrasser and Sölch, 2012; Bickel et al., 2020). The transformation of a single contrail into a contrail cirrus is observable during aircraft spiral flights, as depicted in Figure 4 (Haywood et al., 2009). "Contrail outbreaks" describe scenarios where numerous aged and young contrails coexist, often spanning expansive areas within the same airspace (Duda et al., 2001).

Soot emissions, composed of black carbon particles from aviation, have the potential to alter cirrus properties independently of contrail processing, leading to the formation of "soot cirrus" (Lee et al., 2010). Climate impact assessments of aviation-induced soot cirrus remain inconclusive due to uncertainties in soot abundance and their ice-nucleating properties (Gettelman and Chen, 2013; Zhou and Penner, 2014; Righi et al., 2021). Increased concentrations of small-sized cirrus particles resembling aviation soot emissions have been detected in cirrus regions with dense air traffic (Kristensson et al. 2000). It remains uncertain whether the soot enters the ice during the initial nucleation process or at a later stage through scavenging. The exact mechanism of soot

330 incorporation into cirrus ice remains unclear. Uncertainties persist regarding whether the soot
331 enters the ice during the initial nucleation process or at a later stage through scavenging.

332 A recent study by Testa et al. (2024) examines the processing of aviation soot within contrails and
333 offered further insights into the potential influence of soot on ice nucleation. They specifically
334 investigate the ice nucleation ability of contrail-processed soot particles at cirrus temperatures and
335 found that these particles were generally poor ice nucleating agents. This suggests that soot cirrus
336 formed from processed aviation soot may have a weaker influence on cirrus cloud formation than
337 previously thought.

338 Dischl et al. (2024) demonstrate a significant reduction in non-volatile particle emissions from
339 aircraft engines using sustainable aviation fuel (SAF) compared to traditional jet fuel. This finding
340 indirectly supports the notion that some soot particles might remain dry throughout contrail
341 formation or that some ice particles might sublimate, as these processes could be influenced by
342 particle properties.

343 The sublimation of cirrus particles containing soot and sulfate may lead to the formation of soot
344 aggregates that can potentially act as efficient ice nuclei. A cirrus pattern observed near Munich,
345 Germany, on November 3, 2012, displayed characteristics suggesting an association with aged
346 soot plumes. The cirrus observed between 9.1 and 9.5 km in height, 8-10 km wide, and 35-50 km
347 long, exhibited a distinctive pattern resembling parallel line clouds. Back trajectories indicated that
348 soot was emitted upstream approximately 12 hours before the event by aircraft. The air ascended,
349 forming a cirrus about 4 hours before the event, lasting for about 1-2 hours before subsiding or
350 sublimating. Analyses propose that this could be cirrus formed on preactivated aircraft soot, but
351 certainty is limited, and it cannot be ruled out that the same pattern might have formed without air
352 traffic. (Schumann and Heymsfield, 2017).

353
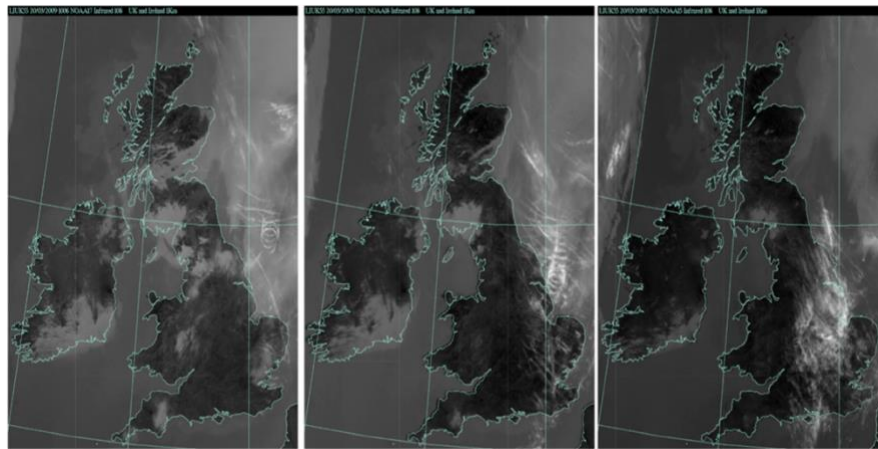
Figure 4. Evolution of contrail cirrus over 1, 3, and 6.5 hours. Contrail cirrus is identified
by bright white areas with low infrared (10.8 mm) brightness temperature. The satellite
scenes are from NOAA AVHRR for 3 UTC times: (left) 1006 (age after emission = 1 hour),
(middle) at 1202 (elapsed time: 3 hours), and (on the right) 1526 (elapsed time: 6.5 hours).
Adapted with permission from Haywood et al. (2009).

354

A comprehensive understanding of the interplay between contrails, cirrus clouds, and aircraft emissions is essential for accurate assessments of their combined effect on Earth's climate. Recent investigations have illuminated this complex relationship, providing valuable scientific insights. Notably, Urbanek et al. (2018) documented ice clouds exhibiting atypical characteristics over Europe, suggesting potential deviations from standard ice crystal behavior. Additionally, these clouds displayed lower ice supersaturation, hinting at a possible modification in the usual ice formation processes (Urbanek et al., 2018). Intriguingly, the spatial distribution of these cloud formations appeared to correlate with regions experiencing high air traffic. While a definitive causal link between these observations and contrail cirrus formation remains elusive, they do suggest a potential indirect influence stemming from aircraft emissions (Urbanek et al., 2018).

In contrast, Kärcher and colleagues (2021) examine the impact of soot particles emitted by aircraft. Kärcher et al. (2021) use modeling to study how these soot particles influence the birth of new cirrus clouds. they found that only a tiny fraction of the soot particles played a role in cloud ice formation via the freezing of liquid aerosol droplets. Consequently, cirrus clouds affected by soot displayed negligible deviations in overall cloud ice content and optical depth compared to their naturally formed counterparts (Kärcher et al., 2021). These findings question the accuracy of current climate models, suggesting they might be overestimating the global radiative impact of interactions between aircraft soot and expansive cirrus clouds.

In a related study, Wolf et al. (2023) delve into the radiative effect (RE) of cirrus clouds, shedding light on the pivotal role played by ice crystal properties. Their investigations unveiled that ice crystal size and concentration are the linchpins dictating the overall RE of cirrus clouds. Intriguingly, smaller ice crystals, often associated with contrails, wield a dual-edged radiative effect, inducing both cooling and warming influences. This intricate interplay generally tips the scale towards an overall warming effect exerted by cirrus clouds (Wolf et al., 2023).

Beyond the realm of ice crystal properties, Wolf et al. (2023) underscores the importance of other variables. Surface albedo emerges as a contributing factor, with cirrus clouds potentially inducing cooling effects over highly reflective surfaces, like ice, while warming effects over less reflective ones. Additionally, the presence of underlying liquid water clouds and the solar zenith angle also influence the radiative effect. Though their focus primarily centered on plane-parallel clouds, Wolf et al. (2023) acknowledge the potential significance of three-dimensional scattering effects, particularly under high sun angles.

2.3 Evolution of contrails and stages of aviation-induced cloud evolution

The review by Paoli and Shariff (2016) examined the primary physical processes and simulation efforts involved in four distinct phases of contrail evolution. These phases are commonly categorized as the jet, vortex, vortex dissipation, and diffusion phases. Contrail evolution is conveniently divided into these four regimes for clarity (Gerz et al., 1998) (see Fig.5).

In the initial seconds after emission (the jet regime), the vortex sheet shed by the wings rolls up into a pair of counter-rotating vortices known as the primary wake. Simultaneously, newly formed ice crystals in the engine exhaust become entrapped around the cores of these vortices. Following this, in the minutes that follow (the vortex regime), the vortices descend into the atmosphere due to their mutually induced downward velocity.
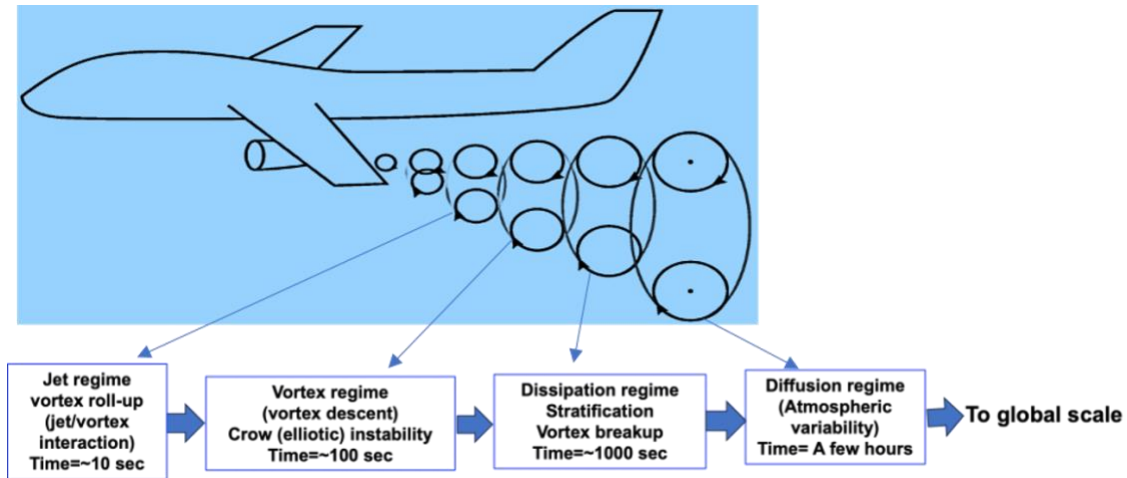
Figure 5. Schematic classification of aircraft wakes evolution into four regimes. Adapted from Paoli and Shariff (2016).

The descent of vortices effects in a contrast in density between the air contained within the vortices (within an oval-shaped region) and the ambient air. This process leads to the generation of vortices with opposite signs (in a stable stratified atmosphere) along the oval boundary. The vorticity shed in the upward direction gives birth to a "secondary wake." Within this secondary wake, a portion of the exhaust gases and ice particles becomes incorporated. Within the regime of vortex dissipation, the primary vortex pair and secondary vorticity disintegrate and disperse, releasing both exhaust and ice crystals that eventually endure sublimation. Ice crystals released in the secondary wake can endure for a longer duration due to the lower temperature. In the fourth regime, known as the diffusion regime, the horizontal and vertical spreading of the contrail is influenced by atmospheric turbulence, particle sedimentation, radiative processes, and wind shear until complete mixing takes place, typically within a few hours.

Figure 6 illustrates the processes that influence the various stages of contrail formation. Exhaust plumes, generated by burning fuel-air mixtures at high temperatures and pressure within turbofan jet engines, contain both gaseous and particulate matter. In the freely expanding and cooling plumes (jet regime), particle types include emitted soot particles and aqueous aerosol particles formed within the exhaust, along with entrained ambient aerosol particles. In scenarios where turbulent mixing occurs, leading to cooling and generating plume supersaturation over liquid water, a significant number of plume particles transform water droplets (depicted as gray circles in Fig. 6).

Water droplets rapidly freeze and increase in size by absorbing water vapor from their surroundings, eventually leading to the formation of a visible contrail. This occurs when the ambient temperature drops below the formation threshold. In exhaust rich in soot, most droplets contain soot inclusions. While droxtals, frozen water droplets with faceted surfaces, and hexagonal prisms and columns likely emerging from them may offer a realistic depiction of small ice crystals in fresh contrails, there is currently no direct observational evidence for their specific shapes.

Plumes from multiple aircraft engines combine with the two wingtip vortices, creating an inhomogeneous wake. The subsequent evolution of ice crystals is contingent upon fluid-dynamical processes, particularly in the vortex regime. The downward movement of the vortex pair warms

424 the surrounding air, resulting in the sublimation of ice crystals in the lower portion of the wake. A
425 small fraction of contrail is amplified by the detrainment of air from the lower wake. Ice crystals
426 present in the upper wake continue to grow by the uptake of entrained ice-supersaturated ambient
427 water vapor. A few minutes past emission, the organized flow pattern collapses and mixes with
428 ambient air (dissipation regime). Table 1 summarizes quantitative comparisons of contrail
429 characteristics across different stages of evolution, including measurement techniques and
430 modeling considerations.

431
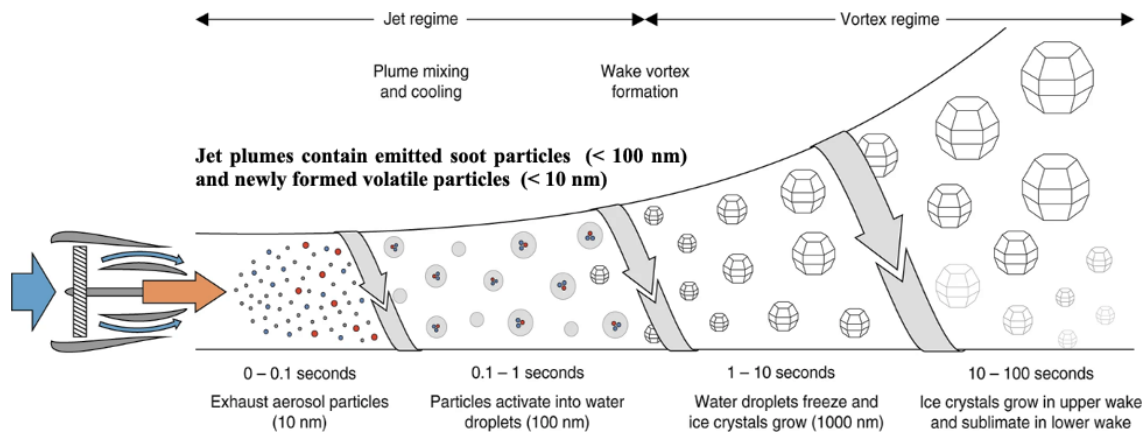
Figure 6. Processes influencing the contrail formation stage. Figure adopted with permission
from Kärcher (2018). (Licensed under CC BY 4.0)

432 **2.4 Contrail coverage**

433 The radiative forcing (RF) for contrails, as determined by Lee et al. (2010), is defined by the
434 product of contrail coverage and optical depth. For a single contrail segment, this product equates
435 to total extinction. However, defining contrail coverage presents challenges for several reasons.
436 Assessing contrail coverage separately from optical depth introduces difficulties. The
437 identification of young contrails versus other cirrus clouds often relies on their distinctive line
438 shape. Yet, using geometric characteristics for contrail coverage classification introduces
439 uncertainty, particularly when contrails undergo deformation or shape changes (Mannstein et al.,
440 1999). Only a small fraction of all linear contrails is detectable from satellites (Kärcher et al., 2009;
441 Mannstein et al., 2010; Minnis et al., 2013).

442 Earlier studies examined global contrail coverage using regional satellite observations, estimating
443 potential contrail coverage based on specific temperature and humidity data and traffic density
444 (Sausen et al., 1998). The integration of observations to achieve hemispheric coverage has only
445 recently become available (Duda et al., 2013). The coverage by contrail cirrus may be significantly
446 higher than determined by line-shaped contrails, and uncertainty factors around an order of 10
447 have been reported (Burkhardt and Kärcher, 2011). However, this ratio is highly uncertain due to
448 detection issues. Burkhardt and Kärcher (2011) conducted a quantification of contrail cirrus using
449 the ECHAM contrail cirrus global climate model (CCmod), which incorporates a subgrid-scale
450 cloud class representing young contrails. This model captures the life cycle of artificial clouds and
451 simulates their global coverage, along with the changes in natural cloudiness they induce. Their

calculations revealed contrail cirrus coverage to be approximately 0.23%. Similar results were obtained from recent attempts to quantify contrail cirrus using MODIS data, accounting for more diffuse contrail contributions (Minnis et al., 2013).

Table 1. Estimated changes in contrail properties during different stages with measurement techniques and modeling consideration.

(The presented values for different stages of contrail properties and measurement techniques/modeling considerations are not based on specific references but represent a general understanding from (Schumann et al.,1998; Schumann, 2005; Schumann et al. 2013; Paoli and Shariff, 2016; Schumann et al. 2017; Heymsfield et al., 2017; Bräuer et al., 2021a, Bräuer et al., 2021b; Schumann et al., 2021; Li et al., 2023; Wang et al., 2023; Geraedts et al., 2024)

Stage	Ice Crystal Size (μm)	Number Density (cm^{-3})	Extinction Coefficient (km^{-1})	Width (m)	Length (km)	Optical Depth
Jet	1-10	10^2-10^4	10^{-2} - 10^{-1}	10 - 20	10 - 100	0.01 - 0.1
Vortex	10 - 30	10 - 10^2	10^{-3}- 10^{-2}	10^2 –10^3	1 - 10	0.001 - 0.01
Dissipation	30-100	1 - 10	10^{-4} - 10^{-3}	10^3 - 10^4	0.1 - 1	0.0001 - 0.001
Diffusion	1000-3000	0.1 - 1	10^{-5} - 10^{-4}	10^4- 10^5	1 - 10	0.00001 - 0.0001

Stage	Measurement Techniques	Modeling Considerations
Jet	Lidar, satellite imagery	Microphysics, Ice Nucleation rates
Vortex	Lidar, In-situ probes	Turbulence, Wind shear effects
Dissipation	Lidar, Ground-based observations	Sedimentation, evaporation rates
Diffusion	Lidar, satellite imagery	Radiative transfer, ice crystal habit

Observations during the COVID-19 pandemic lockdowns provide valuable insights into the relationship between air traffic and contrail coverage. Dauda et al. (2023) documented a significant decrease in contrail coverage (up to 41%) over the conterminous United States during the lockdown period compared to pre-pandemic levels. This decrease highlights the direct impact of air traffic on contrail formation and underscores the potential for mitigating climate impact through air traffic management strategies. However, the study also emphasizes the importance of considering environmental factors alongside air traffic when assessing contrail coverage. While the reduction in air traffic was the primary driver of the observed decrease in contrail formation, changes in atmospheric conditions at cruise altitudes likely played a secondary, but significant, role.

In a modeling study, Huszar et al. (2013) adjusted the concentration of a tracer for contrails by multiplying it with a specific factor and then adding it to the large-scale cloud ice mixing ratio. They fine-tuned this factor through annual simulations spanning 2005 to achieve an appropriate global value of the top-of-the-atmosphere radiative forcing attributable to contrails and contrail-induced cirrus for that year, aiming for a target value of 31 mWm^{-2} as reported by Burkhardt and Kärcher (2011). The distribution of this forcing aligns with Burkhardt and Kärcher (2011) findings, showing peak values exceeding 300 mWm^{-2} over central Europe and the eastern U.S., with significant parts of Europe and the U.S. experiencing a contrail-induced cirrus radiative forcing above 100 mWm^{-2}. However, their estimates for eastern Asia surpass those of Burkhardt and Kärcher (2011), with maximum values exceeding 300 mWm^{-2}, while ranging between 100 and 300 mWm^{-2} elsewhere. They suggested these differences could be attributed to how contrail cirrus is handled (a simpler parameterization in this study versus the more complex contrail-cirrus

486 module used by Burkhardt and Kärcher), variations in simulated thermodynamic conditions over
487 East Asia, and differences in emission inventories.

488 Schumann (2012) developed the Contrail Cirrus Prediction (CoCiP) tool based on a Lagrangian
489 approach. In this model, global contrail coverage is computed by combining the optical depth (τ)
490 contributions from individual contrails and ambient cirrus, counting fractions of areas where
491 contrails cause the optical depth of the total cirrus to surpass a specific threshold (Schumann 2012).

492 Contrails not only augment cloud coverage but also thicken existing cirrus, consequently
493 influencing coverage (Minnis et al., 2013; Schumann and Graf, 2013). This thickening occurs by
494 generating more ice particles with smaller effective radii at constant ice water content (Kristensson
495 et al., 2000). While it is acknowledged that contrails consume humidity and may reduce natural
496 cirrus (Burkhardt and Kärcher, 2011; Unterstrasser and Görsch, 2014; Schumann et al., 2015;
497 Bickel et al., 2020), the prevailing evidence suggests that the thickening effect caused by numerous
498 additional small ice crystals tends to dominate.

499 **2.5 Contrail ice crystal nucleation**

500 Kärcher and Yu (2009) systematically investigated the relationship between nucleated contrail ice
501 crystal numbers and soot particle emissions. In exhaust rich in soot, there is a nearly proportional
502 increase in both ice crystal and soot particle numbers. Close to the contrail threshold, the formation
503 of ice crystals is limited as the low plume supersaturation hinders the activation of water on soot
504 particles, resulting in only a few ice crystals forming. Under conditions rich in soot, the quantity
505 of ice crystals reduces by about one hundred times compared to soot-poor conditions, reaching
506 constant low levels regulated by the number of particles present in the contrail environment. In
507 soot-poor exhaust at low ambient temperatures, there is an increase in ice crystal numbers due to
508 the activation of water and subsequent freezing of abundant aqueous plume particles. Figure 7
509 illustrates the ice crystal number emission index (per kilogram of fuel burnt) in the jet regime,
510 correlating with the number emission index of emitted soot particles as simulated by a parcel model
511 (Kärcher and Yu, 2009). Two sets of results are presented, one for an ambient temperature (T)
512 close to a contrail formation threshold temperature, $\Theta \approx 225$ K (-48°C), commonly encountered in
513 extratropical cruise conditions, and another for a lower temperature of Θ -12 K ≈ 213 K (-60°C).
514 At intermediate ambient temperatures, nucleated ice crystal numbers increase due to enhanced
515 water activation of either soot or ultrafine aqueous plume particles.

516 The hatched area in Figure 7 represents the approximate range of current in-flight soot emission
517 indices. In exhaust rich in soot, the number of soot particles capable of water activation and
518 freezing increases with decreasing ambient temperature. This, in turn, raises plume cooling rates
519 and levels of plume supersaturation over liquid water. It's important to note that the primary driver
520 of the increased cooling and supersaturation is the decreasing ambient temperature, with soot
521 particles acting as additional ice nuclei under these cooler conditions. As the ambient temperature
522 (T) approaches the contrail formation threshold (Θ) in soot-poor exhaust, ambient aerosol particles
523 mixed into exhaust plumes become the sole source of contrail ice crystals. This is because fewer
524 plume particles can be activated due to declining plume supersaturation. The number
525 concentrations of ambient particles in contrails are significantly lower than current levels of soot
526 emissions.

527 The plume cooling rate plays a crucial role in determining the timing of water activation of
528 entrained ambient particles and, consequently, the number of ice crystals derived from them
529 (Kärcher 2015). In soot-poor exhaust, a substantial number of ultrafine aqueous plume particles

530 are formed in the fresh exhaust, especially if the fuel contains condensable vapors besides water
531 vapor. These small particles are anticipated to contribute significantly to ice crystal formation at
532 low ambient temperatures well below average values at cruise levels ($T \approx 218$ K in the extratropic
533 and $T \approx 228$ K in the tropics). If the formation of ultrafine particles cannot be mitigated, ice crystal
534 numbers are expected to be lowest in an intermediate range of soot emissions, specifically between
535 10^{13} and 10^{14} (kg-fuel)$^{-1}$.

536 Ice crystal number (Ni), which quantifies the concentration of ice crystals in the surrounding
537 atmosphere, plays a significant role in contrail properties (Kärcher, 2015). Studies have shown that
538 Ni can influence factors such as contrail persistence, spreading, and optical characteristics (e.g.,
539 Lewellen, 2014). A higher Ni value typically indicates a greater concentration of ice particles
540 within the contrail, which can affect its behavior in several ways.

541 The signs of variation in the number of ice crystals refer to the alteration in the ice particle
542 concentration within a contrail, such as increased ice particle concentration in the contrail, greater
543 persistence, and spreading of the contrail. Increased optical effects, such as increased brightness
544 and reflectivity. The decreased ice crystal particle concentration in the contrail leads to reduced
545 persistence and spreading of the contrail, and weaker optical effects. These variations in Ni may
546 occur due to several factors, comprising changes in atmospheric conditions, aircraft engine
547 emissions, and the presence of ice nuclei or other particles that impact ice particle formation.

548 Lewellen (2014) elucidates the pivotal role of initial ice crystal concentration (Ni) in contrail
549 dynamics through extensive simulations and the proposition of a simplified model. Their
550 simulations elucidate a discernible correlation between elevated Ni values and several significant
551 effects on contrails. First, contrails characterized by higher Ni values demonstrate prolonged
552 lifetimes, persisting for considerably extended durations, with simulations even indicating
553 lifetimes surpassing 40 hours (Lewellen, 2014). This protracted residence within the atmosphere
554 translates to amplified influence on radiative forcing, as contrails with higher Ni values possess
555 increased temporal opportunities for interaction with incident solar radiation. Second, heightened
556 ice particle concentration within the contrail leads to augmented contrail spreading. As Ni
557 escalates, interactions with atmospheric conditions become more conspicuous, potentially
558 precipitating the formation of contrail cirrus, a prevalent cirrus cloud type intimately associated
559 with contrail genesis (Lewellen, 2014). Finally, higher Ni values correlate with intensified optical
560 effects. A greater abundance of ice crystals within the contrail facilitates more efficient scattering
561 of incident sunlight, engendering brighter and more reflective contrails that perturb the radiative
562 equilibrium in the atmosphere (Lewellen, 2014).

563 Lewellen (2014) delineates a valuable framework for understanding the influence of Ni on contrail
564 significance through their simplified model: $S_{\Sigma} = \alpha N \times D$, where S_{Σ} represents the lifetime-
565 integrated ice crystal surface area, a metric for contrail impact, N is the total crystal number per
566 length of flight path (i.e., ice crystal concentration), and D represents the number-averaged fall
567 distance of ice crystals before sublimation. The coefficient 'α' is approximately constant in the
568 regime of interest. This equation underscores the critical role of Ni (N) in determining the overall
569 radiative forcing exerted by contrails. A higher Ni value translates to a larger S_{Σ}, indicating a more
570 significant impact on the atmosphere due to increased light scattering and longer contrail
571 persistence.

572 **2.6 Stages of aviation-induced cloud evolution and spreading stage**

573 The microphysical and optical characteristics of ice crystals within contrails undergo alterations
574 as they disperse or transform into contrail cirrus, contingent upon the prevailing meteorological
575 conditions and microphysical processes (Fig. 8). Over time, persistent contrails undertake a
576 transformation from their initial linear form to become contrail cirrus. In regions of heavy air
577 traffic, these contrail cirrus formations overlap and merge, giving rise to extended layers of ice
578 clouds characterized by alterations in shape, depth, and longevity. These patterns differ from
579 natural cirrus clouds in terms of microphysical, and optical, additionally, geometric properties also
580 play a role. The ice-supersaturated layers that sustain these properties exhibit variations in both
581 vertical structure and horizontal extent, impacting the exchange of water molecules between vapor
582 and ice phases within them. Collectively, these factors contribute to the radiative forcing (RF)
583 potential of aviation-induced cirrus (AIC). Figure 8 illustrates the augmentation in cloud coverage
584 area attributed to the vertical shear of horizontal wind components.

585 The turbulent mixing or entrainment processes result in a gradual reduction (dilution) of ice crystal
586 concentrations over time. The sizes of ice crystals grow through the absorption (deposition) of
587 water vapor from layers that are supersaturated with ice. Continuous deposition growth causes
588 deviations in the shapes (habits) of ice crystals from their initial isometric forms.

589
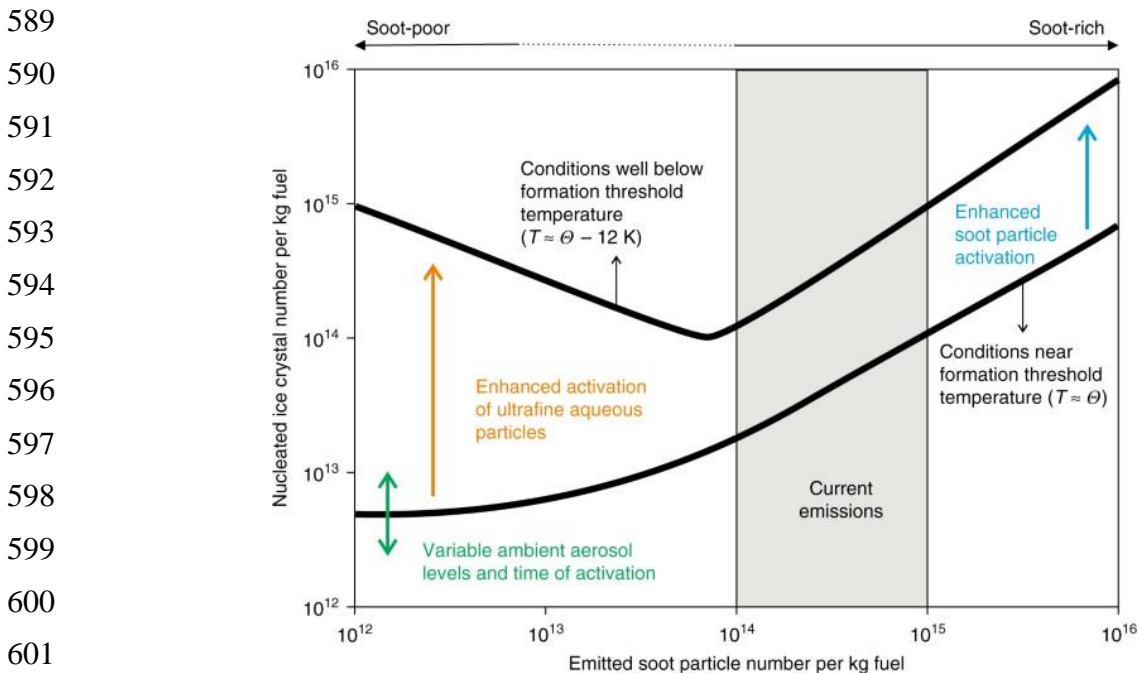
602 **Figure 7.** Nucleation of ice crystals in jet aircraft exhaust plumes. Figure adapted with permission
603 from Kärcher (2018). (Licensed under CC BY 4.0)

604 The shapes and sizes of ice crystals in cirrus clouds significantly impact their growth rates, fall
605 speeds, and optical properties. Larger ice crystals (>30 micrometers) tend to settle due to gravity
606 with fall speeds exceeding 100 meters per hour and are more likely to sublimate in warmer or drier
607 environments. Smaller ice crystals remain suspended around the flight levels due to their negligible
608 fall speeds, provided that some degree of supersaturation can be maintained, which depends on the
609 prevailing meteorological conditions.
610 The efficiency of sedimentation, the process by which ice crystals fall from clouds, is influenced
611 by the depositional growth rate, which in turn is affected by ice supersaturation, the rate of air

612 cooling, and the characteristics of the ice crystals themselves, including their size, shape, and
613 number concentration. Sedimentation increases the vertical extent of cirrus clouds, enhancing their
614 spreading rate and coverage under sheared flow conditions.

615 The settling of ice crystals, known as sedimentation, is a critical factor in determining the lifespan
616 of contrails. As the contrail ages, larger ice particles, due to their increased mass, fall out of the
617 plume more rapidly. This phenomenon can be explained by the concept of terminal velocity
618 (Spichtinger and Gierens, 2009). Researchers have explored methods to calculate this velocity,
619 considering the distribution of ice crystal sizes within the plume (Spichtinger and Gierens, 2009).
620 This approach provides a more comprehensive understanding of the sedimentation process.

621 The size of an individual ice crystal directly influences its falling speed. Larger crystals, typically
622 associated with persistent contrails, descend from the plume quicker than their smaller counterparts
623 found in ephemeral contrails. This sedimentation process significantly impacts the vertical
624 distribution of ice crystals within the contrail and affects its overall persistence. Ice crystals lofted
625 higher, potentially due to weaker updrafts, may experience slower sedimentation and persist for
626 longer durations, especially in colder atmospheric regions.
627

628 **2.7 Lessons learned from observations of contrails and their properties**

629 Contrails, as well as cirrus clouds, are frequently observed in air that lacks saturation (Kübbeler et
630 al., 2011; Krämer et al., 2009). The prevailing explanation suggests that these clouds consist of
631 large ice particles formed under supersaturated conditions, which then descend to lower and drier
632 levels, undergoing slow sublimation. Notably, instances of contrails and contrail cirrus have been
633 documented in ice-sub-saturated air across various scenarios, extending beyond dedicated contrail
634 research flights (Schumann et al., 2017; Voigt et al., 2011; Kübbeler et al., 2011; Gayet et al.,
635 2012; Chauvigné et al., 2018). Such observations have been derived not only from contrail-specific
636 research endeavors but also from In-service Aircraft for a Global Observing System (IAGOS)
637 commercial aircraft data collected in the North Atlantic region (Petzold et al., 2017).

638 Apart from a high number of small contrail ice particles, large particles (ice particle diameter
639 greater than 100 µm) were also detected but at relatively low concentrations (Voigt et al., 2010).
640 Such large ice crystals were also observed in contrail cirrus during the ML-CIRRUS (Midlatitude
641 Cirrus experiment) campaign (Voigt et al., 2017). However, attention to contrail cirrus in ice-sub-
642 saturated environments and the role that large ice particles play in contrail cirrus was raised by
643 Kübbeler et al. (2011) and Schumann (2012).
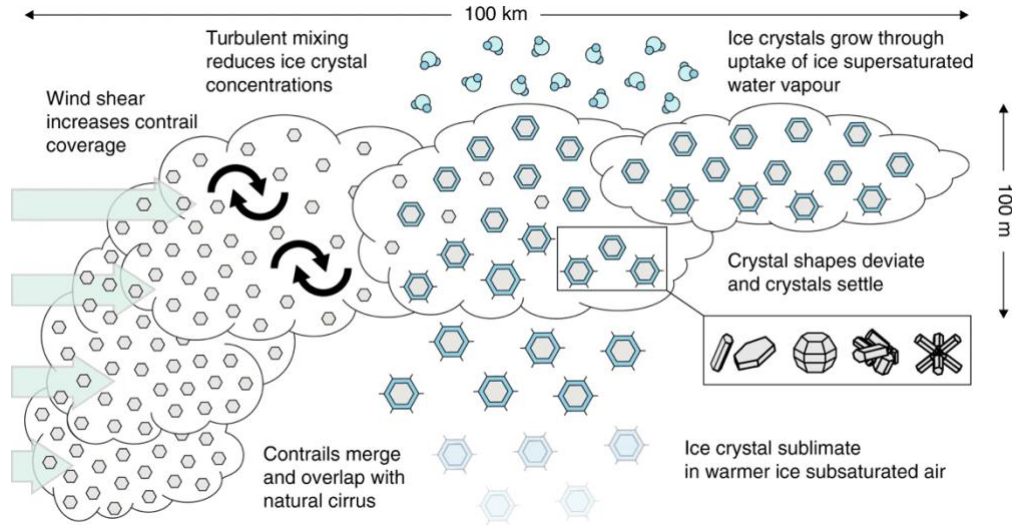
Figure 8. Influential factors in aircraft-induced cloud formation. Figure adopted with permission from Kärcher (2018). (Licensed under CC BY 4.0)

Kübbeler et al. (2011) suggested that the subsaturation observed in contrail cirrus during the CONCERT campaign is caused by the sublimation of large ice particles that may have fallen from higher altitudes after forming under ice supersaturated regions (ISSRs). However, due to the limited contrail cirrus data available, it is difficult to confirm whether contrail cirrus commonly occurs in ice-subsaturated environments.

Li et al. (2023) explored an extended dataset derived from 14.7 hours of cirrus cloud sampling conducted at a frequency of 1 Hz, with a maximum speed of approximately 290 m s^{-1}, obtained during the ML-CIRRUS 2014 campaign. Utilizing readily available parameters that characterize cirrus microphysical properties-including ice number concentration, ice crystal sizes, and ice water content (IWC)-they employed a more straightforward statistical method to distinguish aviation-induced cirrus from natural cirrus, in contrast to the approach adopted by Chauvigné et al. (2018). It consists of the SAC, covering the most common aircraft cruising altitude range, and a recently developed algorithm for detecting aircraft exhaust plumes to identify matured contrail cirrus (>0.5 h lifetime; Voigt et al., 2017; Schumann et al., 2017), and natural cirrus. Contrail cirrus showed sharp differences from natural cirrus during the stages of formation and in the corresponding microphysical properties and occurrence conditions.

Mahnke et al. (2024) investigated the impact of aviation-induced aerosols on cirrus clouds and climate, which remains uncertain. Understanding these properties is vital for assessing aviation's climate effects. From July 2018 to March 2020, the IAGOS-CARIBIC Flying Laboratory identified over 1100 aircraft plume encounters. Findings showed consistent aerosol properties across various altitudes (upper troposphere, tropopause region, and lowermost stratosphere). The exhaust aerosols were primarily externally mixed, even after 1 to 3 hours, with no increase in larger particles (diameter >250 nm) inside the plumes. The particle number emission indices (EIs) from aged plumes matched engine certification values, indicating that aviation aerosols maintain their emission state during plume expansion and that global models use accurate EI values.

Observational Constraints

While there is growing evidence regarding contrail observations in ice-subsaturated environments, it is imperative to acknowledge the inherent limitations associated with measuring contrail properties. These limitations stem from various factors, including:

Spatial and temporal resolution of instrumentation: The comprehensive depiction of contrail phenomena may be impeded by the restricted range or sampling frequency of instruments employed for in-situ or remote sensing observations. For instance, satellite-based observations might fail to capture minute-scale contrail features, while in-situ measurements conducted via research aircraft may not fully encompass the spatial extent of a contrail layer.

Discriminating contrails from natural cirrus formations: The differentiation between contrails and natural cirrus clouds, particularly in ice-subsaturated conditions, presents a significant challenge and often necessitates sophisticated analytical techniques. Both varieties of ice clouds can exhibit comparable characteristics concerning size and ice crystal properties, rendering the definitive identification of their origin based on limited observations a challenging endeavor.

Restricted data availability: Observational datasets, particularly those focusing on fully developed contrail cirrus, may be scarce. This scarcity impedes the ability to draw definitive conclusions regarding the prevalence of contrails in sub-saturated environments and their enduring influence on the climate system.

3 Modeling of Contrails and their Impacts

Understanding the multifaceted impacts of contrails necessitates employing models at various scales. Local-scale process and fluid-dynamic models offer valuable insights into how plume turbulence and wake dynamics influence the nucleation and properties of contrail ice crystals. These simulations can then be validated against in-situ aircraft measurements of nucleated ice crystal concentrations and sublimation losses (Kärcher, 2018). For broader-scale analysis, cloud-resolving and regional models are utilized. These models incorporate meteorological boundary conditions and leverage optical parameterizations to capture the shortwave radiative response of micron-sized ice crystals. By co-locating these simulations with data from aircraft and satellite observations, scientists can gain a more comprehensive understanding of the radiative forcing (RF) exerted by contrail cirrus and its potential influence on pre-existing cirrus clouds (Kärcher, 2018).

The limitations of current instrumentation in measuring the microphysical and optical properties of contrail cirrus elevate the importance of models (Table 2) for estimating their RF. To provide robust predictions of climate change driven by aircraft emissions, models simulating ice nucleation and sublimation must effectively translate the current understanding of contrail formation and evolution processes into frameworks that lack the spatial or temporal resolution to explicitly capture the formation stage. This objective can be achieved by synergistically integrating findings from observations with local-scale, process-oriented models.

3.1 Modeling of individual contrails

Individual contrails have been studied by various authors through approaches ranging from simplified parameterizations to more complex numerical models. Parameterization approaches normally depend on simplified assumptions to estimate contrail properties based on simplified atmospheric and emission conditions. On the contrary, more sophisticated numerical models, such as the Contrail Cirrus Prediction model (CoCiP), utilize detailed representations of atmospheric processes, ice particle growth, and radiative transfer to simulate the formation and evolution of contrails.

Table 2. Modeling the complexities of aircraft-induced cloud radiative effects (Adapted from Kärcher 2018).

Model scale	Spatial resolution		Contrail stages	Major challenges	Approach/solution
	Horizontal	Vertical			
Local	<10 m	<10 m	Formation stage	Ice crystal number and size distribution	Turbulence microphysics coupling
Regional	<1000 m	<100 m	Spreading stage	Radiative flux changes and interaction with natural clouds	Contrail to contrail cirrus transition
Global	<1000km	<1km	Full life cycle	Ice crystal formation and ice supersaturation	Parameterization and high resolution

Improvements in a hierarchy of local- to global-scale models to be realized in conjunction with observations providing data for cloud and radiation parameterization development and overall model validation.

3.1.1 Contrail Cirrus Prediction Tool (CoCiP) for individual contrails

Schumann et al. (2017) compiled a dataset of contrail properties from various sources, including previous publications, additional information gathered from experimenters, reanalysis of existing data, and comparisons with the CoCiP database. The dataset expands upon the work of Schumann and Heymsfield (2017) by incorporating data from the ML-CIRRUS campaign (Voigt et al., 2016). The data includes both in-situ measurements of contrails, such as ice particle size spectra obtained using optical particle spectrometers (Baumgardner et al., 2011; Wendisch and Brenguier, 2013), and remote sensing data from ground-based and airborne lidar, spectroradiometers, satellites, cameras, and visual observations. Remote sensing data provides information on contrail properties such as width and optical depth (Spinhirne et al., 1998; Duda et al., 2004).

3.1.2 MIT Aircraft Plume Chemistry, Emissions, and Microphysics Model (APCEMM)

APCEMM is applied to assess the impact of non-linear plume chemistry and to deliver an initial estimate of the effects of contrails on atmospheric chemistry. Accurately determining the intricate relationship between contrail microphysics and chemistry often necessitates the use of costly large eddy simulations (LESs). APCEMM, through simplified assumptions about plume dynamics, strives to close the disparity between Gaussian plume models and LESs, as outlined by Fritz et al. (2020). APCEMM simulates the growth and chemical progression of an individual aircraft plume. It computes chemical concentrations and aerosol characteristics for a two-dimensional cross-section of the plume, angled perpendicular to the flight path. Dynamics, chemistry, and microphysics are explicitly modeled within the plume, using two different approaches depending on the age of the plume.

3.1.3 NASA's global model for evaluation of individual linear contrails

The NASA Ames Research Center developed a computationally efficient aircraft contrail model designed to simulate aircraft-induced contrail formation. This model relies on the Appleman criterion and operates under static atmospheric conditions (Sridhar et al., 2010; Neil et al., 2010). Subsequently, researchers from NASA Ames extended this model to simulate the dynamic transport of contrails by incorporating a Lagrangian dispersion model and a cloud microphysics model (Li et al., 2013). The computational methods employed are grounded in well-established

approaches utilized in other aircraft contrail models (Pruppacher and Klett, 2000; Schumann et al., 1995).

In comparison with models from Stanford (Naiman et al., 2009; Naiman et al., 2011; Jacobsen et al., 2011) and DLR (Burkhardt and Kärcher, 2009; Burkhardt and Kärcher, 2011; Bier and Burkhardt, 2022), this dynamic contrail model diverges primarily in two aspects: (1) It excludes the initial contrail ice particles down-wash process caused by airplane wake vortex turbulence. This process, typically lasting less than a minute, is crucial in determining contrail ice nucleation, initial contrail ice particle sizes, and displacements through a complex fluid dynamic process dependent on atmospheric, aircraft, and fuel parameters. In this model, the average initial ice particle size is predefined, and the initial contrail location is set based on the cell where contrail formation conditions are met. (2) The results from this model do not yet include additional radiative forcing caused by aircraft contrails. The researchers are in the process of adding a contrail radiative forcing module capable of computing the total aircraft contrail radiative forcing using inputs from the model, such as ice particle size and linear contrail cloud cover area.

3.1.4 DLR's ICON-LEM regional model

Verma and Burkhardt (2022) developed and implemented a model for contrail formation into the ICON-LEM (ICOsahedral Non-hydrostatic Large-Eddy Model; Zängl et al., 2014; Dipankar et al., 2015). This model includes parameterizations for ice nucleation in the jet phase and ice crystal loss during the contrail's vortex phase. It facilitates the investigation of modifications to cirrus clouds resulting from contrail formation. ICON is the new German Numerical Weather Prediction/Climate Model co-developed by DWD and MPI. It solves a set of equations on an unstructured triangular grid based on successive refinement of a spherical icosahedron (Zängl et al., 2014).

The model asserts high horizontal resolution coupled with a vertical resolution of approximately 150 m in the upper troposphere, enabling the resolution of pertinent cloud processes. Within ICON-LEM, a contrail scheme has been developed and implemented, incorporating the parameterization of contrail ice nucleation as proposed by Kärcher et al. (2015) and accounting for the survival of ice crystals within the vortex phase. (Unterstrasser, 2016), to study changes in cloud variables due to contrail formation within cirrus. Contrail formation, dependent on atmospheric as well as aircraft and fuel parameters, is calculated, and contrail ice nucleation and ice crystal loss in the contrail's vortex phase are estimated.

3.1.5 Large-eddy simulations covering the entire life cycle, from initiation to termination

Lewellen et al. (2014) outlined the utilization of large-eddy simulations with size-resolved microphysics to model persistent aircraft contrails and the resulting contrail-induced cirrus clouds. These simulations aim to depict the dynamic evolution of contrails, spanning from a few wing spans behind the aircraft to their dissipation over an extended period. The emphasis of the study lies in the modeling approach, discussing the development of schemes for efficient numerical computation. The authors introduced dynamic local ice binning and updating, along with coupled radiation, to accurately capture microphysical processes and radiative properties within individual columns. The paper also addresses the challenge of maintaining realistic ambient turbulence over extended simulation times, proposing a "quasi 3D" approach as a computationally feasible approximation of the full dynamics, allowing for exploration across a broader parameter space.

803 Lewellen (2014) provides an extensive analysis encompassing over 200 instances of long-lived
804 contrails, spanning from their formation at several seconds old to their termination. The study
805 investigated the complete lifespan of long-lived contrails originating from a single aircraft. Various
806 factors were explored, including the effective ice crystal number emission index, temperature,
807 relative humidity concerning ice, stratification, shear, supersaturated-layer depth,
808 uplift/subsidence, and coupled radiation. The analysis delved into the scaling behaviors of contrail
809 lifetime, width, ice mass, and surface area. The simulations unveiled contrail lifetimes exceeding
810 40 hours, widths surpassing 100 kilometers, and ice masses exceeding 50 kg per meter of the flight
811 path. The paper identified distinct behavioral regimes influenced by radiative forcing and proposed
812 a simplified model to predict these regimes.

813 Key insights from the simulations highlight the notable impact of ice crystal number loss resulting
814 from competition among different crystal sizes, influencing both young contrails and aging contrail
815 cirrus. The sensitivity of contrail properties to the initial number of ice crystals decreases over
816 time, highlighting the importance of uncertainties in ice crystal deposition coefficients and the
817 Kelvin effect. The influence of atmospheric turbulence on contrail properties and lifetime is also
818 emphasized. Additionally, the paper discusses the effects of ice crystal shape, coupled radiation,
819 precipitation dynamics, and the role of water from fuel consumption in reducing ice crystal loss in
820 colder contrails.

821 Lewellen's simulations provide valuable insights into contrail behavior, shedding light on the
822 significance of crystal number loss mechanisms, the interaction between shear and ice
823 sedimentation, the depth of the supersaturated layer, and the potential impact of "cold" subvisible
824 contrails. The findings from these simulations contribute to estimating the effects of intricate
825 contrail scenarios, formulating mitigation strategies, and enhancing our comprehension of the
826 dynamics of natural cirrus clouds.

827 **3.2 Treatment of contrails in global models**

828 The consideration of contrail cirrus in global climate models has greatly improved in recent years.
829 Despite these advancements, notable uncertainties persist, particularly in the depiction of contrail
830 microphysics and the interaction between contrail-cirrus and cirrus-radiation. As mentioned
831 earlier, the characteristics of young contrail cirrus diverge from those of natural cirrus primarily
832 due to the elevated ice crystal number concentration typical in contrails. Consequently,
833 microphysical process rates in contrail cirrus, influencing its lifespan, can exhibit significant
834 deviations from those observed in natural cirrus. In this section, we examine the treatments of
835 contrail and contrail cirrus in global models. Very few models account for contrails, so our focus
836 is on those models that have been published extensively on contrail impacts, including modeling
837 studies done by the Institute for Atmospheric Physics (DLR), the National Center for Atmospheric
838 Research (NCAR), and Stanford University. The focus is on their modeling approaches and
839 findings. We start with a description of the approach used to treat contrails in these models.

840 **3.2.1 DLR Contrail Cirrus Prediction Model (CoCiP)**

841 CoCiP can be implemented within a GCM and used to study the global distributions of contrails
842 and contrail cirrus (Schumann et al., 2015). The model is specifically crafted for the estimation of
843 contrail cirrus coverage and the analysis of contrail climate impact, particularly in the context of
844 aviation system optimization processes. It is engineered to simulate the entire life cycle of
845 contrails. Contrail segments arise between waypoints along individual aircraft tracks in air masses
846 that are cold and humid enough. The initial characteristics of contrails are contingent upon the

847 specific aircraft involved. The advection and progression of contrails adhere to a Lagrangian
848 Gaussian plume model. This model treats the contrail life cycle using bulk contrail ice physics,
849 incorporating several simplifying assumptions. Notably, the model demonstrates efficiency in
850 handling mixing and cloud processes in a quasi-analytical manner (Schumann, 2012). Contrails
851 become extinct when the bulk ice content endures sublimation or precipitation.

852 The model takes into consideration the impact of both aircraft properties and ambient
853 meteorological conditions. This encompasses established contrail formation thresholds, the effects
854 of advection, turbulent mixing, and the formation of ice mass from both emitted and ambient
855 humidity. The number of ice crystals is contingent upon the quantity of soot particles emitted. The
856 model incorporates simplified approximations for the survival of ice particles in adiabatically
857 sinking wake vortices and the loss of particles in aged contrails (Schumann, 2012).

858 CoCiP (Contrail Cirrus Prediction) depicted in Figure 9 simulates the formation of contrails under
859 specific meteorological conditions, either regionally or globally. Numerical weather prediction
860 data are utilized to determine ambient meteorological conditions through linear interpolation at
861 given positions and times. The model has been effectively employed to simulate contrails in both
862 global and specific cases, and its results have been compared with outcomes from other models
863 and in-situ measurements (Schumann, 2012).

864 **3.2.2 DLR version of the ECHAM5-HAM model**

865 The global climate model ECHAM5-HAM (European Center for Medium-Range Weather
866 Forecasts (ECMWF) and Hamburg) was developed at the Max Planck Institute (MPI) for
867 Meteorology in Hamburg, Germany (Roeckner et al., 2003, 2006; Stier et al., 2005), and adapted
868 to study of aviation effects on climate, including the modeling of the effects from contrails. The
869 aerosol-climate modeling system ECHAM5-HAM is based on a flexible microphysical approach,
870 and it predicts the evolution of an ensemble of microphysically interacting internally and externally
871 mixed aerosol populations as well as their size distribution and composition. Bier and Burkhardt
872 (2022) applied the ECHAM5-HAM model, incorporating a two-moment microphysical scheme
873 that was expanded to introduce a novel cloud category-contrail cirrus. The contrail cirrus scheme
874 encompasses a parameterization addressing contrail ice nucleation, the loss of ice crystals during
875 the vortex phase, plume dilution, the spreading of contrails influenced by vertical wind shear, and
876 inclusive microphysical and macrophysical processes aligned with the natural cloud scheme.

877 The contrail cirrus parameterization implemented in ECHAM5-HAM follows the framework
878 established by Burkhardt and Kärcher (2009), who introduced contrail cirrus as a distinct cloud
879 class alongside natural cirrus clouds within the model's natural cloud scheme. The water and heat
880 budgets are balanced, with natural cirrus and contrails competing for available water vapor.
881 Prognostic variables, including ice water content, contrail coverage, and the length of contrail
882 cirrus, are computed based on factors such as persistence, advection, spreading, and
883 deposition/sublimation.

884

885

886

887

888

889

890

891

892

893

894

895

896

897

898

899
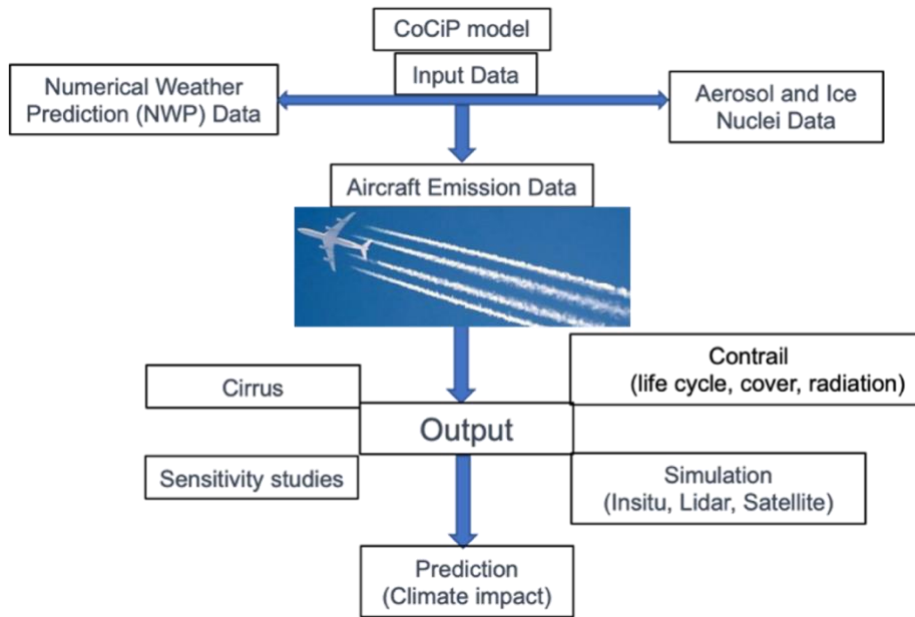
Figure 9. Schematic of the CoCiP model. Adapted from Schumann (2012). Contrail Image (Credit: Adrian Pingstone (public domain)

Bock and Burkhardt (2016) extended this parameterization (CCMod) by incorporating a microphysical two-moment scheme (Lohmann et al., 2008). This enhancement significantly improved the representation of microphysical processes by introducing contrail cirrus ice crystal number concentration and volume as additional prognostic variables. This advancement is crucial for studies investigating the impact of aircraft particle number emissions on contrail cirrus properties and their overall climate influence.

Bier and Burkhardt (2022) describe the initialization of contrails within the model. However, the chosen initialization time of 450 seconds (7.5 minutes) warrants further discussion. This value represents half of a model time step, potentially suggesting computational efficiency as a factor in its selection. Nevertheless, a 450-second delay in contrail formation might be too long for accurate simulations, especially for studies focusing on the early stages of contrail evolution. Future investigations need to explore the sensitivity of model results to this initialization time and potentially refine it for a more realistic representation of contrail formation processes.

In instances of contrail cirrus volumes exhibiting very low ice crystal number concentrations, as observed in aged contrails associated with heightened ice crystal sedimentation, the deposition of ice water is constrained, aligning with the depositional growth of ice crystals (Bock and Burkhardt, 2016). In more recent iterations of the model, specifically, ECHAM5-CCMod, Bier and Burkhardt (2019) incorporated the contrail ice nucleation parameterization proposed by Kärcher et al. (2015). In their model approach, they suggest that the plume cools over time due to continuous mixing of the exhaust with ambient air, eventually becoming water-supersaturated when the SAC criterion is met. The number of activated aerosol particles, stemming from soot and ambient particles, is computed based on ambient conditions, fuel/engine characteristics, and exhaust particle properties. Additionally, Bier and Burkhardt (2022) introduced a parameterization for ice crystal loss during the vortex phase and conducted a thorough evaluation of their model.

Figure 10. Stages of contrails and their corresponding treatment into the global climate model ECHAM5-CCMod. [Adapted from Bier and Burkhardt (2022). Contrail Image (Credit: Adrian Pingstone (public domain)

3.2.3 NCAR CAM6 model with Contrails

In the first NCAR study of the radiative forcing of linear contrails and contrail cirrus, Chen and Gettelman (2013) used the Community Atmosphere Model version 5 (CAM5), the atmospheric component of the National Center for Atmospheric Research (NCAR) Community Earth System Model (CESM). More recently, they have used the updated atmospheric component from the new version of CESM2 (Danabasoglu et al., 2020). The current atmospheric model implemented in CESM2 is CAM, version 6.2 (CAM6; Gettelman et al., 2020). CAM6 incorporates a detailed two-moment cloud microphysics scheme (Gettelman and Morrison, 2015) coupled with an aerosol microphysics and chemistry model (Liu et al., 2016; Gettelman et al., 2019). The latest version of the contrail parameterization (Chen et al., 2012) was utilized with CAM6 (Gettelman et al., 2021). While the ice cloud microphysics and aerosols exhibit minimal differences between CAM5 and CAM6, the aerosol activation in CAM6 significantly differs, impacting natural cirrus clouds but not contrails. The assumed emission ice particle diameter was adjusted from the original parameterization (10 µm) to 7.5 µm to better align with observations (e.g., Lee et al., 2021).

For contrail studies at NCAR, the standard version of CESM with 32 levels (to 3 hPa) vertical and ∼ 1∘ horizontal resolution was employed. Winds and optional temperatures were relaxed to NASA's data assimilation analyses, specifically the Modern-Era Retrospective analysis for Research and Applications, version 2 (MERRA2; et al., 2015), with wind nudging (Gettelman et al., 2020, 2021). CESM2 features a fully interactive land surface model (the Community Land Model, version 5; et al., 2020). Sea surface temperatures (SSTs) are fixed to MERRA2 SST, and there is no interactive ocean.

These simulations allow for adjustments in atmospheric and surface temperatures, resulting in radiative flux perturbations representing an Effective Radiative Forcing (ERF). Sensitivity tests were conducted, with temperatures nudged to MERRA2. The results were compared with previous

965 contrail simulations using this model and others, as well as observational data. The pattern of
966 contrail-induced changes to cloud fraction closely resembled the previous model documented in
967 CAM5 (Chen and Gettelman 2013), with peak effects observed in the Northern Hemisphere at
968 mid-latitudes. The radiative forcing in the CAM6 simulations exceeded that of the earlier Chen
969 and Gettelman (2013) study due to a smaller initial contrail area (100 vs. 300 m) and smaller initial
970 ice crystal sizes (7.5 vs. 10 μm diameter). The radiative forcing pattern and magnitude were
971 qualitatively and quantitatively consistent with the analysis conducted by Lee et al. (2021),
972 aligning with the intercomparison between contrail simulation models.

3.2.4 Stanford global model for contrail evaluation

974 Although it is no longer actively utilized in aviation studies, Stanford University developed a low-
975 order contrail model and a Large Eddy Simulation (LES) model (Naiman et al., 2009; Naiman et
976 al., 2011; Jacobsen et al., 2011). In their work, Jacobsen et al. (2011) assessed mass-conservative,
977 positive-definite, unconditionally stable, and non-iterative numerical techniques for simulating the
978 evolution of discrete, size, and composition-resolved aerosol and contrail particles within
979 individual aircraft exhaust plumes. This simulation was conducted in a global or regional 3-D
980 atmospheric model, incorporating the coupling of subgrid exhaust plume information to the grid
981 scale (see Fig. 11). This approach represents a distinct method for simulating the impacts of aircraft
982 on climate, contrails, and atmospheric composition.

983 The microphysical processes addressed within each plume include size-resolved coagulation
984 among and between aerosol and contrail particles, aerosol-to-hydrometeor particle ice and liquid
985 nucleation, deposition/sublimation, and condensation/evaporation. Each plume is characterized by
986 its own emission and supersaturation, and the spreading and shearing of each plume's cross-section
987 are calculated over time. Aerosol and contrail-particle core compositions are tracked for each size
988 and affect optical properties within each plume. When linear contrails sublimate or evaporate, their
989 size and composition-resolved aerosol cores and water vapor are introduced to the grid scale,
990 where they influence large-scale clouds. The model's algorithmic properties were analyzed, and
991 the final model was evaluated against in situ and satellite data. Table 3 summarizes the cross-
992 model intercomparison of contrail simulation models covered in this study.
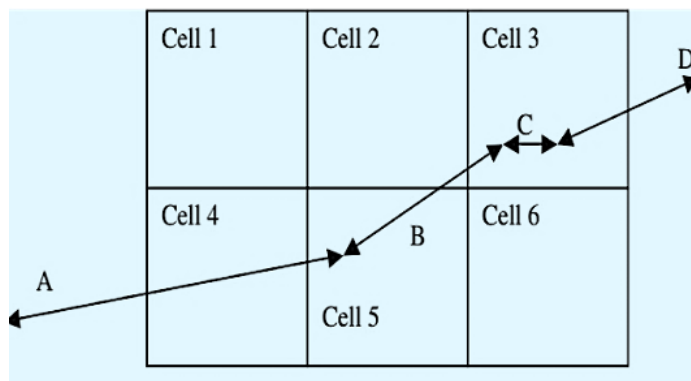
Figure 11. Example of how flight segments cross grid cell boundaries in the Jacobsen et al., model. Segments A, B, C, and D are original segments. These are partitioned or aggregated into individual model grid cells 2, 3, 4, and 5 to form ''new'' segments. Adapted with permission from Jacobson et al. (2011).

4 Radiative Forcing for Contrail Cirrus in Global Models

4.1 Contrail radiative forcing and efficacy

Contrails during the day can warm or cool depending on optical depth, zenith angle, and ice crystal shape (Meerkötter et al., 1999; Stuber et al., 2006; Newinger and Burkhardt, 2012). Stuber et al. (2006) suggested that moving all air traffic to the day decreases RF. Newinger and Burkhardt (2012) stated that we need to consider the lifetime of the contrails since daytime air traffic can cause a large contrail coverage at night. After all, it is the long-lived contrail cirrus outbreaks that are responsible for a large part of the climate impact (Burkhardt et al., 2018). As illustrated in Fig. 1, the overall effect reveals a positive net radiative forcing (RF), signifying a warming impact. The examination of this phenomenon is undertaken here in contrast to the comprehensive RF, the local RF (RF′) can be defined as the instantaneous change in net incoming radiation for 100% contrail coverage in a specific location.

Contrail RF comprises both a long-wave (LW) and a short-wave (SW) component, with each influenced by flight characteristics and the time of day. Unlike the systematic dependency on optical depth (τ), the relationship between RF and ice water path (IWP) is less consistent (De Leon et al., 2012; Schumann et al., 2012). The LW RF is positive both day and night, with the largest impact observed for a cold contrail (located near the tropopause) over a warm, cloud-free Earth surface. The shortwave radiative forcing (RF) is predominantly negative, with the greatest impact observed for contrails over darker surfaces, such as cloud-free oceans (Meerkötter et al., 1999). Studies conducted by Schumann et al. (2012), utilizing both their model and observational evaluations, suggest the existence of substantial regional RF′ values. The calculation of contrail RF within a global model is contingent on factors such as the representation of contrails, the atmospheric conditions, and the radiation transfer model employed (Myhre et al., 2009).

While radiative forcing (RF) provides a valuable measure of the impact of contrails on the radiative balance, it doesn't fully account for the efficacy of different forcing agents in driving surface temperature changes. Recent studies by Bickel et al. (2020) and Ponater et al. (2021) highlight the importance of effective radiative forcing (ERF) as a superior metric. ERF considers feedback mechanisms that can influence the ultimate climate impact of a forcing agent.

In instances of contrail cirrus volumes exhibiting very low ice crystal number concentrations, as observed in aged contrails associated with heightened ice crystal sedimentation, the deposition of ice water is constrained, aligning with the depositional growth of ice crystals (Bock and Burkhardt, 2016). In more recent iterations of the model, specifically, ECHAM5-CCMod, Bier and Burkhardt (2019) incorporated the contrail ice nucleation parameterization proposed by Kärcher et al. (2015). In their model approach, they suggest that the plume cools over time due to continuous mixing of the exhaust with ambient air, eventually becoming water-supersaturated when the SAC criterion is met. The number of activated aerosol particles, stemming from soot and ambient particles, is computed based on ambient conditions, fuel/engine characteristics, and exhaust particle properties. Additionally, Bier and Burkhardt (2022) introduced a parameterization for ice crystal loss during the vortex phase and conducted a thorough evaluation of their model.

Bickel et al. (2020) analyzed the feedback processes and quantified the effective radiative forcing (ERF) of contrail cirrus, which refers to the cloud formations produced by aircraft engine exhaust. They highlighted that feedback analysis is a valuable tool for understanding climate sensitivity and the differences in efficacies between various climate-forcing agents. Previous climate model simulations have suggested a relatively low efficacy of contrails in forcing global mean surface

1049 temperature changes. They employed a climate model that incorporates a state-of-the-art
1050 representation of contrail cirrus and conducted the simulations with fixed sea surface temperatures
1051 to determine the ERF resulting from contrail cirrus.

1052
1053 **Table 3** Cross-model intercomparison of contrail simulation models
1054

Model Name	Developer	Simulations	Strengths	Weaknesses	Evaluation
CoCiP	DLR	Full life cycle	Efficient computation, considers aircraft/fuel	Simplified mixing, neglects radiation	In-situ measurements, remote sensing data
APCEMM	MIT	Individual microphysics/chemistry	Detailed microphysics	High computational cost, limited global use	Primarily theoretical, limited observations
NASA Global Contrail Model	NASA Ames	Individual formation/transport	Computationally efficient	Neglects downwash, excludes radiative forcing	Reanalysis data
ICON-LEM (Contrail Scheme)	DLR	Contrail formation (regional model)	Considers ice nucleation/survival	Relies on parameterizations, limited microphysics	Satellite data
LES Model	Stanford University	Full life cycle (individual & cirrus)	High-resolution microphysics	Computationally expensive, limited scalability	In-situ measurements

Model Name	Validation Method		Model Uncertainties		
CoCiP	In-situ measurements, remote sensing data		*In-situ measurements*: May not fully capture contrail variability; calibration and processing uncertainties affect accuracy. *Satellite retrievals*: Uncertainties in thin contrails; cloud backgrounds can misidentify or underestimate contrails. *Data Coverage:* CoCiP dataset may not cover all contrail properties, limiting model generalizability.		
APCEMM	Primarily theoretical, limited observations		*Validation data:* Simplified plume dynamics may not accurately reflect real-world contrail behavior due to limited validation. *Parameterization:* Uncertainties in microphysical process parameterizations can affect model accuracy.		
NASA Global Contrail Model	Reanalysis data		*Reanalysis biases:* Temperature and humidity biases in reanalysis data affect contrail formation accuracy. *Static atmosphere:* Model ignores wind shear and dynamic factors in contrail evolution. *Downwash exclusion:* Omits ice particle downwash from wake turbulence, impacting contrail properties.		
ICON-LEM (Contrail Scheme)	Satellite data		*Satellite retrievals:* Cloud backgrounds cause uncertainties in satellite detection and contrail property estimation. *Parameterization:* Uncertainties in ice nucleation and crystal survival parameterizations affect contrail persistence accuracy.		
LES Model	In-situ measurements		*Spatial and temporal coverage*: In-situ measurements may miss full variability of contrail properties in large-scale simulations. *Computational limits*: LES models are expensive, limiting simulation scope and number of contrails, affecting behavior capture. *Microphysics schemes:* Uncertainties in ice binning and microphysical processes impact contrail microphysics accuracy.		

1055

1056

1057 Bickel et al. (2020) noticed that significant scaling up of aviation density is necessary to obtain
1058 statistically significant results from the simulations. Their study found that the ERF of contrail
1059 cirrus is less than 50% of the respective instantaneous or stratosphere-adjusted radiative forcings.
1060 The best estimate of contrail cirrus ERF is approximately 35%. In comparison, the reduction of
1061 ERF is more substantial for contrail cirrus than for a similar magnitude increase in CO_2
1062 concentrations. They identified the main factor contributing to the reduction in contrail cirrus ERF
1063 as a compensating effect of natural clouds that provide negative feedback. Additionally, they
1064 observed that the combined water vapor and lapse rate adjustment, which affects the distribution
1065 of water vapor in the atmosphere and the lapse rate (temperature decrease with altitude), has a less
1066 positive impact on contrail cirrus ERF compared to the reference case of CO_2 forcing.
1067 Nevertheless, the negative feedback provided by natural clouds has a more pronounced effect in
1068 reducing contrail cirrus ERF compared to these adjustments.

1069 Overall, Bickel et al. (2020) suggested that contrail cirrus has a lower climate impact than initially
1070 thought, with the reduction in ERF attributed to the compensating effect of natural clouds.
1071 Understanding the specific feedback processes and quantifying the ERF of different climate
1072 forcing agents, such as contrail cirrus, is crucial for accurately assessing their contributions to
1073 surface temperature changes and overall climate dynamics.

1074 While radiative forcing (RF) provides a measure of contrail impact on radiative balance, it doesn't
1075 fully account for the efficacy of different forcing agents in driving surface temperature changes.
1076 Recent studies by Ponater et al. (2021) emphasize the importance of effective radiative forcing
1077 (ERF) as a superior metric. ERF considers feedback mechanisms that influence a forcing agent's
1078 ultimate climate impact. Their findings suggest a potentially lower climate impact from contrail
1079 cirrus than previously assumed based on ERF calculations. However, as acknowledged by Ponater
1080 et al. (2021), further research is needed to confirm the efficacy of ERF in assessing the complete
1081 surface temperature response to contrail cirrus. Direct simulations of this response would be
1082 crucial for validating ERF as a reliable metric for contrail cirrus impact.

1083 Similar to findings by Bickel (2023), this study highlights the potential limitations of using RF
1084 alone to estimate contrail cirrus impact. Here, climate model simulations revealed a significant
1085 reduction in the effective radiative forcing (ERF) of contrail cirrus compared to its conventional
1086 RF. This suggests a potentially lower climate impact from contrail cirrus than previously assumed
1087 based solely on RF calculations. The primary contributor to this reduced ERF is likely a negative
1088 cloud adjustment, where contrail cirrus formation leads to a decrease in natural cirrus cover.
1089 Further research is needed to confirm these findings across different climate models and refine our
1090 understanding of contrail cirrus efficacy in driving surface temperature changes.

1091 Long-lasting contrails contribute to global climate change. These contrails can form cirrus clouds,
1092 which are a type of high-altitude cloud that can trap heat in the atmosphere. This trapping of heat
1093 is known as radiative forcing. While the exact contrail contribution to radiative forcing remains
1094 uncertain, it is thought to be a significant factor in climate change (Brasseur et al., 2016). The RF
1095 metric is a backward-looking measure of the effect of emissions on the radiative flux balance and
1096 is commonly used to compare changes in climate forcings (Wuebbles et al., 2010). The RF linked
1097 to non-CO_2 aviation emissions arises from processes occurring over different time scales. Contrails
1098 generally exist for a few hours after an aircraft emissions occur, but other emissions can last much
1099 longer. Effects on the distribution of aerosols and on ozone produced from NOx emissions can

1100 remain for a few days to months, while changes in CH_4 can be affected for longer than a decade.
1101 The limitations of using RF as a comprehensive metric for global non-CO_2 aviation climate
1102 impacts are well-recognized due to such associated spatiotemporal variations (Wuebbles et al.,
1103 2007). The nonlinear interactions involved make it imprecise to represent the sum of RF for various
1104 non-CO_2 components as a single value. Similarly, distinct climate responses are observed for
1105 different forcing mechanisms.

1106 In 2016, Brasseur et al. investigated the radiative forcing (RF) through analyses involving seven
1107 global models (CAM4, CAM5, IGSM, GISS-E2, GEOSCCM, GATOR-GCMOM, and GEOS-
1108 CHEM) as part of the Federal Aviation Administration's (FAA) Aviation Climate Change
1109 Research Initiative (ACCRI) program. The assessment covered climate impacts for 2006, and the
1110 initial five models projected impacts for 2050 scenarios, specifically focusing on selected aircraft
1111 emission components. In a separate study, Chen and Gettelman (2016) used the CAM5 model to
1112 estimate RF for contrails and contrail cirrus in the 2050 future scenario, employing the 2006 AEDT
1113 dataset. Notably, the research highlighted the tendency to overestimate global linear contrail (LC)
1114 net RF when using the natural ice cloud optical property parameterization as a stand-in for contrail
1115 counterparts in modeling studies. Furthermore, the distribution of regional RF indicated that in
1116 densely trafficked airspaces, such as the United States, RF could be up to ten times higher than the
1117 global average (Brasseur et al., 2016).

1118 Schumann and Graf (2013) determined a more significant AIC impact by using both observational
1119 data and the contrail cirrus prediction model (CoCiP; Schumann, 2012). They found an "aviation
1120 fingerprint" ascribed to a daily air traffic cycle within the diurnal cycle of cirrus properties in the
1121 North Atlantic region (NAR), associating with the annual mean diurnal patterns of cirrus cover
1122 and outgoing longwave radiation (OLR) derived from Meteosat data (Graf et al., 2012).

1123 Figure 12 shows the global average annual radiative forcing (RF) values and uncertainty ranges
1124 for persistent contrails alone and together with contrail cirrus. The values are compiled from
1125 selected studies and assessments published since 1999 and include a recent development by
1126 Kärcher (2018). Over time, early assessments of contrail RF have been confirmed and the range
1127 of uncertainty has been narrowed down considerably.

1128 The figure shows that the RF due to persistent contrails alone is -0.01 W/m² (with an uncertainty
1129 range of 0.005-0.03 W/m²), and the RF due to persistent contrails together with contrail cirrus is
1130 ~0.05 W/m² (with an uncertainty range of 0.02-0.15 W/m²). (Kärcher, 2018). Figure. 12 shows
1131 that analyses accounting only for linear contrails underestimate the total RF for contrails. More
1132 recent analyses tend to show an overall warming of around ~45mWm^{-2} (Bier and Burkhardt, 2022).

1133 The models applied by DLR and NCAR's groups are summarized in Table 4 (updated from. Bock
1134 and Burkhardt, 2016). Bock and Burkhardt (2016) evaluated the year 2002 using the AERO2k
1135 inventory and for year 2006 using the AEDT 2006 slant distance inventory. The corrected NCAR
1136 analyses and their more recent results are consistent with those from the DLR modeling studies
1137 (Lee et al., 2021). These findings further amplify the conclusions from Fig. 12.

1138
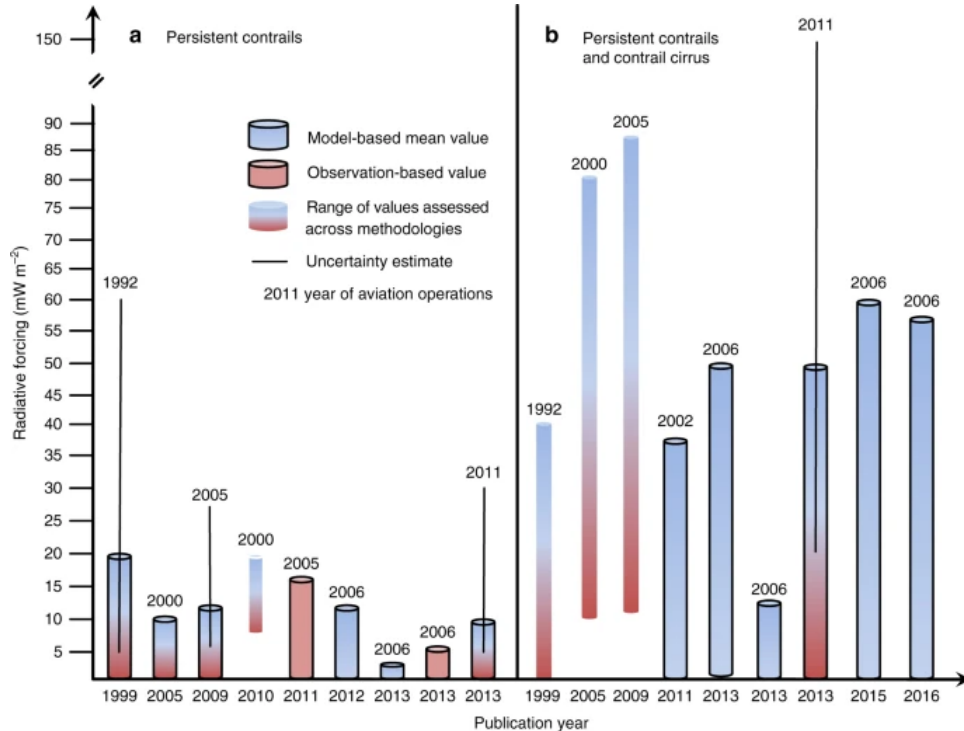
Figure 12. Global annual average amount of radiative forcing caused by aircraft-induced clouds Figure adapted with permission from Kärcher (2018). (Licensed under CC BY 4.0)

4.2 Future RF projections

4.2.1 DLR's study for future RF projections

Bock and Burkhardt (2019) investigated how changes in air traffic between 2006 and 2050, including both volume increase and upward shift in flight altitudes (0.3-1.5 km), would impact contrail cirrus properties and radiative forcing. Table 5 shows their simulations considering this combined scenario. It projects a fourfold increase in air traffic and a maximum flight density at a lower altitude (200 hPa in 2050 compared to 240 hPa in 2006), which has climate implications.

In Table 5, the air traffic distance is specified as the ground-projected track distance. The coverage is sketched out for all contrail cirrus, and the visibility of contrail cirrus (visible optical depth > 0.05) is indicated in brackets (Bock and Burkhardt, 2016). Radiative forcing estimates exist for both track distance and slant distance within brackets (Table 5). Remarkably, Bock and Burkhardt (2019) determined that the projected future increase in air traffic, coupled with a minor shift to higher altitudes, outcomes in a substantial rise in contrail cirrus coverage, optical depth, and radiative forcing. Particularly, air traffic contrail cirrus radiative forcing is estimated to increase threefold, from 49 to 159 mW m^{-2} (Fig. 13). The findings are a result of a future air traffic inventory, where the measurement of air traffic is signified in terms of track distance (ground projected) rather than slant distance (3-D). Declining the initial contrail ice particle number by 50% results in a substantial drop in the climate impact of contrail cirrus, leading to a global decline in radiative forcing for the year 2050. The reduction is significant, amounting to a 14% reduction from 160 to 137 mWm^{-2} (Fig. 13).

1176 **Table 4.** Summary of existing contrail cirrus simulations and RF from the DLR and NCAR
1177 models. Adapted from of Bock and Burkhardt (2016).
1178

Model	Inventory	Flight distance	RF (mW/m^2)	References
ECHAM5-CCMod	AERO2k 2002	track	35	
ECHAM5-CCMod	AEDT 2006	track	49	*Burkhardt and Kärcher* (2011)
ECHAM5-CCMod	AEDT 2006	slant	56	
ECHAM4-CCMod	AERO2k 2002	track	38	
ECHAM4-CCMod	REACT4C 2006	track	45	*Schumann et al,* (2015)
COCIP	AEDT 2006	flight vectors	63	*Schumann et al.* (2015)
CAM5	AEDT 2006	slant	13 (57)*	*Chen and Gettelman* (2013)
CAM6	AEDT 2006	slant	62 (ERF)**	*Gettelman et al.* (2021)

* The approximation of Chen and Gettelman (2013) was revised.

**ERF (the scaling technique was derived from Lee et al.2021 for 2006 to 2018 and then 9% per year scaled (2018 to 2019) by Gettelman et al. (2021)

AERO2k – Global aircraft emissions data project for climate impacts evaluation

AEDT- Aviation Environmental Design Tool

REACT4C- Reducing Emissions from Aviation by Changing Trajectories for the benefit of Climate

1179

1180 **4.2.2 RF projections from the NCAR model**

1181 The study conducted by Chen and Gettelman (2016) investigated the radiative forcing curbing
1182 from aviation-induced cloudiness, using the Community Atmosphere Model Version 5 (CAM5)
1183 for both present (2006) and future (up to 2050) scenarios. The researchers found a projected four-
1184 fold increase in global flight distance from 2006 to 2050. Despite this, the simulated radiative
1185 forcing from contrail cirrus in 2050 is predicted to reach 87 mWm^{-2}, representing a seven-fold rise
1186 compared to 2006. This underlines a non-linear correlation between radiative forcing and fuel
1187 emission mass, accredited to non-uniform regional escalations in air traffic and changes in contrail
1188 radiative forcing sensitivity through different regions.

1189 The CAM5 simulations also indicate that the negative radiative forcing resulting from the indirect
1190 effect of aviation sulfate aerosols on liquid clouds in 2050 could be as large as -160 mWm^{-2}, a
1191 four-fold increase from 2006. Consequently, when considering both aviation aerosols and contrail
1192 cirrus, the total radiative forcing in 2050 could possibly employ a cooling impact on the planet.
1193 Aerosols, particularly aviation sulfate aerosols distributed at cruise altitudes, may be transferred
1194 to the lower troposphere. This procedure raises aerosol concentrations and consequently enhances
1195 the cloud drop number concentration and persistence of low-level clouds. On the other hand, the
1196 study suggests that aviation black carbon aerosols have an insignificant net forcing affect globally,
1197 both in 2006 and 2050.

1198 The researchers focus on specific regions, for instance, Central Europe, eastern North America,
1199 and East Asia, and recommend quantitative evaluations of the forcing in each region for several
1200 scenarios. For example, in Central Europe, the predicted contrail cirrus radiative forcing in 2050
1201 is anticipated to locally peak at 2 Wm^{-2}, marking a 2 to 3-fold increase compared to 2006. In the
1202 eastern United States, the contrail cirrus radiative forcing could reach 800 mWm^{-2} in 2050,
1203 revealing a higher percentage increase compared to 2006. The most prominent rise in contrail

1204 cirrus radiative forcing is estimated in East Asia, where a 6-fold increase is projected for 2050,
1205 associated with the region's anticipated significant rise in consumption of aviation fuel.

1206 **Table 5.** Overview of the model simulations: Air traffic distance exists as ground-projected track
1207 distance. Coverage is furnished for all contrail cirrus, with coverage for visible contrail cirrus
1208 (visible optical depth > 0.05) shown in brackets (Bock and Burkhardt, 2016). The radiative
1209 forcing is represented for both track distance and slant distance, with values enclosed in brackets.
1210 (Adapted from Bock and Burkhardt (2019)

Background	Inventory	Air traffic volume (km yr^{-1})	Propulsion efficiency	Initial ice number concentration (cm^{-3})	Coverage (%)	RF (mW m^{-2})
2006	2006	3.7×10^{10}	0.3	150	1.1 (0.7)	49 (56)
2006	2050 Baseline	15.4×10^{10}	0.3	150	2.9 (2.0)	159 (182*)
2050 (RCP6)	2050 Baseline	15.4×10^{10}	0.3	150	2.8 (2.0)	160 (183*)
2050 (RCP6)	2050 Scenario1	15.4×10^{10}	0.42	75	2.98(1.7)	137 (157*)

RCP6-Representative Concentration Pathway 6.0

*Asterisks denote extrapolated values resultant from the factor resolute by the radiative forcing in 2006, which is connected to air traffic volume and computed using slant distance and track distance (Bock and Burkhardt, 2016).

1211 The inclusion of aviation aerosols in the simulations suggests a slight reduction in positive forcing
1212 over land, as compared to the forcing solely caused by contrail cirrus. On the other hand, over the
1213 ocean, a negative forcing rising from aviation emissions is measured. This can be accredited to the
1214 lower surface albedo and cleaner environment (fewer aerosols) in comparison to land areas. In the
1215 three regions with the highest projected air traffic in 2050 (eastern United States, Central Europe,
1216 and East Asia), aviation aerosols reduce the regionally averaged positive radiative forcing induced
1217 by contrail cirrus by approximately 50%, as indicated by the blue boxes in Fig. 14. The peak
1218 positive forcing within each of these regions is also reduced by 50% due to aviation aerosols. The
1219 study provides detailed regional estimates of these effects (Table 6).

1220 The negative radiative forcing result from aviation aerosols, as detected in this study, supports the
1221 inferences represented by Righi et al. (2013). The extent of the cooling effect is estimated to be
1222 affected by the background cloud drop number concentration.
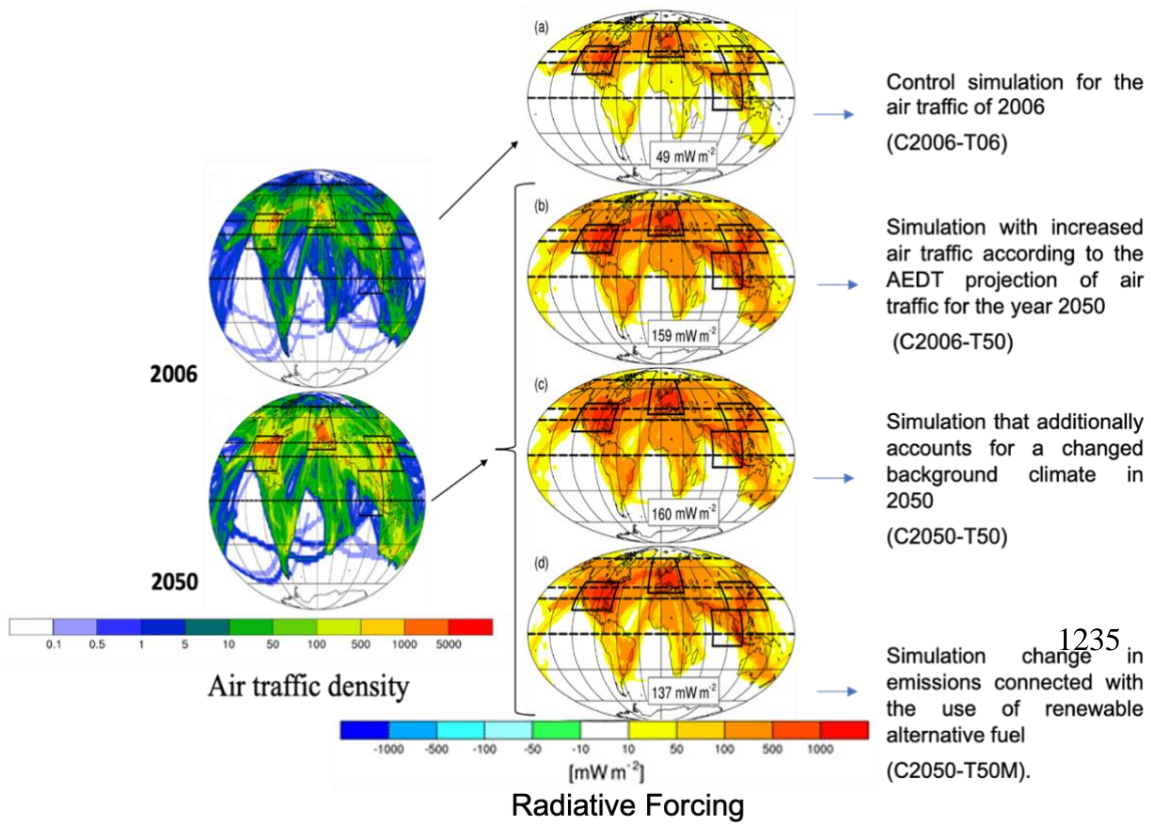
1240 **Figure 13.** The horizontal distribution depicts the vertically incorporated air traffic density (km
1241 $m^{-2}s^{-1}$) for the years 2006 and 2050, along with the radiative forcing in scenarios C2006-T06 (a),
1242 C2006-T50 (b), C2050-T50 (c), and C2050-T50M (d) Figure adapted with permission from Bock
1243 and Burkhardt (2019). (Licensed under CC BY 4.0).

1244 **Table 6.** Radiative forcing (mWm^{-2}) attributed to aviation H_2O emissions, with uncertainties
1245 derived from 2 standard deviations of the four-member ensemble. (Adapted from Chen and
1246 Gettelman, 2016)

Meteorology	Scenario	Global	North America	Central Europe	East Asia
Present	2006 AIR	12 ± 4	195 ± 30	483 ± 69	41 ± 8
2050 RCP4.5	2050 BL	87 ± 6	798 ± 152	1682 ± 535	272 ± 39
2050 RCP4.5	2050 SC1	76 ± 7	724 ± 136	1568 ± 489	231 ± 36
2050 RCP4.5	2050 SC2	76 ± 7	724 ± 136	1568 ± 489	231 ± 36
2050 RCP4.5	2050 SC3	80	681	1952	213
2050 RCP8.5	2050 BL	83 ± 3	852 ± 92	1558 ± 226	248 ± 25
2050 RCP8.5	2050 SC1	73 ± 4	777 ± 96	1442 ± 235	211 ± 24
2050 RCP8.5	2050 SC2	73 ± 4	777 ± 96	1442 ± 235	211 ± 24
2050 RCP8.5	2050 SC3	75	865	1597	221

1247 RCP4.5-Representative Concentration Pathway 4.5
1248 RCP8.5 -Representative Concentration Pathway 8.5. BL-Base line
1249 SC1. SC2, and SC3- Scenarios 1, 2 and 3
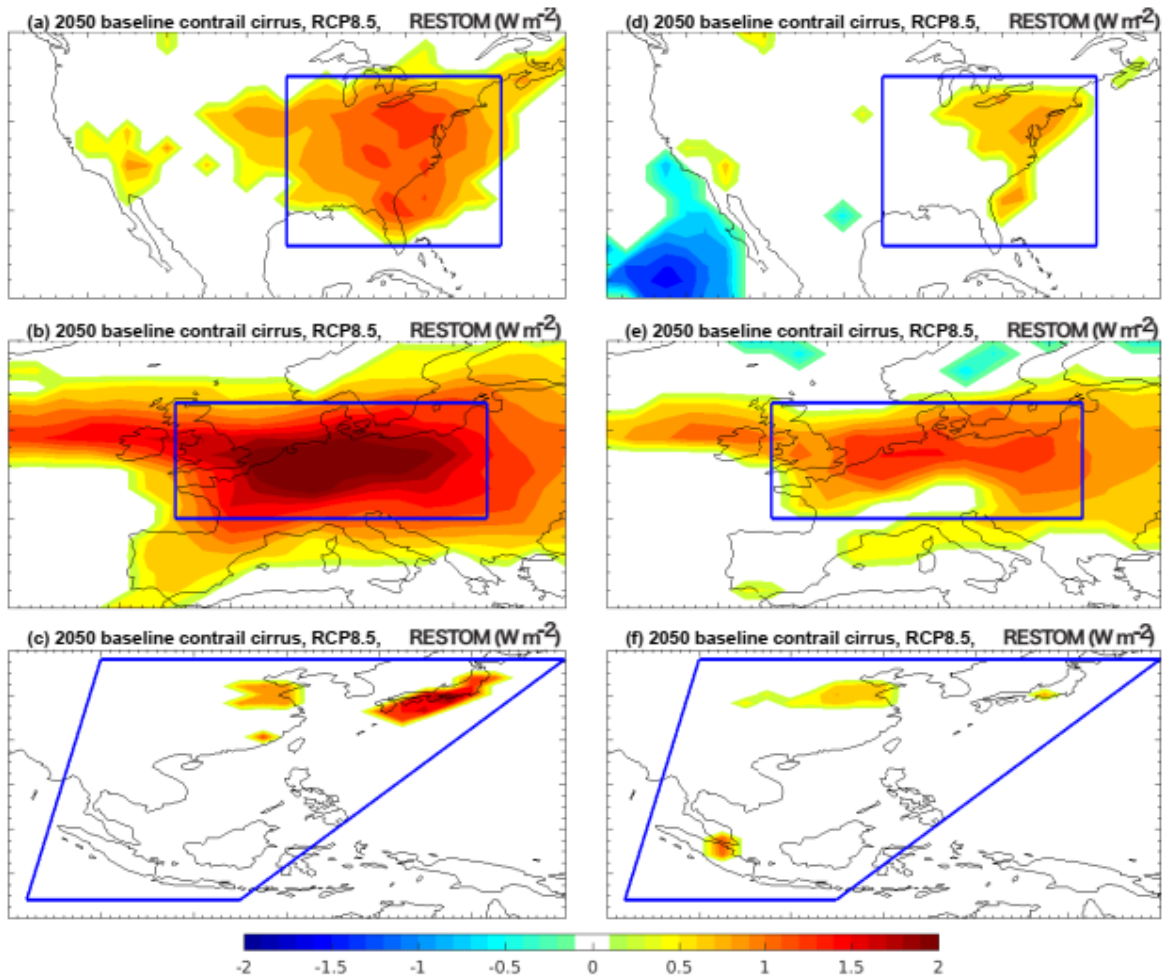
1250

Figure 14. Ensemble of the average regional radiative forcing in Wm^{-2}, utilizing the baseline emission scenario for the year 2050 with RCP8.5 meteorology, focusing on contrail cirrus alone (a–c) and contrail cirrus combined with aviation aerosols (d–f). The term "RESTOM" represents the alteration in the net residual radiative flux at the top of the model. The plot includes only ensemble-mean perturbations that surpass 2 standard deviations of the averaged control simulations. (Figure adopted with permission from Chen and Gettelman, 2016) (Licensed under CC BY 4.0

4.3 Issues representing cloud-contrail and contrail-contrail overlaps in modeling studies

A thorough examination of past methodologies for modeling cloud layer overlaps and several modeling studies recommends that overlapping with other cloud layers is prone to reduce both the shortwave (cooling) and longwave (warming) radiative forcing linked to contrails (Sanz-Morère et al., 2021). However, there is inadequate agreement on how the overlap between clouds and contrails might modify the net radiative forcing due to uncertainties regarding whether it would more strongly mitigate the shortwave or longwave components. Particularly, the precise impact of contrail-contrail overlap on global contrail radiative forcing has yet to be measured. In this section, we review previous literature referring to the treatment of multiple-layer overlap in the context of contrail radiative forcing calculations.

1268 Schumann et al. (2012) determined that the net radiative forcing may augment if contrails overlap
1269 with low-level clouds but could go through significant variations when passing under natural cirrus
1270 clouds. This underscores the significance of precisely modeling natural clouds in contrail
1271 simulations. Nevertheless, when utilizing this method to simulate single contrails, accounting for
1272 the radiative interactions among multiple contrails turns into a challenging task. In prior examples
1273 of modeling contrail-contrail overlap, when simulating contrails in global climate models, various
1274 treatments have been utilized, as outlined in. Contrail parametrizations have been formulated for
1275 ECHAM4 (Ponater et al., 2002; Burkhardt and Kärcher, 2009), where maximum-random overlap
1276 is presumed between contrail and cloud layers, as well as among different contrails (Burkhardt and
1277 Kärcher, 2011; Marquart et al., 2003; Bock and Burkhardt, 2016; Frömming et al., 2011). Rädel
1278 and Shine (2008) and Rap et al. (2010) also use this parameterization, calibrating the outcomes by
1279 using satellite observations. Table 7 summarizes the existing methods for modeling contrail–
1280 contrail overlaps.

1281

1282 **Table 7.** Existing methods for modeling contrail–contrail overlap when estimating global contrail
1283 RF. MRO: maximum-random overlap, defined by Geleyn and Hollingsworth (1978) as assuming
1284 that clouds in adjacent layers maximally overlap, while clouds separated by one or more clear
1285 layers randomly overlap (Adapted from Sanz-Morère et al. 2021).

Source	Model used to represent contrail–contrail overlap
Minnis et al. (1999)	No overlap considered (fractional coverage from observations)
Marquart et al. (2003)	MRO in the vertical for each column
Rädel and Shine (2008)	Random overlap
Rap et al. (2010)	Random overlap
Frömming et al. (2011)	MRO in the vertical for each column
Burkhardt and Kärcher (2011)	MRO in the vertical for each column
Chen and Gettelman (2013)	Zero contrail–contrail overlap in grid box
Schumann and Graf. (2013)	Linear RF addition
Bock and Burkhardt (2016)	MRO in the vertical for each column

1286

1287 Chen and Gettelman (2013) included contrails in the CAM5 model by portraying them as an
1288 increase in the 3-D cloud fraction, where the model presumes maximum-random overlap.
1289 Nevertheless, in their method, they considered zero overlaps between newly formed contrails when
1290 placed at the same vertical level (approximately 1 km). Finally, the CoCiP Lagrangian contrail
1291 model (Schumann, 2012) reports contrail-contrail overlaps indirectly by linearly summing the
1292 radiative forcing of all contrails, taking into consideration any observed cirrus present above the
1293 simulated contrail. Nonetheless, this method does not clearly consider the overlap between
1294 simulated contrails. Inconsistencies rise in how contrail-contrail overlaps are modeled across
1295 various studies. The most efficient approach remains uncertain, and as of now, no analysis has
1296 measured the impact of contrail-contrail overlaps on global contrail RF. Since further expansion
1297 of the aviation sector is expected, it is anticipated that an increased number of instances of contrail
1298 overlap will occur. Hence, a more inclusive understanding of the degree and dynamics of contrail-
1299 contrail overlap is a necessity. Table 8 summarizes the agreement and disagreement between
1300 climate models on contrail cirrus radiative forcing.

5 Observation Datasets for Contrail Studies

The vast majority of observations, comprised of airborne, satellite, and ground-based approaches, encompass jet aircraft exhaust contrails from 1972 onward. Nevertheless, it is remarkable that records of contrail observations date back to as early as 1915, as published by Ettenreich in 1919.

Early measurements performed behind a propeller-driven aircraft offered data supporting the concept that contrail ice formation requires liquid saturation to originate, associating with the Schmidt-Appleman criterion that is now well-established (Schmidt, 1941, Appleman,1953 and Schumann, 1996.). These remarks, which encompassed the collection of ice particles on impactors and halo observations, also furnished initial insights into the size and shape of both contrail and cirrus ice particles (Weickmann, 1945).

The precise testing of models necessitates reliable quantitative data, covering not only information on contrail and plume properties but also on contrail age, the generating aircraft, atmospheric conditions during contrail formation, and the observational methods employed (Schumann et al., 2017). Mean properties of individual contrails are characterized for a wide range of jet aircraft as a function of age during their life cycle from seconds to 11.5 h (7.4-18.7 km altitude, -88 to -31°C ambient temperature), based on a compilation of about 230 in-situ and remote sensing measurements (Schumann et al., 2017). Contrails from individual aircraft can remain visible for extended periods, as reported in analyses by Minnis et al. 1998, 2013) and Vázquez-Navarro et al. (2015). Schumann et al. (2017) furnished a brief description of individual datasets, integrating new analyses for their study, and combined them to create a "contrail library" (COLI). This dataset was then compared with the outcomes of the Contrail Cirrus Prediction (CoCiP) model. The observations corroborate that the quantity of ice particles in contrails is controlled by both the engine exhaust and the formation process in the jet phase. Some particle losses ensue in the wake vortex phase, with succeeding gradually diminishes over time.

Publicly available air traffic data are usually limited, but certain projects have gathered flight data from sources such as air traffic control or ground-based observations (Schumann et al., 2013; Schumann et al., 2017). Distinguishable projects with air traffic subsets since 2005 are accredited. Garber et al. (2005) compiled traffic data for the United States and southern Canada for the years 2000-2005. In Germany, the Deutsche Flugsicherung (DFS) has been gathering and filing away traffic data from 2006 onwards for more new projects. The Aviation and Climate Change Research Initiative (ACCRI; Brasseur et al., 2016) furnished a global waypoint dataset for the year 2006 to researchers included in the ACCRI project.

The existing observation datasets on contrail properties and formation conditions are constantly expanding with the inclusion of innovative resources. The recently developed Global Aviation Emissions Inventory based on ADS-B (GAIA) (Teoh et al., 2024). leverages historical flight paths derived from Automatic Dependent Surveillance-Broadcast (ADS-B) technology, coupled with reanalyzed weather data from 2019 to 2021. GAIA paints a detailed picture of global aviation activity, encompassing the spatial and temporal variations in flight patterns, fuel consumption, and emissions of key pollutants like CO_2, NOx, and particulate matter. This information proves particularly valuable for contrail research by offering insights into the connections between aircraft types, flight routes, and the potential for contrail formation in diverse regions. For example, by analyzing short-haul versus long-haul flight emissions within GAIA, researchers can glean insights into the contribution of various aircraft categories to contrail formation patterns across different geographical areas.

1345 Table 8 . Agreement and disagreement between climate models on contrail cirrus radiative forcing.
1346 (The models discussed include CoCiP, ECHAM5-HAM, CAM6, and the Stanford Global Model. Detailed
1347 descriptions of these models can be found in Sections 3.2.1 through 3.2.4).
1348

Aspect	Agreement	Disagreement	Potential Causes	Recommendations for Future Research
Net Radiative Forcing (RF)	Likely positive net RF, signifying warming			
Longwave vs. Shortwave RF		Models show some variation in the relative contribution of longwave (warming) and shortwave (cooling) components to the net RF depending on factors like ice crystal shape and optical depth.	Complexity of ice crystal parameterizations Treatment of solar radiation transfer	Improve ice crystal parameterizations in models to better capture the variation in radiative properties. Conduct studies to refine the treatment of solar radiation transfer in contrail simulations.
Regional Variations	Models concur on significant regional variations in RF			
High-traffic vs. Low-traffic areas		Models show discrepancies in the magnitude of the regional variations.	Input data on air traffic patterns	Improve the quality and resolution of air traffic data used in climate models.
Future RF Projections	Models predict a significant increase in contrail cirrus RF by 2050 due to rising air traffic and flight altitude			
Impact of aviation aerosols		Models show variations in the projected net effect (warming vs. cooling) due to the counteracting impact of aviation aerosols on low-level clouds.	Uncertainties in how models represent aviation aerosol properties and their interactions with clouds.	Conduct dedicated studies to improve the representation of aviation aerosols and their interactions with clouds in climate models.
Cloud Overlap	Overlap with other clouds (natural cirrus, low-level clouds) can affect RF, but the extent of impact (shortwave vs. longwave dominance) is uncertain.	Contrail-contrail overlap is not well understood and might be more frequent in the future.	Need for a better understanding of cloud-contrail and contrail-contrail overlap and their impact on global RF.	Develop improved methods for simulating cloud-contrail and contrail-contrail overlap in climate models. Conduct observational studies to quantify the frequency and radiative effects of contrail overlap.

- *CoCiP:* Agreements on overall contrail effects, but some discrepancies in initial ice crystal formation.
- *ECHAM5-HAM:* Captures basic contrail formation but has different ice crystal properties affecting long-term impacts.
- *CAM6:* Aligns with others in radiative forcing but shows minor differences in contrail-induced cloud changes.
- *Stanford Global Model:* Agrees on initial formation but has contrasting plume mixing and microphysical schemes leading to varied impact predictions.

1349 By seamlessly integrating GAIA with existing observation datasets like COLI (Schumann et al.,
1350 2017), researchers can cultivate a more nuanced understanding of the interplay between aviation
1351 activity, atmospheric conditions, and contrail occurrence. This enhanced knowledge ultimately
1352 empowers the improvement of contrail prediction models and informs strategies to mitigate their
1353 impact on climate.

1354 Particulars about aircraft assets, including size, mass, speed, fuel consumption, and propulsion
1355 efficiency, were tracked from various references, including the BADA (EUROCONTROL, 2009).
1356 Added engine properties, such as fuel consumption and emissions at surface pressure, can be
1357 attained from the ICAO Aircraft Engine Emissions Databank (EASA, 2023) and the 2006 AEDT
1358 emissions inventory (Barrett, 2010; Wilkerson, 2010).

1359 Poll (2018) devised a straightforward model to estimate fuel burn for commercial aircraft, offering
1360 a transparent, publicly accessible option apart from the BADA and PIANO codes (Piano-X,
1361 software, Lissys Ltd., 2008)). Utilizing this method necessitates understanding the Mach number
1362 and flight level where an aircraft, under specific conditions, achieves its absolute minimum fuel
1363 burn rate. Yet, acquiring this data proves challenging, although an initial effort is outlined in Poll
1364 and Schumann (Poll, 2018), where input files are supplied for 53 aircraft types.

1365 Two sets of observational-based capabilities exist that can provide the coverage needed to help
1366 evaluate the global modeling analyses for treating the effects of contrails, the Contrail Library
1367 (COLI) and the satellite-based record. The Contrail Library results are useful for evaluating limited
1368 areas of contrails but not for global analyses.

1369 **5.1 Contrail Library (COLI)**

1370 The COLI database includes 236 entries describing properties of contrails with known ages,
1371 including mean data for one hundred cases of in-situ measurements, more than 70 cases from
1372 ground-based and airborne lidar observations, 50 cases from satellites, and a few camera
1373 observations. The data come from 33 observation projects during the last 45 years. The comparison
1374 of the data from various measurements shows notable differences among the various instruments
1375 utilized across the dataset. Nevertheless, a notable accord endures among each approach, as well
1376 as uniformity between in-situ and remote sensing results, along with agreement with Schumann et
1377 al (2017) model outcomes. Moreover, in-situ data resultant from contrail measurements, the
1378 investigation integrates remote sensing data found from ground-based or airborne lidar and
1379 spectroradiometer, satellites, cameras, and visual interpretations. Table 9 summarizes some of the
1380 projects that contributed to the COLI database, including the aircraft used and the primary location,
1381 the mode of reference, and the primary reference of the study.

1382 Accurate forecasting of contrail occurrence and persistence holds significant importance in
1383 addressing their potential climate impact. For this purpose, research conducted by Gierens et al.
1384 (2020) underscores the limitations of reanalysis data, primarily due to their coarse vertical
1385 resolution. This study shows the necessity for high-resolution observational data, especially
1386 concerning temperature and relative humidity in the upper troposphere and tropopause region, to
1387 understand contrail formation and behavior better. Initiatives such as the In-service Aircraft for a
1388 Global Observing System (IAGOS) (Gierens et al., 2020) are pivotal in providing such data by
1389 utilizing advanced instruments installed on passenger aircraft. The assessment of contrail
1390 formation models demands dependable data encompassing both contrail characteristics and
1391 atmospheric conditions during their formation. While the study by (Gierens et al., 2020) evaluates
1392 the predictability of contrails using the Schmidt-Appleman criterion based on reanalysis data, it

1393 underscores the critical role of high-resolution data in assessing more advanced contrail prediction
1394 models. The availability of observational datasets containing parameters such as temperature,
1395 relative humidity, and air traffic data, as discussed in this section, is indispensable for such model
1396 assessments.
1397

5.2 Satellite-based datasets

1399 Over the past two decades, the detection of contrail in satellite imagery has primarily depended on
1400 the algorithm developed by Mannstein et al. (2003) (e.g., Palikonda et al., 2005; Vazquez-Navarro
1401 et al., 2010). This algorithm contains a series of convolution and thresholding operations related
1402 to brightness temperature images and, subsequently the detection of linear associated components
1403 of fitting size. While the algorithm has been fine-tuned to attain either high precision or high
1404 remembrance in contrail detections, no single model has simultaneously surpassed in both aspects.
1405 Subsequently, empirical observations of contrail coverage often need broad lower-bound/upper-
1406 bound approaches (Duda et al., 2013). Minnis et al. (2013) reported the properties of contrail cirrus
1407 clouds formed during 11 different contrail outbreaks, in the context of objectively determined
1408 linear contrails and their properties. It was observed that the ratio of contrail cirrus to linear
1409 contrails is substantially affected by the satellite analysis algorithm utilized to allocate linear
1410 contrails. Furthermore, this ratio seems to be affected by the presence of overlapping contrails,
1411 which can obscure individual contrails.

1412 The contrail cirrus optical depths were found to be 2-3 times greater than their linear contrail
1413 counterparts and the associated ice crystal particle diameters were 20% greater than the contrail
1414 particle sizes. The analyses of such satellite datasets are likely to be useful for evaluating global
1415 models of contrail radiative effects.

1416 An exception to the application of the Mannstein et al. (2013) algorithm is prominent in Kulik
1417 (2019) and Meijer et al. (2021). These analyses employed a deep learning model for pixel-level
1418 contrail detection using GOES-16 satellite imagery. Upon detecting a contrail, these studies
1419 facilitate the assessment of its lifetime impact and the ascription of potentially relevant flights
1420 (Vazquez-Navarro et al., 2010; Vazquez-Navarro et al., 2013; Vazquez-Navarro et al., 2015.
1421 Mutually, these practices furnish a means to evaluate the efficacy of flight diversions in avoiding
1422 contrail formations. McCloskey et al. (2021) officially released the first large dataset of pixel-level
1423 contrail locations in Landsat-8 satellite imagery labeled by humans. Labelers should be able to
1424 accurately differentiate contrails from naturally occurring cirrus due to Landsat-8's high spatial
1425 resolution and the advected flight history information provided. This dataset will be useful in
1426 benchmarking contrail detection models and validating contrail research in collocated
1427 geostationary satellite imagery.

1428 Satellite-based datasets offer valuable insights into global contrail occurrence and variability,
1429 although challenges arise when estimating contrail radiative forcing. Retrieving contrail optical
1430 thickness, a crucial parameter for such calculations, from current satellite observations, is
1431 particularly difficult. Moreover, distinguishing contrails from overlapping features and natural
1432 cirrus clouds remains challenging, especially with limited spatial resolution. Addressing these
1433 challenges is essential for enhancing the contribution of satellite observations to contrail radiative
1434 forcing estimations. Advancements in retrieval algorithms for contrail optical thickness and
1435 methods to differentiate contrails from overlapping features are necessary for more accurate
1436 assessments.

1437
1438 Despite these challenges, satellite-based contrail datasets have significant potential for monitoring
1439 contrail occurrence and coverage over time. This information is valuable for evaluating the
1440 effectiveness of flight diversion strategies aimed at minimizing contrail formation. Furthermore,
1441 the emergence of human-labeled contrail datasets like McCloskey et al. (2021) provides a valuable
1442 resource for training and validating future advancements in contrail detection using deep learning
1443 and machine learning algorithms. Continuous collaboration among satellite data providers,
1444 atmospheric scientists, and AI researchers is vital for realizing the full potential of satellite-based
1445 contrail datasets for contrail mitigation and climate impact assessments.
1446
1447 Ng et al. (2023) presented a human-labeled dataset named open contrails to train and evaluate
1448 contrail detection models based on GOES-16 Advanced Baseline Imager (ABI) data. Ng et al.
1449 (2023) proposed and evaluated a contrail detection model that incorporates temporal context for
1450 improved detection accuracy. The human-labeled dataset and the contrail detection outputs are
1451 publicly available on Google Cloud Storage at gs://goes_contrails_dataset.

1452 Persuading policymakers and airlines about the climate benefits of flight diversions becomes more
1453 reasonable with the availability of satellite corroboration capabilities. Geostationary satellites like
1454 GOES-16 and low-earth orbit satellites such as Landsat-8 present both complementary strengths
1455 and weaknesses when employed for the task of contrail detection (i.e., coverage versus persistence
1456 of the observations). An automated contrail detection system is essential for developing and
1457 evaluating contrail avoidance systems. Deep neural networks can be employed as an automated
1458 contrail detection system, a form of artificial intelligence (AI) and machine learning (ML), that
1459 has been advanced to connect and categorize contrails in satellite imagery or other relevant data
1460 sources. This system can effectively analyze complex patterns and features associated with
1461 contrails, by leveraging the competencies of deep neural networks. By utilizing deep neural
1462 networks and machine learning techniques, the automated contrail detection system offers an
1463 efficient and reliable solution for detecting and monitoring contrails, facilitating further research
1464 and analysis of their impact on climate and aviation.

1465 **Table 9.** Observations from the year 2000 to 2014 were incorporated into the COLI for the study
1466 of contrail (Adapted from Schumann et al. 2016).

Year	Project name	Source aircraft	Carrier/location	Measurement	Reference
2000	Cluster	airliners	Great Lakes	satellite	Duda et al.,(2004)
2001	Shutdown	B747+C fighters	Northwestern USA	satellites	Minnis et al.,(2002)
2002	CRYSTAL-FACE	WB-57	NASA WB-57	in situ	Gao et al.,(2006)
2003	Fallstreaks 2003	airliners	Goddard	lidar	Atlas and Wang (2010)
2005	PAZI-2	airliners	DLR Falcon	in situ	Febvre et al.,(2009)
2006	CR-AVE	WB-57	NASA WB-57	in situ	Flores et al.,(2006)
2008	CONCERT	airliners	DLR Falcon	in situ	Voigt et al.,(2010)
2008	ACTA	airliners	Europe andNorth Atlantic	satellite	Vázquez-Navarro et al.,(2015)
2011	CONCERT2011	airliners	DLR Falcon	in situ	Kaufmann et al.,(2014)
2011	COSIC	Bae 146	FAAM Bae-146	in situ	Jones et al.,(2012)
2012	Cameras	airliners	Munich	cameras	Schumann et al.,(2013)
2014	ML-CIRRUS	B772 or F900	HALO	in situ	Voigt et al.,(2016)

1467

1468 Siddiqui (2020) conducted a study where a neural network was used to distinguish contrail cirrus
1469 clouds from regular cirrus clouds on TSI images. The study found that the neural network
1470 triumphed with a high accuracy of 98.5% on the validation set, implying that the model was able
1471 to learn significant visual features of contrails that differentiate them from regular cirrus clouds.
1472 The success of this model opens various practical applications for studying contrails. For instance,
1473 the model can be used to analyze images from different months of data, agreeing for researchers
1474 to investigate the frequencies of contrail occurrences. This can impart valuable insights into air
1475 traffic trends, as well as how physical conditions like temperature and humidity vary seasonally
1476 and their potential impact on contrail formation. Researchers can better understand contrail
1477 behavior and their relationship with various environmental factors by leveraging the neural
1478 network's ability to detect and classify contrails accurately. This knowledge can be used to refine
1479 models and predictions related to contrail formation and persistence and contribute to a more
1480 comprehensive understanding of aviation's impact on the atmosphere.

6 Supersonic contrails

1482 Contrail studies have primarily focused on subsonic aviation due to the predominance of subsonic
1483 air traffic since the retirement of the Concorde in 2003. Contrail formation and persistence for
1484 supersonic commercial aircraft pose challenges -- persistent contrails are unlikely to form in the
1485 stratosphere when these aircraft are flying at supersonic speeds but societal requirements for flying
1486 at subsonic speeds over land to avoid noise issues would still potentially produce persistent
1487 contrails. The importance of understanding the global climate effect of contrails linked to
1488 supersonic aviation is well-established (Stenke et al., 2008). Matthes et al. (2022) recently
1489 published a comprehensive review on the climate effects of supersonic aviation, encompassing
1490 non-CO2 effects like contrail formation. Their work highlights the need for a thorough
1491 understanding of existing research in this area and uncertainties persist regarding parameters
1492 controlling contrail ice crystal distribution evolution for these aircraft. Consequently, the presence
1493 or absence of contrails becomes a discernible marker of the aircraft's speed regime. Additionally,
1494 limited research, such as observations by Schumann et al. (2017) suggested the possibility of
1495 contrail formation even at high altitudes (18.7 km) under specific atmospheric conditions. These
1496 factors highlight the need for a comprehensive understanding of contrail formation and persistence
1497 for future supersonic aircraft.

7 Uncertainties and Research Gaps

7.1 Uncertainties

1500 There are several crucial areas of uncertainty and research gaps that require focused investigation
1501 to achieve a more comprehensive understanding of contrail formation, evolution, and their effects:
1502 • *Humidity Observations and Predictions:* An important uncertainty lies in the accuracy and
1503 reliability of humidity observations and predictions at different altitudes. Improved
1504 measurements and modeling of humidity are critical for assessing the conditions conducive to
1505 persistent contrail formation and their subsequent behavior. Addressing this uncertainty will
1506 lead to more precise insights into contrail persistence and its associated radiative impacts.
1507 • *Interaction with Natural Cirrus Clouds:* The interplay between natural cirrus clouds and
1508 contrails initiates an additional level of uncertainty, fostering obscuring the understanding of
1509 their individual and mutual effects on radiative forcing (RF).
1510 • *Regional Variations in Atmospheric Conditions:* The sensitivity of contrail radiative impacts
1511 to regional variations in atmospheric conditions is not well understood and remains uncertain.

- *Uncertainties and Soot Particles*: The role of soot particles in contrail formation remains subject to uncertainties, particularly regarding their ability to nucleate ice. Despite the presence of numerous ice particles in fresh contrails, ongoing debates, as highlighted in recent studies such as Righi et al. (2021), question whether soot particles directly facilitate ice nucleation. Clarifying this relationship is essential for comprehending the impact of soot emissions on contrail formation and subsequent evolution. To address this knowledge gap, further research efforts are imperative to explore the influence of soot particles on ice nucleation processes within contrails.
- *Radiative Transfer Scheme:* Quantifying the radiative forcing exerted by contrails on Earth's climate remains an intricate task. Studies by Schumann and Graf (2013) identified a distinct signature, an "aviation fingerprint," in cirrus cloud cover and outgoing longwave radiation (OLR) that mirrored air traffic patterns. This observation suggests a robust correlation between aviation activity and cirrus cloud formation. Their analysis even estimated a regional increase in heat-trapping (longwave radiative forcing) of 600-900 mWm^{-2}, highlighting the potential influence of aviation on these high-altitude ice clouds. However, a crucial challenge lies in accurately modeling the net impact on Earth's energy balance. This difficulty stems from the fact that different climate models employ various approaches to simulate radiative transfer processes, which govern the movement of heat through the atmosphere. These variations in how models handle these radiative processes can significantly influence the estimated impact of contrails on our planet's energy equilibrium.

Significant uncertainties persist regarding the radiative forcing caused by aircraft contrails. These uncertainties arise from numerous factors, starting with uncertainties in the background meteorology and specific aircraft emissions. When assessing the climate impact of contrail cirrus, the primary uncertainties lie in (1) determining upper tropospheric water vapor concentrations and regions of supersaturation; (2) adequately representing contrail cirrus processes in global models; and (3) understanding the radiative response resulting from the contrail cirrus presence, typically, only approximate assessments of uncertainties associated with these processes are furnished.

Assessing the radiative response of contrail cirrus involves handling several crucial uncertainties, including:

Uncertainties in Contrail Cirrus Radiative Forcing: Estimating the radiative forcing (RF) of contrail cirrus clouds is inherently uncertain. Lee et al. (2021) categorizes these uncertainties into two main areas: (A) uncertainties related to the radiative response of contrail cirrus and (B) uncertainties associated with the upper-tropospheric water budget and the contrail cirrus scheme within climate models.

(A) *Uncertainties in Radiative Response*

Radiative Transfer Scheme (A1): Myhre et al. (2009) estimated an uncertainty of approximately 35% arising from the radiative transfer scheme employed in climate models. This scheme simulates how different wavelengths of radiation interact with various atmospheric components, including contrail cirrus.

Cloud Heterogeneity (A2*):* The inhomogeneity of ice crystals within a model grid box, vertical cloud overlap, and limitations of plane-parallel geometry contribute an estimated uncertainty of 35% (Carlin et al., 2002; Pomroy and Illingworth, 2000; Gounou and Hogan, 2007).

Ice Crystal Habit (A4): Variations in the shape and form (habit) of ice crystals within contrail cirrus can significantly impact how they interact with radiation. Markowicz and Witek (2011) suggest an uncertainty of 20% due to this factor.

Soot Core Impact (A5): The radiative transfer uncertainty associated with soot cores embedded within contrail cirrus ice crystals is significant, particularly for shortwave albedo (reflectivity), but remains unquantified (Liou et al., 2013). Soot cores can absorb radiation, potentially leading to a warming effect that is not currently accounted for in models.

(*B) Uncertainties in Water Budget and Contrail Cirrus Scheme*

Ice Supersaturation (B1): Uncertainties in the representation of upper-tropospheric ice supersaturation (Lamquin et al., 2012) contribute an estimated 20% uncertainty.

Ice Crystal Number Density (B2): and Radiative Transfer for Young Contrails (A3): Uncertainties in ice crystal number densities (Karcher et al., 2015, 2018) are linked to factors like water vapor saturation and soot emissions. Lee et al. (2021) recognized the dependence between A3 (radiative transfer for young contrails) and B2 (ice crystal number density). Consequently, they included the uncertainty from A3 within their overall category B uncertainty estimate.

Contrail Cirrus Lifetime (B3): The effect of contrail cirrus lifetime on estimated RF is relatively small, with an associated uncertainty estimated at 5-10% (Chen and Gettelman, 2013; Newinger and Burkhardt, 2012). While Lewellen (2014) highlights the potential importance of lifetime through large-eddy simulations demonstrating contrail cirrus lifetimes exceeding 40 hours and widths exceeding 100 km, several factors contribute to the seemingly counterintuitive finding in this context of estimated RF. Lewellen's (2014) simulations highlight the potential significance of contrail cirrus with extended lifetimes, particularly for their ice crystal surface area and overall radiative impact. However, the study focuses on the integrated effect over the entire lifetime, whereas the uncertainty estimate (5-10%) pertains to the impact of variations in lifetime on the average RF. Further research is needed to better understand the complex interplay between contrail cirrus lifetime, ice crystal growth processes, atmospheric conditions, and their combined effect on radiative forcing.

Air Traffic Data Resolution (B4): Sensitivity studies suggest an uncertainty of about 10% arising from the temporal resolution of air traffic data used in climate models (Lee et al., 2021).

Natural Cloud Feedback (B5): The feedback mechanism by which contrail cirrus alters the upper tropospheric water budget, affecting natural clouds, introduces a significant uncertainty that remains unquantified (Burkhardt and Karcher, 2011; Schumann et al., 2015). Lee et al. (2021) assumed an uncertainty of 15% for this factor.

Initial Ice Crystal Assumptions (B6): The estimation of RF by Chen and Gettelman (2013) is subject to uncertainties associated with assumptions about initial ice crystal radii and contrail cross-sectional areas, leading to an estimated uncertainty of 33%.

Overall Uncertainty

Following Lee et al. (2021), the uncertainty in the radiative response to contrail cirrus (excluding soot cores) is estimated to be around 55%, assuming independence of different uncertainties. This aligns with their findings and highlights the dominance of radiative response uncertainties (category A) in the overall uncertainty budget. Category B uncertainties (water budget and contrail

1595 cirrus scheme) remain significant and require further investigation, particularly the combined
1596 effect of ice crystal number density and radiative transfer for young contrails.

1597 The Uncertainty Tightrope
1598 While scientists continue to refine their understanding of how contrails form and influence our
1599 climate, the ever-present threat of climate change demands that we don't wait for complete
1600 certainty before taking action. The evidence of our warming planet is undeniable, and aviation's
1601 contribution to this issue necessitates exploring all possible solutions, even in the face of some
1602 lingering unknowns.

1603 Fortunately, research like that conducted by Frias et al. (2024) offers a glimmer of hope. Their
1604 study suggests that practical strategies to avoid contrail formation can be implemented with
1605 minimal disruption to flight operations, while significantly reducing the overall climate impact of
1606 these contrails. This finding underscores the potential for immediate action alongside ongoing
1607 scientific inquiry. By embracing a two-pronged approach that combines continued research with
1608 real-world mitigation efforts, we can work towards minimizing aviation's environmental footprint.

1609
1610 **7.2 Research needs and gaps**

1611 In the pursuit of a comprehensive understanding of contrail impacts on climate, there is a critical
1612 need to establish clear research needs and requirements.

1613 Improving weather models demands better predictions of humidity and clouds with enhanced
1614 resolution in time, space, and altitude. The models must also adapt to evolving weather conditions.
1615 Accurate water vapor data during cruise altitudes is crucial, emphasizing the need for small, cost-
1616 effective humidity sensors. To achieve this, there is a need for the production, testing, and
1617 evaluation of precise sensors. Lidar technology and weather model assessments play a key role in
1618 advancing observational capabilities for more accurate predictions. Enhancing cirrus cloud
1619 forecasts requires a dual focus on data and artificial intelligence. Ensemble simulations are vital
1620 for estimating uncertainties in cirrus cloud predictions. Additionally, there is an urgent need for
1621 more climate and contrail models, ensuring a comprehensive understanding and evaluation of these
1622 complex atmospheric processes.

1623 Gierens et al. (2020) highlighted a significant issue with the ERA-5 reanalysis data, showing that
1624 it underestimates the frequency and degree of ice supersaturation. This underestimation impacts
1625 the reliability of forecasts for contrail persistence and the accuracy of estimates for contrail optical
1626 thickness and instantaneous radiative forcing. Their research, which involved comparing
1627 predictions from weather and climate models with actual atmospheric data from the
1628 IAGOS/MOZAIC project and the EMAC model, revealed that while temperature predictions are
1629 generally accurate, relative humidity predictions are often significantly off. This discrepancy
1630 undermines the effectiveness of using reanalysis data to predict real-world contrail formation along
1631 aircraft trajectories. The study underscores the necessity of improving ice supersaturation
1632 predictions to enhance the reliability of contrail avoidance strategies and ensure they can be
1633 operationally viable (Gierens et al.,2020).

1634 Research by Ovarlez et al. (2000) highlights discrepancies between measured water vapor content
1635 and data from weather forecasts. Their findings emphasize the importance of accurate humidity
1636 measurements, particularly for studies on contrail formation and persistence. Weather forecasts
1637 might underestimate actual humidity, potentially leading to inaccurate assessments of contrail

1638 behavior. This underlines the need for ongoing research to improve the accuracy of humidity data
1639 in weather models.

1640 Furthermore, high-quality observations, effectively integrated into weather models, are crucial for
1641 setting accurate starting points for forecasts (Bauer et al., 2015). This highlights the need for robust
1642 data collection strategies that combine information from diverse sources. These sources can
1643 include in-situ measurements taken directly within the atmosphere, radar systems that track
1644 precipitation patterns, and satellite sensors that provide a global view. Advanced data assimilation
1645 techniques then play a vital role by merging these observations with model outputs. This combined
1646 approach creates a more precise picture of the initial atmospheric state, ultimately leading to
1647 improved weather forecasts (Bauer et al., 2015).

1648 Sun and Roosenbrand (2023) reported the limitations in traditional computer vision approaches
1649 for contrail detection, particularly in handling the complexity of satellite images under varying
1650 conditions. Earlier machine learning methods relied on simpler convolutional neural network
1651 models, primarily demanding extensive labeled data for contrail presence determination. Notably,
1652 there is a gap in the existing literature, lacking research specifically tailored to machine learning
1653 approaches for contrail detection, setting it apart from other image segmentation or detection tasks.
1654 A significant challenge lies in the absence of adequate loss functions optimized for linear features
1655 like contrails during training, making detection notably difficult at lower resolutions, especially
1656 when multiple contrails are close. Addressing these gaps is crucial for advancing the efficacy of
1657 contrail detection methods (Sun and Roosenbrand, 2023).

1658 While a complete understanding of contrail effects on climate may not be achievable, further
1659 research is crucial to reduce uncertainties and improve our ability to predict and mitigate their
1660 impact. Here are some of the key areas of research gaps that should be explored to address existing
1661 uncertainties:

1662 ▪ *Properties of Contrail Particles*: Understanding contrail effects on climate requires
1663   reflection of key factors such as particle size, layer height, cloud overlap, and optical
1664   properties. Larger particles tend to have a different radiative impact than smaller ones. The
1665   altitude of contrail formation impacts their interaction with solar and terrestrial radiation.
1666   Precise climate modeling requires proper accounting for cloud overlap, impacting radiative
1667   calculations. Contrail optical properties, comprising albedo and emissivity, determine their
1668   reflective and trapping abilities for solar and terrestrial radiation. The concentration and
1669   size distribution of contrail particles affect their formation and radiative impact. Accurate
1670   estimation of contrail forcing, important for climate modeling and policy decisions,
1671   depends on understanding particle number, size, and layer height.
1672 ▪ *Assessment of Effective Radiative Forcing:* Effective Radiative Forcing (ERF) is a valuable
1673   tool for evaluating the global mean radiative impact of contrail cirrus on climate. However,
1674   it's important to recognize that ERF primarily focuses on this average effect and may not
1675   fully capture regional variations or complex feedback mechanisms associated with contrail
1676   formation and persistence.
1677 ▪ *Emissions and Alternative Fuels*: Corroborating a precise connection between soot and
1678   contrail ice crystal numbers is important for understanding the environmental impact of
1679   sustainable aviation fuels, such as biofuels. Biofuels are being studied as a more sustainable
1680   alternative to conventional aviation fuels, and evaluating their impact on contrail formation
1681   is crucial for assessing environmental benefits. Scientific research, notifying regulatory
1682   decisions, relies on the interpretation of the correlation between soot and ice crystal

numbers. This connection is integral for complete visions of the environmental implications of alternative aviation fuels. Precise data on contrail formation, containing the impact of biofuels, is crucial for climate models predicting the impact of aviation emissions on climate. The experimental establishment of the soot-ice crystal connection gives this understanding.

- *Properties of Soot Particle*: A study into the bimodal size distributions of soot particles in aircraft emissions is critical for focusing uncertainties on contrail formation and properties, with inferences for climate science and aviation practices (Schumann et al., 2002). In-flight measurements typically show a single peak in the number-size distribution of freshly emitted soot particles (Schumann et al., 2002). However, some cases reveal a second, larger particle mode in near-field contrails and dry plumes. The source of this larger mode remains uncertain, suggesting that the bimodal distribution might be present in unrefined jet engine emissions rather than being solely caused by contrail processing or coagulation during plume development (Schumann et al., 2002). Precise data on soot particle properties, including any potential bimodal size distribution, is essential for climate models incorporating contrail effects. Resolving the origin of this bimodal distribution is crucial to improving model representations of contrail properties. Policymakers and regulatory bodies rely on scientific research for progressing aviation-related environmental policies, making an understanding of soot particle size distributions significant for up-to-date decision-making.

- Examining the microphysical interaction between soot particles and contrail ice crystals emerges as a critical research priority. Laboratory experiments simulating contrail formation conditions offer valuable insights into the ice nucleating potential of soot particles under controlled environments. Moreover, field measurements focusing on the in-situ characterization of soot particles and ice crystals within nascent contrails provide indispensable data for validating models. By integrating these methodologies, researchers can advance their understanding of the role of soot particles in contrail formation and refine climate models accordingly.

- *Remote Sensing for Contrail-Cirrus*: Organized regional campaigns are important for estimating key variables in aging contrail-cirrus and aircraft plumes. This contains in-situ and remote sensing to portray the growth, decay, and trajectories of contrail ice particles, delivering essential data for interpretation of transformation and radiative effects. Estimation of contrail particles, ambient aerosols, and gaseous aerosol precursors notifies climate modeling and environmental assessments, connecting emissions to contrail properties. Gathered data validates climate models, enhancing their accuracy and improving the representation of contrail-cirrus effects. Understanding contrail-cirrus development supports developing mitigation strategies, informing contrail avoidance, and reducing aviation's climate impact.

In addition to these research issues, there is a need to bridge the gaps with the assessment of the above-reported uncertainties and to investigate and improve the understanding of contrail avoidance and climate tradeoffs. Research should explore how to mitigate the climate impact of contrails without compromising aviation safety and efficiency.

7.3 Contrail avoidance and climate tradeoffs

While existing studies explore contrail avoidance strategies and their impact on fuel burn and climate, a comprehensive large-scale evaluation remains elusive. Ideally, such an evaluation would encompass a significant number of routes, account for weather variations, enable full flight level optimization, quantify contrail impacts on individual flights, and compare results to a fuel-optimal baseline to isolate the specific effects of contrail avoidance. This comprehensive approach would provide a more definitive understanding of the fuel-climate tradeoffs associated with contrail avoidance strategies.

Recent studies investigating targeted contrail avoidance strategies offer promising results. Teoh et al. (2020) suggest that focusing on a small percentage of flights with the highest contrail impact could be an effective approach, minimizing the overall increase in fuel consumption and CO2 emissions. Additionally, advancements in engine design hold promise as a long-term solution for reducing contrail formation.

Molloy et al. (2022) address a critical step towards implementing effective contrail avoidance strategies in practice. Their work outlines the practical considerations for conducting large-scale trials, which are essential for evaluating the feasibility and effectiveness of these strategies in real-world conditions. The proposed deployable options based on existing air traffic management processes offer a promising path forward for initiating such trials.

Frias et al. (2024) present a compelling case for the practicality and economic viability of contrail avoidance. Their findings demonstrate that significant reductions in contrail climate impact can be achieved with minimal operational burdens. This study provides strong motivation for airlines and air traffic controllers to embrace contrail avoidance strategies as a means to reduce aviation's overall climate footprint.

Gierens et al. (2008) proposed several potential ways to mitigate the impact of contrails, encompassing both technical and operational approaches. Regarding the technical aspect, they recognized the challenge of completely preventing contrail formation due to its primarily thermodynamic nature. However, they suggested the exploration of new engine cycles and technical infrastructures that might help suppress contrails. Additionally, reducing the number of emitted particles was considered to mitigate contrail formation. While such evaluations would not eliminate contrails completely, they would produce thinner contrails with rarer but larger crystals. These heavier ice crystals would incline more rapidly on average, causing shorter contrail lifetimes. The analysis also investigated operational mitigation options. Striking strict constraints, such as fixed maximum flight levels, was studied unreasonably due to the significant challenges it would pose for air traffic controllers and the resulting safety concerns. Their proposed strategies focused on addressing contrail formation both at the technical level through engine and infrastructure improvements and at the operational level by implementing flexible measures that consider real-time weather conditions. These approaches aimed to strike a balance between contrail reduction and the practical needs of aviation.

In a recent study, Sausen et al. (2023) presented an experiment that aimed to avoid contrail formation during real-world operations. This experiment took place in the Maastricht Upper Area Control region, covering parts of Germany, the Benelux countries, and the North Sea, in the year 2021. The researchers highlighted that contrail avoidance could serve as an effective method for mitigating the climate impact of aviation. To conduct their trial experiment, air traffic was

1771 deliberately diverted every other day by adjusting the flight altitude, either increasing or decreasing
1772 it by up to 2000 ft, whenever potential persistent contrails were predicted. The effectiveness of
1773 these deviations was assessed by analyzing satellite images of high clouds and employing a
1774 contrail detection algorithm that utilized contrail properties. Despite the ongoing challenge of
1775 accurately forecasting persistent contrails, the trial achieved a significant level of success, reaching
1776 97.5%, suggesting that on average, persistent contrails can be avoided during regular flights in the
1777 real world through minor adjustments in the vertical flight path. Contrail avoidance through minor
1778 adjustments in flight paths represents a practical approach to mitigate the formation of persistent
1779 contrails. It demonstrates the feasibility of implementing such measures within air traffic
1780 management to reduce the environmental impact of aviation. The study highlights the potential for
1781 real-world applications of contrail avoidance as a means of addressing the climate effects of
1782 contrails. The findings of this experiment mark an important milestone in implementing
1783 operational measures in air traffic management to decrease the impact of climate from aviation.

1784 The limitations of simply avoiding all contrails become evident when we consider their diverse
1785 climate effects. While some contrails can have a net cooling effect, others contribute to warming.
1786 This distinction necessitates a more nuanced approach to contrail avoidance. We should focus on
1787 mitigating the formation of contrails that contribute to warming, while potentially allowing or even
1788 encouraging the formation of those with a net cooling effect. This distinction requires reliable
1789 methods for differentiating between the two contrail types.

1790 *Future considerations: optimizing contrail avoidance.*

1791 The Sausen et al. (2023) study represents a significant step forward, demonstrating the feasibility
1792 of operational contrail avoidance through minor flight adjustments. To optimize this approach for
1793 maximum climate benefit, future research should focus on three key areas:

1794 *Distinguishing warming from cooling contrails:* Developing robust methods to differentiate
1795 between these contrail types is crucial. Improved weather forecasting models and contrail
1796 prediction algorithms that consider factors like altitude, atmospheric conditions, and cirrus cloud
1797 cover can contribute to this goal.

1798 *Large-scale implementation:* Evaluating the broader applicability of contrail avoidance strategies
1799 necessitates conducting large-scale trials across diverse airspace with varying weather patterns.
1800 This will provide a more comprehensive understanding of the effectiveness and potential trade-
1801 offs associated with contrail avoidance in different operational contexts.

1802 *Integration with air traffic management:* For widespread adoption, efficient protocols for
1803 integrating contrail avoidance measures within existing air traffic management systems are
1804 essential. This may involve developing streamlined decision-making tools and communication
1805 channels for air traffic controllers and pilots.

1806 By addressing these considerations, contrail avoidance can evolve from a general strategy to a
1807 targeted approach that maximizes its potential for mitigating aviation's climate impact. This
1808 approach would focus on reducing the formation of warming contrails while allowing for or even
1809 encouraging the formation of cooling contrails.

1810 In a recent Ph.D. thesis, Elmourad (2023) evaluated the fuel-climate tradeoffs arising from contrail
1811 avoidance strategies applied on a large scale. This study raises several key questions about
1812 contrails avoidance: What fraction of aviation's global total contrail length can be avoided using
1813 vertical re-routing exclusively? What is the fuel penalty of such an avoidance strategy? How does

1814 the fuel penalty or contrail reduction vary between flights or seasons? Can the fuel penalty be
1815 constrained? What effect does that have on the ability to do contrail avoidance? What net climate
1816 benefit can be achieved from contrail avoidance strategies? How does this differ from avoiding all
1817 contrails or only nighttime contrails? What are the relative orders of magnitude between the
1818 climate benefits from contrail avoidance and the climate damages from additional fuel burn? How
1819 does this difference compare with the uncertainties associated with contrail impacts?

1820 As the global volume of air traffic continues to rise, the aviation industry grapples with a
1821 significant challenge in mitigating its environmental impact on climate change. Contrails, which
1822 contribute to global warming by trapping terrestrial radiation, have the potential to counteract the
1823 benefits of reduced emissions resulting from optimized flight paths. In a study by Roosenbrand et
1824 al. (2023), the authors conducted a global assessment of flights that contribute to contrail formation
1825 and assessed the altitude adjustments required to avoid these contrail-prone areas. This analysis
1826 utilized a combination of data from the Integrated Global Radiosonde Archive (IGRA), which
1827 provides measurements from weather balloons with global coverage and high vertical resolution,
1828 and flight data from OpenSky. The study identified Mid-Western Europe, the Eastern United States
1829 of America, and Japan as regions characterized by both high air traffic volumes and a substantial
1830 percentage of flights forming contrails. Importantly, these regions offer opportunities for altitude
1831 adjustments of less than one kilometer to minimize contrail formation. The research also
1832 pinpointed other regions where relatively minor operational interventions could yield significant
1833 climate benefits.

1834 *Fuel-climate tradeoffs*: While there have been numerous studies on operational contrail avoidance,
1835 there are still some research gaps in the field when it comes to understanding the fuel-climate
1836 tradeoffs that would follow a large-scale global application of contrail avoidance strategies.

1837 *Sustainable Aviation Fuel (SAF)*: Much still needs to be understood about what SAF will look like
1838 as it becomes the dominant fuel of the future. The emissions of soot and other particles from SAF
1839 are still not well understood and will have a significant effect on future contrail production and
1840 lifetimes. According to Bräuer et al. (2021b), sustainable aviation fuels have been identified as
1841 capable of reducing both contrail ice numbers and the radiative forcing caused by contrail cirrus.
1842 Their study involved the measurement of apparent ice emission indices across different fuels with
1843 varying aromatic content at altitudes ranging from 9.1 to 9.8 km and 11.4 to 11.6 km. The data
1844 were collected during the ECLIF II/NDMAX flight experiment in January 2018, encompassing a
1845 variety of fuels differing in aromatic quantity and type. A comparison between a sustainable
1846 aviation fuel blend and a reference fuel Jet A-1 revealed a maximum reduction of 40% in apparent
1847 ice emission indices, highlighting the potential impact of sustainable aviation fuels on mitigating
1848 contrail-related environmental effects.

1849 Moore et al. (2017) examined the impact of biofuel blends compared to traditional jet fuel on
1850 aircraft emissions. They found that biofuel blends significantly reduced the quantity and weight of
1851 particles emitted, suggesting biofuels can reduce aviation's environmental impact. Their
1852 measurements showed a notable decrease in total and non-volatile particles with the biofuel blend
1853 and a shift to smaller particle sizes. This is due to a larger reduction in bigger soot particles acting
1854 as condensation nuclei. The drop in soot emissions enhances the formation of new particles.
1855 Mixing petroleum fuels with HEFA bio-jet fuel cut volatile and non-volatile particle emissions by
1856 50%-70% during cruise conditions. However, soot particle emissions remain high, indicating
1857 biofuels help but don't eliminate issues related to contrail formation.

Alternative aircraft and new fuels: There is a lot of ongoing discussion about the potential development of aircraft using hydrogen as fuel. Such an aircraft engine would still emit water vapor and therefore could produce contrails. However, the major reduction in particulates, e.g., no soot, could affect the lifetime of the contrail and whether it could result in contrail cirrus. Research is needed to evaluate the potential for contrail production and resulting lifetimes. Other alternative fuels would also need to be evaluated.

There is a necessity for government research organizations as well as industry partners to venture into the investigation and establishment of sensor prototypes. An example is a humidity sensor prototype with a range of great precision covering 20 parts per million by volume to more than 10,000 ppmv. The purpose is to improve the accuracy of measurements, especially on parameters like temperature and relative humidity, at altitudes preserved during flight to counteract contrail mitigation. Additionally, improving measurement at lower altitudes is vital for improving the precision of weather forecasting. This accumulated data will play a pivotal role in evaluating and integrating these insights into forecast models, enhancing the robustness of these calculations. An additional area of focus is the refinement of model calculations on the impact of contrails, necessitating improved handling of variables such as clouds, aerosols, and specific aircraft characteristics.

Tackling the pressing challenge of climate change requires the exploration and adoption of effective contrail mitigation strategies. Recent studies show promise in the utilization of alternative fuels, particularly sustainable aviation fuels (SAFs), which boast lower soot particle emissions compared to conventional jet fuel. Initial flight trials have shown a marked decrease in contrail formation when SAFs are used, potentially attributed to the reduced concentration of ice nucleation particles in SAF exhaust. Moreover, ongoing research focuses on optimizing flight path planning and air traffic management (ATM) to minimize contrail formation and persistence. Research conducted by Sausen et al. (2023) demonstrates the feasibility of contrail avoidance through minor adjustments in flight paths during real-world operations. Continued progress and application of these strategies, coupled with advancements in contrail observation technologies such as high-precision humidity sensors, offer significant potential to mitigate the climate impact of aviation.

8 Conclusions

This study reviews the current understanding of the impacts of contrail formation by aircraft on the Earth's climate system; it provides insights into the current state of contrail research, offering perspectives on contrail formation, characteristics, life cycle, and potential future impacts. The study underscores the importance of confronting uncertainties in climate models and emphasizes the need for further research to enhance our understanding of contrail effects.

Aviation emissions, encompassing both contrail cirrus clouds and carbon dioxide emissions, exert an important influence on the Earth's climate. Extensive research efforts have significantly improved our understanding of contrail formation and aging; however, key microphysical processes remain a subject of ongoing investigation. Our examination of global observational data and projections highlights the potential for a significant increase in contrail cirrus radiative forcing by the mid-21st century, driven by factors such as anticipated growth in air traffic, potential improvements in fuel efficiency, and evolving atmospheric conditions. While uncertainties regarding the precise magnitude of this increase exist, the potential consequences necessitate proactive mitigation strategies. Several promising approaches are being explored, including operational measures to optimize flight paths, the development of new contrail suppression

technologies, and the adoption of sustainable aviation fuels. Implementing a combination of these strategies, while continuously refining our understanding of contrail effects, is crucial for minimizing the overall climate impact of aviation.

Author contributions. DKS prepared the manuscript with partial support from SS and supervision from DJW

Competing interests. The author declares that they have no competing interests.

Acknowledgment.
This work was supported by the National Aeronautics and Space Administration (NASA) under award number NNA16BD14C for NASA Academic Mission Services (NAMS).
We thank Drs. Andrew Gettelman (Pacific Northwest National Laboratory, PNNL, USA), Ulrike Burkhardt (German Aerospace Center, DLR, Germany), Bernd Kärcher (DLR), Phillip J Ansell (University of Illinois at Urbana-Champaign, USA), D.S. Lee (Manchester Metropolitan University, UK), and Steven L Baughcum (The Boeing Company) for reviewing prior drafts of this report.
Financial support. The authors would like to thank for support from the Universities Space Research Association (USRA) through project subcontract 08600-031.

References

Airbus Global Market Forecast: 2023-2042. Retrieved from https://www.airbus.com/en/products services/commercial-aircraft/market/global-market-forecast), 2022.

Appleman, H.: The formation of exhaust condensation trails by jet aircraft. Bull. Amer. Meteor. Soc., 34(1), 14-20, https://doi.org/10.1175/1520-0477-34.1.14, 1953.

Atlas, D., Wang, Z., and Duda, D. P.: Contrails to cirrus: Morphology, microphysics, and radiative properties. J. Appl. Meteor., 45, 5–19, https://doi.org/10.1175/JAM2335.1, 2006.

Aufm Kampe, H. J.: Die Physik der Auspuffwolken hinter Flugzeugen, Luftwissen, 10, 171–173, 1943.

Barrett, S., Prather, M., Penner, J., Selkirk, H., Balasubramanian, S., Dopelheuer, A., Fleming, G., Gupta, M., Halthore, R., Hileman, J., Jacobson, M.: Guidance on the use of AEDT gridded aircraft emissions in atmospheric models. A technical note, Aug 17, https://doi.org/10.2172/993261, 2010.

Bauer, H.S., Schwitalla, T., Wulfmeyer, V., Bakhshaii, A., Ehret, U., Neuper, M. and Caumont, O.: Quantitative precipitation estimation based on high-resolution numerical weather prediction and data assimilation with WRF–a performance test. Tellus A: Dynamic Meteorology and Oceanography, 67(1), p.25047, https://doi.org/10.3402/tellusa.v67.25047, 2015.

Baumgardner, D., Brenguier, J. L., Bucholtz, A., Coe, H., DeMott, P., Garrett, T. J., Gayet, J. F., Hermann, M., Heymsfield, A., Korolev, A., Krämer, M.: Airborne instruments to measure atmospheric aerosol particles, clouds and radiation: A cook's tour of mature and emerging technology. Atmos. Res., 102(1-2), 10-29. Oct 1, https://doi.org/10.1016/j.atmosres.2011.08.010, 2011.

Bickel, M., Ponater, M., Bock, L., Burkhardt, U. and Reineke, S.,. Estimating the effective radiative forcing of contrail cirrus. Journal of Climate, 33(5), pp.1991-2005, https://doi.org/10.1175/JCLI-D-19-0531.1, 2020.

Bickel, M.: Climate Impact of Contrail Cirrus. Ph.D. Thesis, Ludwig-Maximilians-Universität München, 133 pp. doi: 10.57676/mzmg-r403., 2023.

Bier, A., and Burkhardt, U.: Variability in contrail ice nucleation and its dependence on soot number emissions. J. Geophys. Res. Atmos., 124(6), 3384–3400, https://doi.org/10.1029/2018JD030132, 2019.

Bier, A., and Burkhardt, U.: Impact of parametrizing microphysical processes in the jet and vortex phase on contrail cirrus properties and radiative forcing. J. Geophys. Res. Atmos., 127, e2022JD036677, https://doi.org/10.1029/2022JD036677, 2022.

Bier, A., Burkhardt, U., and Bock, L.: Synoptic control of contrail cirrus life cycles and their modification due to reduced soot number emissions. J. Geophys. Res. Atmos., 122(21), 11,584–11,603, https://doi.org/10.1002/2017JD027182, 2017.

Bock, L., and Burkhardt, U.: Reassessing properties and radiative forcing of contrail cirrus using a global climate model. J. Geophys. Res. Atmos., 121(16), 9717–9736, https://doi.org/10.1002/2015JD024688, 2016.

Bock, L., and Burkhardt, U.: The temporal evolution of a long-lived contrail cirrus cluster: Simulations with a global climate model, J. Geophys. Res. Atmos., 121, 3548–3565, https://doi.org/10.1002/2015JD024282, 2016.

Bock, L., and Burkhardt, U.: Contrail cirrus radiative forcing for future air traffic. Atmos. Chem. Phys., 19(12), 8163–8174, https://doi.org/10.5194/acp-19-8163-2019, 2019

Boeing: Commercial Market Outlook 2022–2041. https://www.boeing.com/commercial/market/commercial-market-outlook/index.page, 2022.

Bräuer, T., Voigt, C., Sauer, D., Kaufmann, S., Hahn, V., Scheibe, M., Schlager, H., Diskin, G. S., Nowak, J. B., DiGangi, J. P., Huber, F.: Airborne measurements of contrail ice properties-Dependence on temperature and humidity, Geophys. Res. Lett., 48(8), e2020GL092166, https://doi.org/10.1029/2020GL092166, 2021a.

Bräuer T, Voigt C, Sauer D, Kaufmann S, Hahn V, Scheibe M, Schlager H, Huber F, Le Clercq P, Moore RH, Anderson BE. Reduced ice number concentrations in contrails from low-aromatic biofuel blends. Atmos. Chem. Phys., 21(22), 16817-26., https://doi.org/10.5194/acp-21-16817-2021, 2021b.

Burkhardt, U., Kärcher, B., Ponater, M., Gierens, K., and Gettelman, A.: Contrail cirrus supporting areas in model and observations. Geophys. Res. Lett., 35, https://doi.org/10.1029/2008GL034056, 2008.

Burkhardt, U., and Kärcher, B.: Process-based simulation of contrail cirrus in a global climate model. J. Geophys. Res. Atmos., 114(D16), D16201, https://doi.org/10.1029/2008JD011675, 2009.

Burkhardt, U., Bock, L., and Bier, A.: Mitigating the contrail cirrus climate impact by reducing aircraft soot number emissions. npj Clim. Atmos. Sci., 1, 37, https://doi.org/10.1038/s41612-018-0044-x, 2018.

Burkhardt, U., and Kärcher, B.: Global radiative forcing from contrail cirrus. Nat. Clim. Change., 1, 54–58, https://doi.org/10.1038/nclimate1068, 2011.

Burkhardt, U., Kärcher, B., and Schumann, U.: Global modeling of the contrail and contrail cirrus climate impact. Bull. Am. Meteorol. Soc., 91(4), 479–484, https://doi.org/10.1175/2010BAMS2966.1, 2010.

Caiazzo, F., Agarwal, A., Speth, R. L., and Barrett, S. R. H.: Impact of biofuels on contrail warming. Environ. Res. Lett., 12, 114013, https://doi.org/10.1088/1748-9326/aa8c25, 2017.

Carlin, B., Fu, Q., Lohmann, U., Mace, G., Sassen, K., and Comstock, J.: High-cloud horizontal inhomogeneity and solar albedo bias. J. Climate, 15, 2321–2339, https://doi.org/10.1175/1520-0442(2002), 2002.

Chauvigné, A., Jourdan, O., Schwarzenboeck, A., Gourbeyre, C., Gayet, J. F., Voigt, C., Schlager, H., Kaufmann, S., Borrmann, S., Molleker, S., Minikin, A.: Statistical analysis of contrail to cirrus evolution during the Contrail and Cirrus Experiment (CONCERT). Atmos. Chem. Phys., 18(13), 9803-22, Jul 12, https://doi.org/10.5194/acp-18-9803-2018, 2018.

Chen, C.-C., Gettelman, A., Craig, C., Minnis, P., and Duda, D.: Global contrail coverage simulated by CAM5 with the inventory of 2006 global aircraft emissions. J. Adv. Model. Earth Syst., 4(4), https://doi.org/10.1029/2012MS000088, 2012.

Chen, C.-C., and Gettelman, A.: Simulated radiative forcing from contrails and contrail cirrus. Atmos. Chem. Phys. Discuss., 13, 10,939–10,959, https://doi.org/10.5194/acpd-13-10939-2013, 2013.

Chen, C.-C., and Gettelman, A.: Simulated 2050 Aviation Radiative Forcing from Contrails and Aerosols. Atmos. Chem. Phys., 16 (11), 7317–33, https://doi.org/10.5194/acp-16-7317-2016, 2016.

Comstock, J. M., Ackerman, T. P., and Turner, D. D.: Evidence of high ice supersaturation in cirrus clouds using ARM Raman lidar measurements. Geophys. Res. Lett., 31, L11106, https://doi.org/10.1029/2004GL019705, 2004.

Danabasoglu, G., Lamarque, J. F., Bacmeister, J., Bailey, D. A., DuVivier, A. K., Edwards, J., Emmons, L. K., Fasullo, J., Garcia, R., Gettelman, A., Hannay, C.: The community earth system model version 2 (CESM2). J. Adv. Model. Earth Syst., 12(2), e2019MS001916, https://doi.org/10.1029/2019MS001916, Feb, 2020.

De Leon, R. R., M. Krämer, M., Lee, D. S., and Thelen, J. C.: Sensitivity of radiative properties of persistent contrails to the ice water path. Atmos. Chem. Phys., 12, 7893–7901, https://doi.org/10.5194/acp-12-7893-2012, 2012.

Dischl, R. K., Sauer, D., Voigt, C., Harlaß, T., Sakellariou, F., Märkl, R. S., Schumann, U., Scheibe, M., Kaufmann, S., Roiger, A., Dörnbrack, A., Renard, C., Gauthier, M., Swann, P., Madden, P., Luff, D., Johnson, M., Ahrens, D., Sallinen, R., Schripp, T., Eckel, G., Bauder, U., and Le Clercq, P.: Measurements of particle emissions of an A350-941 burning 100 % sustainable aviation fuels in cruise, EGUsphere [preprint], https://doi.org/10.5194/egusphere-2024-1224, 2024.

Dietmüller, S., et al.: A new radiation infrastructure for the Modular Earth Submodel System (MESSy, based on version 2.51). Geosci. Model Dev., 9, 2209–2222, https://doi.org/10.5194/gmd-9-2209-2016, 2016.

Dipankar, A., Stevens, B., Heinze, R., Moseley, C., Zängl, G., Giorgetta, M., and Brdar, S.: Large eddy simulation using the general circulation model ICON. J. Adv. Model. Earth Syst., 7, 963–986, https://doi.org/10.1002/2015MS000431, 2015.

Duda, D. P., Minnis, P., Nguyen, L., and Palikonda, R.: A case study of the development of contrail clusters over the Great Lakes. J. Atmos. Sci., 61, 1132–1146, https://doi.org/10.1175/1520-0469(2004)061<1132:ACOTDO>2.0.CO;2, 2004.

Duda, D. P., Minnis, P., Khlopenkov, K., Chee, T. L., and Boeke, R.: Estimation of 2006 Northern Hemisphere contrail coverage using MODIS data. Geophys. Res. Lett., 40, 612–617, https://doi.org/10.1002/grl.50126, 2013.

Duda, D. P., Smith, W. L., Bedka, S., Spangenberg, D., Chee, T., and Minnis, P.: Impact of COVID-19-Related Air Traffic Reductions on the Coverage and Radiative Effects of Linear MicrphysicalPersistent Contrails Over Conterminous United States and Surrounding Oceanic Routes, J. Geophys. Res.-Atmos., 128, e2022JD037554, https://doi.org/10.1029/2022JD037554, 2023.

EASA (European Union Aviation Safety Agency) ICAO Aircraft Engine Emissions Databank 2023: http://www.easa.europa.eu/document-library/icao-aircraft-engine-emissions-databank.

Ettenreich, R.: Wolkenbildung über einer Feuersbrunst und an Flugzeugabgasen. Meteorol. Z., 36, 355–356, 1919.

Elmourad, J. A.: Evaluating Fuel-Climate Tradeoffs in Contrail Avoidance (Doctoral dissertation, Massachusetts Institute of Technology), 2023.

EUROCONTROL.: Aircraft Performance Summary Tables for the Base of Aircraft Date (BADA), 3.7, European Organisation for the Safety of Air Navigation, Brétigny-sur-Orge, 103, 2009.

Frias, A.M., Shapiro, M.L., Engberg, Z., Zopp, R., Soler, M. and Stettler, M.E.J.: Feasibility of contrail avoidance in a commercial flight planning system: an operational analysis. Environmental Research: Infrastructure and Sustainability, 4(1), p.015013, doi 10.1088/2634-4505/ad310c, 2024.

Fritz, T. M., Eastham, S. D., Speth, R. L., and Barrett, S. R. H.: The role of plume-scale processes in long-term impacts of aircraft emissions. Atmos. Chem. Phys., 20, 5697–5714, https://doi.org/10.5194/acp-20-5697-2020, 2020.

Frömming, C., Ponater, M., Burkhardt, U., Stenke, A., Pechtl, S., and Sausen, R.: Sensitivity of contrail coverage and contrail radiative forcing to selected key parameters, Atmos. Environ., 45, 1483–1490, https://doi.org/10.1016/j.atmosenv.2010.12.039, 2011.

Fuglestvedt, J. S., and coauthors: Transport impacts on atmosphere and climate: Metrics. Atmos. Environ, 44, 4648–4677, https://doi.org/10.1016/j.atmosenv.2009.04.044, 2010.

Garber, D. P., Minnis, P., and Costulis, P. K.: A commercial flight track database for upper tropospheric aircraft emission studies over the USA and southern Canada, Meteorologische Zeitschrift, 14, 445–452, https://doi.org/10.1127/0941-2948/2005/0040, 2005.

Gayet, J. F., Shcherbakov, V., Voigt, C., Schumann, U., Schäuble, D., Jessberger, P., Petzold, A., Minikin, A., Schlager, H., Dubovik, O., Lapyonok, T.: The evolution of microphysical and optical properties of an A380 contrail in the vortex phase, Atmos. Chem. Phys., 12(14), 6629-6643, https://doi.org/10.5194/acp-12-6629-2012, 2012.

Geleyn, J. F., Hollingsworth, A.: An economical analytical method for the computation of the interaction between scattering and line absorption of radiation, Beiträge zur Physik der Atmosphäre, 52, 1–16, 1978.

Gerz, T., Durbeck, T., Konopka, P.: Transport and effective diffusion of aircraft emissions, J. Geophys. Res., 103, 25905–25914, https://doi.org/10.1029/98JD01819, 1998.

Geraedts, S., Brand, E., Dean, T. R., Eastham, S., Elkin, C., Engberg, Z., Hager, U., Langmore, I., McCloskey, K., Ng, J. Y. H., and Platt, J. C.: A scalable system to measure contrail formation on a per-flight basis, Environ. Res. Commun., 6, 015008, 2024.

Gettelman, A., Chen, C. C., Bardeen, C. G.: The climate impact of COVID-19-induced contrail changes, Atmos. Chem. Phys., 21(12), 9405-9416, https://doi.org/10.5194/acp-21-9405-2021, 2021.

Gettelman, A., Chen, C.: The climate impact of aviation aerosols, Geophys. Res. Lett., 40(11), 2785-2789, https://doi.org/10.1002/grl.50539, 2013.

Gettelman, A., Morrison, H.: Advanced Two-Moment Bulk Microphysics for Global Models. Part I: Off-Line Tests and Comparison with Other Schemes, J. Climate, 28, 1268–1287, https://doi.org/10.1175/JCLI-D-14-00102.1, 2015.

Gettelman, A., Bardeen, C. G., McCluskey, C. S., Järvinen, E., Stith, J., Bretherton, C., McFarquhar, G., Twohy, C., D'Alessandro, J., Wu, W.: Simulating Observations of Southern Ocean Clouds and Implications for Climate, J. Geophys. Res., 125, https://doi.org/10.1029/2019JD031872, 2020.

Gettelman, A., Gagne, D. J., Chen, C.-C., Christensen, M. W., Lebo, Z. J., Morrison, H., Gantos, G.: Machine Learning the Warm Rain Process, J. Adv. Model. Earth Syst., 13, https://doi.org/10.1029/2020MS002273, 2021.

Gettelman, A., Hannay, C., Bacmeister, J. T., Neale, R. B., Pendergrass, A. G., Danabasoglu, G., Lamarque, J.-F., Fasullo, J. T., Bailey, D. A., Lawrence, D. M., Mills, M. J.: High Climate Sensitivity in the Community Earth System Model Version 2 (CESM2), Geophys. Res. Lett., 46, https://doi.org/10.1029/2019GL083978, 2019.

Gierens, K. M., Lim, L., Eleftheratos, K.: A review of various strategies for contrail avoidance, Open Atmos. Sci. J., 2, 1-7, https://doi.org/10.2174/1874282300802010001, 2008.

Gierens, K., Matthes, S., Rohs, S.: How Well Can Persistent Contrails Be Predicted?, Aerospace, 7, 169, https://doi.org/10.3390/aerospace7110169, 2020.

Gounou, A., Hogan, R. J.: A sensitivity study of the effect of horizontal photon transport on the radiative forcing of contrails, J. Atmos. Sci., 64, 1706–1716, https://doi.org/10.1175/JAS3943.1, 2007.

Graf, K., Schumann, U., Mannstein, H., Mayer, B.: Aviation induced diurnal North Atlantic cirrus cover cycle, Geophys. Res. Lett., 39, https://doi.org/10.1029/2012GL053403, 2012.

Grewe, V., Gangoli Rao, A., Grönstedt, T., Xisto, C., Linke, F., Melkert, J., Middel, J., Ohlenforst, B., Blakey, S., Christie, S., Matthes, S., Dahlmann, K.: Evaluating the climate impact of aviation emission scenarios towards the Paris agreement including COVID-19 effects, Nat. Commun., 12, 3841, https://doi.org/10.1038/s41467-021-24046-4, 2021.

Haywood, J. M., Allan, R. P., Bornemann, J., Forster, P. M., Francis, P. N., Milton, S., Rädel, G., Rap, A., Shine, K. P., Thorpe, R.: A case study of the radiative forcing of persistent contrails evolving into contrail-induced cirrus. J. Geophys. Res. Atmos., 114(D24), https://doi.org/10.1029/2009JD012650, 2009.

Heymsfield, A. J., Krämer, M., Luebke, A., Brown, P., Cziczo, D. J., Franklin, C., Lawson, P., Lohmann, U., McFarquhar, G., Ulanowski, Z., and Van Tricht, K.: Cirrus clouds, Meteorol. Monogr., 58, 2.1–2.26, 2017.

Huszar, P., Teyssèdre, H., Michou, M., Voldoire, A., Olivié, D. J. L., Saint-Martin, D., Cariolle, D., Senesi, S., Salas Y Melia, D., Alias, A., Karcher, F., Ricaud, P., and Halenka, T.: Modeling the present and future impact of aviation on climate: an AOGCM approach with online coupled chemistry, Atmos. Chem. Phys., 13, 10027–10048, https://doi.org/10.5194/acp-13-10027-2013, 2013.

ICAO Future Of Aviation 2012, 2012. Retrieved from https://www.icao.int/Meetings/FutureOfAviation/Pages/default.aspx

Immler, F., Treffeisen, R., Engelbart, D., Krüger, K., Schrems, O.: Cirrus contrails, and ice supersaturated regions in high-pressure systems at northern mid-latitudes, Atmos. Chem. Phys., 8, 1689–1699, https://doi.org/10.5194/acp-8-1689-2008, 2008.

IPCC: Climate Change 2021: The Physical Science Basis. Contribution of Working Group I to the Sixth Assessment Report of the Intergovernmental Panel on Climate Change, 2021.

IPCC: Summary for Policymakers 2018: In V. Masson-Delmotte, P. Zhai, H. O. Pörtner, et al. (Eds.), Global warming of 1.5°C. An IPCC Special Report on the Impacts of Global Warming of 1.5°C above Pre-industrial Levels and Related Global Greenhouse Gas Emission Pathways, World Meteorological Organization Technical Document, pp. 32, 2018.

IPCC: Aviation and the global atmosphere 1999: In: Penner, J.E., Lister, D.H., Griggs, D. J., Dokken, D.J., McFarland, M. (Eds.), Intergovernmental Panel on Climate Change Special Report. Cambridge University Press, Cambridge, UK, 1999.

Irvine, E. A., Hoskins, B. J., Shine, K. P.: A Lagrangian analysis of ice-supersaturated air over the North Atlantic, J. Geophys. Res.: Atmospheres, 119, 90–100, https://doi.org/10.1002/2013JD019843, 2013.

Iwabuchi, H., Yang, P., Liou, K.N. and Minnis, P.: Physical and optical properties of persistent contrails: Climatology and interpretation. J. Geophys. Res: Atmospheres, 117(D6), https://doi.org/10.1029/2011JD017003, 2012.

Jacobson, M. Z., Wilkerson, J. T., Naiman, A. D., Lele, S. K.: The effects of aircraft on climate and pollution. Part I: Numerical methods for treating the subgrid evolution of discrete size-and composition-resolved contrails from all commercial flights worldwide. J. Comput. Phys., 230(12), 5115-32, https://doi.org/10.1016/j.jcp.2011.03.021, Jun 1, 2011.

Jacobson, M. Z.: Short-term effects of controlling fossil-fuel soot, biofuel soot and gases, and methane on climate, Arctic ice, and air pollution health. J. Geophys. Res., 115, D14209, https://doi.org/10.1029/2009JD013795, 2010.

Jensen, E., Ackermann, A.S., Stevens, D.E., Toon, O.B., Minnis, P.: Spreading and growth of contrails in a sheared environment. J. Geophys. Res., 103, 13557–13567, https://doi.org/10.1029/98JD00642, 1998.

Jensen, E., Toon, O., Vay, S., Ovarlez, J., May, R., Bui, T., Twohy, C., Gandrud, B., Pueschel, R., and Schumann, U.: Prevalence of ice-supersaturated regions in the upper troposphere: Implications for optically thin ice cloud formation, J. Geophys. Res., 106, 17253–17266, https://doi.org/10.1029/2000JD900774, 2001.

Kärcher, B.: Formation and radiative forcing of contrail cirrus. Nat. Commun., 9, 1824, https://doi.org/10.1038/s41467-018-04272-2, 2018.

Kärcher, B., Burkhardt, U., Bier, A., Bock, L., and Ford, I. J.: The microphysical pathway to contrail formation. J. Geophys. Res. Atmos., 120, 7893–7927, https://doi.org/10.1002/2015JD023293, 2015.

Kärcher, B.: Formation and radiative forcing of contrail cirrus. Nat. Commun., 9(1), 1824, https://doi.org/10.1038/s41467-018-04272-2, 2018.

Kärcher, B., and Yu, F.: Role of aircraft soot emissions in contrail formation. Geophys. Res. Lett., 36(1), L01804, https://doi.org/10.1029/2008GL036649, 2009.

Kärcher, B., Burkhardt, U., Bier, A., Bock, L., and Ford, I. J.: The microphysical pathway to contrail formation. J. Geophys. Res. Atmos., 120(15), 7893–7927, https://doi.org/10.1002/2015JD023293, 2015.

Klöwer, M., Allen, M. R., Lee, D. S., Proud, S. R., Gallagher, L., and Skowron, A.: Quantifying aviation's contribution to global warming. Environ. Res. Lett., 16, 104027, https://doi.org/10.1088/1748-9326/ac24ff, 2021.

Krämer, M., Rolf, C., Spelten, N., Afchine, A., Fahey, D., Jensen, E., Khaykin, S., Kuhn, T., Lawson, P., Lykov, A., Pan, L. L. (2020 Nov 2). A microphysics guide to cirrus–Part 2: Climatologies of clouds and humidity from observations. Atmos. Chem. Phys., 20(21), 12569-608, https://doi.org/10.5194/acp-20-12569-2020, 2020.

Krämer, M., Schiller, C., Afchine, A., Bauer, R., Gensch, I., Mangold, A., Schlicht, S., Spelten, N., Sitnikov, N., Borrmann, S., de Reus, M., and Spichtinger, P.: Ice supersaturations and cirrus cloud crystal numbers, Atmos. Chem. Phys., 9, 3505–3522, https://doi.org/10.5194/acp-9-3505-2009, 2009.

Kristensson, A., Gayet, J.-F., Ström, J., and Auriol, F.: In situ observations of a reduction in effective crystal diameter in cirrus clouds near flight corridors, Geophys. Res. Lett., 27, 681–684, https://doi.org/10.1029/1999GL010858, 2000.

Kübbeler, M., Hildebrandt, M., Meyer, J., Schiller, C., Hamburger, Th., Jurkat, T., Minikin, A., Petzold, A., Rautenhaus, M., Schlager, H., Schumann, U., Voigt, C., Spichtinger, P., Gayet, J.-F., Gourbeyre, C., and Krämer, M.: Thin and subvisible cirrus and contrails in a subsaturated environment, Atmos. Chem. Phys., 11, 5853–5865, https://doi.org/10.5194/acp-11-5853-2011, 2011.

Kulik, L.: Satellite-based detection of contrails using deep learning, Master's thesis, Massachusetts Institute of Technology, 2019.

Kurz, C.: Entwicklung und Anwendung eines gekoppelten Klima-Chemie-Modellsystems: Globale Spurengastransporte und chemische Umwandlungsprozesse (Doctoral thesis), Ludwigs-Maximilians-University Munich, DLR Forschungsbericht, 2007.

Lamquin, N., Stubenrauch, C.J., Gierens, K., Burkhardt, U., and Smit, H.: A global climatology of upper tropospheric ice supersaturation occurrence inferred from the Atmospheric Infrared Sounder calibrated by MOZAIC, Atmos. Chem. Phys., 12, 381–405, https://doi.org/10.5194/acp-12-381-2012, 2012.

Lee, D.S., Pitari, G., Grewe, V., Gierens, K., Penner, J.E., Petzold, A., Prather, M.J., Schumann, U., Bais, A., Berntsen, T. and Iachetti, D.: Transport impacts on atmosphere and climate: Aviation, Atmospheric environment, 44(37), pp.4678-4734, https://doi.org/10.1016/j.atmosenv.2010.06.045, 2010.

Lee, D. S., Fahey, D. W., Forster, P. M., Newton, P. J., Wit, R. C. N., Lim, L. L., Owen, B., and Sausen, R.: Aviation and global climate change in the 21st century, Atmos. Environ., 43, 3520-3537, https://doi.org/10.1016/j.atmosenv.2009.04.024, 2009.

Lee, D. S., Fahey, D. W., Skowron, A., Allen, M. R., Burkhardt, U., Chen, Q., Doherty, S. J., Freeman, S., Forster, P. M., Fuglestvedt, J., Gettelman, A., De León, R. R., Lim, L. L., Lund, M. T., Millar, R. J., Owen, B., Penner, J. E., Pitari, G., Prather, M. J., Sausen, R., and Wilcox, L. J.: The contribution of global aviation to anthropogenic climate forcing for 2000 to 2018, Atmos. Environ., 244, 117834, https://doi.org/10.1016/j.atmosenv.2020.117834, 2021.

Lewellen, D. C.: Analytic Solutions for Evolving Size Distributions of Spherical Crystals or Droplets Undergoing Diffusional Growth in Different Regimes, J. Atmos. Sci., 69, 417–434, https://doi.org/10.1175/JAS-D-11-0193.1, 2012.

Lewellen, D. C.: Persistent contrails and contrail cirrus. Part II: Full lifetime behavior, J. Atmos. Sci., 71, 4420–4438, https://doi.org/10.1175/JAS-D-14-0004.1, 2014.

Lewellen, D. C., Meza, O., Huebsch, W.: Persistent contrails and contrail cirrus. Part 1: Large-eddy simulations from inception to demise, J. Atmos. Sci., 71, 4399–4419, https://doi.org/10.1175/JAS-D-14-0003.1, 2014.

Li, J., Caiazzo, F., Chen, N. Y., Sridhar, B., Ng, H., and Barrett, S.: Evaluation of aircraft contrails using dynamic dispersion model, AIAA Guidance Navigation, and Control (GNC) Conf., 2013–5178 pp., https://doi.org/10.2514/6.2013-5178, 2013.

Li, Y., Mahnke, C., Rohs, S., Bundke, U., Spelten, N., Dekoutsidis, G., Groß, S., Voigt, C., Schumann, U., Petzold, A., and Krämer, M.: Upper-tropospheric slightly ice-subsaturated

2222   regions: frequency of occurrence and statistical evidence for the appearance of contrail cirrus,
2223   Atmos. Chem. Phys., 23, 2251–2271, https://doi.org/10.5194/acp-23-2251-2023, 2023
2224 Li, J., Kim, J. H., Sridhar, B., and Ng, H. K.: Ames Contrail Simulation Model: Modeling Aviation
2225   Induced Contrails and the Computation of Contrail Radiative Forcing Using Air Traffic Data,
2226   NASA Tech. Memo., NASA/TM-20230014633, 2023.
2227 Liou, K.N., Takano, Y., Yue, Q., and Yang, P.: On the radiative forcing of contrail cirrus
2228   contaminated by black carbon, Geophys. Res. Lett., 40, 778–784,
2229   https://doi.org/10.1002/grl.50214, 2013.
2230 Liu, X., Ma, P.-L., Wang, H., Tilmes, S., Singh, B., Easter, R. C., Ghan, S. J., and Rasch, P. J.:
2231   Description and evaluation of a new four-mode version of the Modal Aerosol Module (MAM4)
2232   within version 5.3 of the Community Atmosphere Model, Geosci. Model Dev., 9, 505–522,
2233   https://doi.org/10.5194/gmd-9-505-2016, 2016.
2234 Lohmann, U., Spichtinger, P., Heidt, S., Peter, T., and Smit, H.: Cirrus clouds and ice
2235   supersaturation regions in a global climate model, Environ. Res. Lett., 3(4), 045022,
2236   https://doi.org/10.1088/1748-9326/3/4/045022, 2008.
2237 Luebke, A. E., Afchine, A., Costa, A., Grooß, J.-U., Meyer, J., Rolf, C., Spelten, N., Avallone, L.
2238   M., Baumgardner, D., and Krämer, M.: The origin of midlatitude ice clouds and the resulting
2239   influence on their microphysical properties, Atmos. Chem. Phys., 16, 5793–5809,
2240   https://doi.org/10.5194/acp-16-5793-2016, 2016.
2241 Mahnke, C., Gomes, R., Bundke, U., Berg, M., Ziereis, H., Sharma, M., Righi, M., Hendricks, J.,
2242   Zahn, A., Wahner, A., and Petzold, A.: Properties and Processing of Aviation Exhaust Aerosol
2243   at Cruise Altitude Observed from the IAGOS-CARIBIC Flying Laboratory, Environ. Sci.
2244   Technol., 58, 6945–6953, 2024.
2245 Mannstein, H., Brömser, A., and Bugliaro, L.: Ground-based observations for the validation of
2246   contrails and cirrus detection in satellite imagery, Atmos. Meas. Tech., 3, 655–669,
2247   https://doi.org/10.5194/amt-3-655-2010, 2010.
2248 Mannstein, H., Meyer, R., and Wendling, P.: Operational detection of contrails from NOAA-
2249   AVHRR data, Int. J. Remote Sens., 20, 1641–1660,
2250   https://doi.org/10.1080/014311699212470, 1999.
2251 Märkl, R. S., Voigt, C., Sauer, D., Dischl, R. K., Kaufmann, S., Harlaß, T., Hahn, V., Roiger, A.,
2252   Weiß-Rehm, C., Burkhardt, U., Schumann, U., Marsing, A., Scheibe, M., Dörnbrack, A.,
2253   Renard, C., Gauthier, M., Swann, P., Madden, P., Luff, D., Sallinen, R., Schripp, T., and Le
2254   Clercq, P.: Powering aircraft with 100 % sustainable aviation fuel reduces ice crystals in
2255   contrails, Atmos. Chem. Phys., 24, 3813–3837, https://doi.org/10.5194/acp-24-3813-2024,
2256   2024.
2257 Markowicz, K. M., Witek, M. L.: Simulations of contrail optical properties and radiative forcing
2258   for various crystal shapes, J. Appl. Meteorol. Climatol., 50, 1740–1755,
2259   https://doi.org/10.1175/JAMC-D-11-071.1, 2011.
2260 Marquart, S., Ponater, M., Mager, F., and Sausen, R.: Future Development of Contrail Cover,
2261   Optical Depth, and Radiative Forcing: Impacts of Increasing Air Traffic and Climate Change,
2262   J. Climate, 16, 2890–2904, https://doi.org/10.1175/1520-0442(2003)016<2890:FDOCCO>2.0.CO;2,
2263   2003.
2264 Matthes S, Lee DS, De Leon RR, Lim L, Owen B, Skowron A, Thor RN, Terrenoire E.: The effects
2265   of supersonic aviation on ozone and climate, Aerospace, 9(1), 41,
2266   https://doi.org/10.3390/aerospace9010041, 2022.

2267   Mayer, B., and Kylling, A.: The libRadtran software package for radiative transfer calculations:
2268   Description and examples of use, Atmos. Chem. Phys., 5, 1855–1877,
2269   https://doi.org/10.5194/acp-5-1855-2005, 2005.
2270   McCloskey, K., Geraedts, S., Van Arsdale, C., and Brand, E.: A human-labeled landsat-8 contrails
2271   dataset. In ICML 2021 Workshop on Tackling Climate Change with Machine Learning,
2272   https://www.climatechange.ai/events/iclr2023#about, 2021.
2273   Meerkötter, R., Schumann, U., Doelling, D. R., Minnis, P., Nakajima, T., and Tsushima, Y.:
2274   Radiative forcing by contrails, Ann. Geophys., 17, 1080–1094,
2275   https://doi.org/10.1007/s00585-999-1080-0, 1999.
2276   Meijer, V. R., Kulik, L., Eastham, S. D., Allroggen, F., Speth, R. L., Karaman, S., and Barrett, S.
2277   R.: Contrail coverage over the United States before and during the COVID-19 pandemic,
2278   Environ. Res. Lett., 17, 034039, https://doi.org/10.1088/1748-9326/ac52f4, 2021.
2279   Minnis, P.: Contrails. In G. R. North (Ed.), Encyclopedia of Atmospheric Sciences (2nd ed., Vol.
2280   2, pp. 121-132). Oxford, UK: Elsevier Ltd., 2015.
2281   Minnis, P., Bedka, S. T., Duda, D. P., Bedka, K. M., Chee, T., Ayers, J. K., Palikonda, R.,
2282   Spangenberg, D. A., Khlopenkov, K. V., and Boeke, R.: Linear contrail and contrail cirrus
2283   properties determined from satellite data, Geophys. Res. Lett., 40, 3220–3226,
2284   https://doi.org/10.1002/grl.50557, 2013.
2285   Minnis, P., Schumann, U., Doelling, D. R., Gierens, K. M., and Fahey, D. W.: Global distribution
2286   of contrail radiative forcing, Geophys. Res. Lett., 26, 1853–1856,
2287   https://doi.org/10.1029/1999GL900391, 1999.
2288   Molod, A., Takacs, L., Suarez, M., and Bacmeister, J.: Development of the GEOS-5 atmospheric
2289   general circulation model: evolution from MERRA to MERRA2, Geosci. Model Dev., 8,
2290   1339–1356, https://doi.org/10.5194/gmd-8-1339-2015, 2015.
2291   Molloy, J., Teoh, R., Harty, S., Koudis, G., Schumann, U., Poll, I. and Stettler, M.E.: Design
2292   principles for a contrail-minimizing trial in the north atlantic, Aerospace, 9(7), p.37,
2293   https://doi.org/10.3390/aerospace9070037, 2022.
2294   Moore, R.H., Thornhill, K.L., Weinzierl, B., Sauer, D., D'Ascoli, E., Kim, J., Lichtenstern, M.,
2295   Scheibe, M., Beaton, B., Beyersdorf, A.J. and Barrick, J.: Biofuel blending reduces particle
2296   emissions from aircraft engines at cruise conditions, Nature, 543(7645), pp.411-415,
2297   https://doi.org/10.1038/nature21420, 2017.
2298   Myhre, G., and Stordal, F.: On the tradeoff of the solar and thermal infrared radiative impact of
2299   contrails, Geophys. Res. Lett., 28, 3119–3122, https://doi.org/10.1029/2001GL013916, 2001.
2300   Myhre, G., Kvalevåg, M., Rädel, G., Cook, J., Shine, K. P., Clark, H., Kärcher, F., Markowicz,
2301   K., Kardas, A., Wolkenberg, P., Balkanski, Y., Ponater, M., Forster, P., Rap, A., and De Leon,
2302   R. R.: Intercomparison of radiative forcing calculations of stratospheric water vapour and
2303   contrails, Meteorol. Z., 18, 585–596, https://doi.org/10.1127/0941-2948/2009/0405, 2009.
2304   Naiman, A. D., Lele, S. K., Wilkerson, J. T., and Jacobson, M. Z.: Parameterization of subgrid
2305   plume dilution for use in large-scale atmospheric simulations, Atmos. Chem. Phys., 10, 2551–
2306   2560, https://doi.org/10.5194/acp-10-2551-2010, 2009.
2307   Naiman, A. D., Lele, S. K., Wilkerson, J. T., and Jacobson, M. Z.: A low order contrail model for
2308   use with global-scale climate models, 47th AIAA Aerospace Science Meeting, Orlando, FL,
2309   2011.
2310   Naiman, A. D., Lele, S. K., and Jacobson, M. Z.: Large Eddy simulations of persistent aircraft
2311   contrails, 49th AIAA Aerospace Science Meeting, Orlando, 2011.

Newinger, C., Burkhardt, U.: Sensitivity of contrail cirrus radiative forcing to air traffic scheduling, J. Geophys. Res. Atmos., 117, D1020, https://doi.org/10.1029/2011JD016815, 2012.

Neil Y. Chen, N., Sridhar, B., and Ng, H. K.: Prediction and use of contrail frequency index for contrail reduction strategies, AIAA Guidance, Navigation, and Control Conference, Toronto, Canada, 2010.

Ng, J. Y. H., McCloskey, K., Cui, J., Brand, E., Sarna, A., Goyal, N., ... and Geraedts, S.: OpenContrails: Benchmarking Contrail Detection on GOES-16 ABI, arXiv preprint arXiv:2304.02122, 2023.

Niklaß, M., Grewe, V., Gollnick, V., and Dahlmann, K.: Concept of climate-charged airspaces: a potential policy instrument for internalizing aviation's climate impact of non-CO2 effects, Climate Policy, 21, 1066–1085, https://doi.org/10.1080/14693062.2020.1809243, 2021.

Ovarlez, J., van Velthoven, P., Sachse, G., Vay, S., Schlager, H., and Ovarlez, H.: Comparison of water vapor measurements from POLINAT 2 with ECMWF analyses in high-humidity conditions, J. Geophys. Res., 105, 3737–3744, https://doi.org/10.1029/1999JD900591, 2000.

Ovarlez, J., Gayet, J.-F., Gierens, K., Strom, J., Ovarlez, H., Auriol, F., Busen, R., and Schumann, U.: Water vapour measurements inside cirrus clouds in Northern and Southern hemispheres during INCA, Geophys. Res. Lett., 29, 1813–1817, https://doi.org/10.1029/2002GL016301, 2002.

Palikonda, R., Minnis, P., Duda, D. P., and Mannstein, H.: Contrail coverage derived from 2001 AVHRR data over the continental United States of America and surrounding areas, Meteorol. Z., 14, 525–536, https://doi.org/10.1127/0941-2948/2005/0055, 2005.

Paoli, R. and Shariff, K.: Contrail Modeling and Simulation, Annu. Rev. Fluid Mech., 48, 393–427, https://doi.org/10.1146/annurev-fluid-010719-060304, 2016.

Penner, J. E., Lister, D. H., Griggs, D. J., Dokken, D. J., and McFarland, M., Eds.: Aviation and the Global Atmosphere, Cambridge University Press, 373 pp., 1999.

Petters, M. D., and Kreidenweis, S. M.: A single parameter representation of hygroscopic growth and cloud condensation nucleus activity, Atmos. Chem. Phys., 7(8), 1961–1971, https://doi.org/10.5194/acp-7-1961-2007, 2007.

Petzold, A., Busen, R., Schröder, F. P., Baumann, R., Kuhn, M., Ström, J., Hagen, D. E., Whitefield, P. D., Baumgardner, D., Arnold, F., Borrmann, S., and Schumann, U.: Near-field measurements on contrail properties from fuels with different sulfur content, J. Geophys. Res. Atmos., 102, 29867–29880, https://doi.org/10.1029/97JD02686, 1997.

Petzold, A., Krämer, M., Neis, P., Rolf, C., Rohs, S., Berkes, F., Smit, H. G. J., Gallagher, M., Beswick, K., Lloyd, G., Baumgardner, D., Spichtinger, P., Nédélec, P., Ebert, V., Buchholz, B., Riese, M., and Wahner, A.: Upper tropospheric water vapor and its interaction with cirrus clouds as seen from IAGOS long-term routine in situ observations, Faraday Discuss, 200, 229–249, https://doi.org/10.1039/C7FD00040A, 2017.

Petzold, A., Hoor, P., Järvinen, E., Lauer, A., Meyer, J., Neuberger, T., Schiller, C., Veselovskii, I., and Woiwode, W.: Ice-supersaturated air masses in the northern mid-latitudes from regular in situ observations by passenger aircraft: vertical distribution, seasonality and tropospheric fingerprint, Atmos. Chem. Phys., 20, 8157–8179, https://doi.org/10.5194/acp-20-8157-2020, 2020.

Poellot, M. R., Arnott, W. P., and Hallett, J.: In situ observations of contrail microphysics and implications for their radiative impact, J. Geophys. Res., 104, 12 077–12 084, https://doi.org/10.1029/1999JD900006, 1999.

Poll DI. On the relationship between non-optimum operations and fuel requirement for large civil transport aircraft, with reference to environmental impact and contrail avoidance strategy, The Aeronautical Journal, Dec;122(1258):1827-70, 2018.

Pomroy, H.R., and Illingworth, J.A.: Ice cloud inhomogeneity: quantifying bias in emissivity from radar observations, Geophys. Res. Lett., 27, 2101–2104, https://doi.org/10.1029/2000GL011429, 2000.

Ponater, M., Marquart, S., and Sausen, R.: Contrails in a comprehensive global climate model: Parameterization and radiative forcing results, J. Geophys. Res. Atmos., 107, ACL 2-1–ACL 2-15, https://doi.org/10.1029/2001JD001227, 2002.

Ponater, M., Bickel, M., Bock, L. and Burkhardt, U.: Towards determining the contrail cirrus efficacy, Aerospace, 8(2), p.42, https://doi.org/10.3390/aerospace8020042, 2021.

Pruppacher, H. R. and Klett, J. D.: Microphysics of Clouds and Precipitation, Atmospheric and Oceanographic Sciences Library, 2nd Edn., Kluwer Academic Publishers, Dordrecht, the Netherlands, ISBN 978-0792344094, 1997.

Pruppacher, H. R. and Klett, J. D.: Microphysics of clouds and precipitation, Kluwer Academic, Norwell, Mass., 2000.

Rädel, G. and Shine, K. P.: Radiative forcing by persistent contrails and its dependence on cruise altitudes, J. Geophys. Res. Atmos., 113, D07105, https://doi.org/10.1029/2007JD009401, 2008.

Rap, A., Forster, P. M., Jones, A., Boucher, O., Haywood, J. M., Bellouin, N., and De Leon, R. R.: Parameterization of contrails in the UK Met Office Climate Model, J. Geophys. Res., 115, D10205, https://doi.org/10.1029/2009JD012152, 2010.

Reutter, P., Konopka, P., Pappalardo, L., Lembras, A., Müller, R., Euler, F., Baklanov, A., and Hegerl, G.: Ice supersaturated regions: properties and validation of ERA-Interim reanalysis with IAGOS in situ water vapor measurements, Atmos. Chem. Phys., 20, 787–804, https://doi.org/10.5194/acp-20-787-2020, 2020.

Righi, M., Hendricks, J., and Sausen, R.: The global impact of the transport sectors on atmospheric aerosol: simulations for year 2000 emissions, Atmos. Chem. Phys., 13, 9939–9970, https://doi.org/10.5194/acp-13-9939-2013, 2013.

Righi M, Hendricks J, Beer CG. Exploring the uncertainties in the aviation soot–cirrus effect, Atmos. Chem. Phys., 21(23), pp.17267-17289, https://doi.org/10.5194/acp-21-17267-2021, 2021.

Roeckner, E., Baeuml, G., Bonventura, L., Brokopf, R., Esch, M., Giorgetta, M., Hagemann, S., Kirchner, I., Kornblueh, L., Manzini, E., Rhodin, A., Schlese, U., Schulzweida, U., and Tompkins, A.: The atmospheric general circulation model ECHAM5. PART I Model description, Report 349. Max Planck Institute for Meteorology, Hamburg, Germany.

Roosenbrand, E., Sun, J., & Hoekstra, J.: Optimizing Global Flight Altitudes for Contrail Reduction. Insights from Open Flight and Weather Balloon Data. In: Fifteenth USA/Europe Air Traffic Management Research and Development Seminar (ATM2023), 2023.

Sanz-Morère, I., Eastham, S. D., Allroggen, F., Speth, R. L., & Barrett, S. R. H.: Impacts of multi-layer overlap on contrail radiative forcing. Atmos. Chem. Phys., 21, 1649–1681, doi:10.5194/acp-21-1649-2021, 2021.

Sausen, R., Gierens, K., Ponater, M., & Schumann, U.: A diagnostic study of the global distribution of contrails. Part I: Present-day climate. Theor. Appl. Climatol., 61, 127–141, doi:10.1007/s007040050076, 1998.

Sausen, R., Hofer, S. M., Gierens, K. M., Bugliaro Goggia, L., Ehrmanntraut, R., Sitova, I., ... & Miller, N.: Can we successfully avoid persistent contrails by small altitude adjustments of flights in the real world?. Meteorol. Z., 2023.

Schmidt, E.: Die Entstehung von Eisnebel aus den Auspuffgasen von Flugmotoren. Schr. Dtsch. Akad. Luftfahrtforsch., 44, 1–15, 1941.

Schröder, F., Kärcher, B., Duroure, C., Ström, J., Petzold, A., Gayet, J.-F., ... & Borrmann, S.: On the Transition of Contrails into Cirrus Clouds. J. Atmos. Sci., 57, 464–480, doi:10.1175/1520-0469(2000)057<0464:OTTOCI>2.0.CO;2, 2000.

Schumann, U., & Graf, K.: Aviation-induced cirrus and radiation changes at diurnal timescales. J. Geophys. Res., 118, 2404–2421, doi:10.1002/jgrd.50283, 2013.

Schumann, U., & Heymsfield, A.: On the lifecycle of individual contrails and contrail cirrus-Ice Formation and Evolution in Clouds and Precipitation: Measurement and Modeling Challenges: Chapter 3, Meteor. Monogr, 3.1–3.24, 2017.

Schumann, U., & Wendling, P.: Determination of contrails from satellite data and observational results. In: Air Traffic and the Environment-Background, Tendencies and Potential Global Atmospheric Effects, U. Schumann (Ed.), Lecture Notes in Engineering, Springer-Verlag, 138–153, 1990.

Schumann, U., Baumann, R., Baumgardner, D., Bedka, S. T., Duda, D. P., Freudenthaler, V., ... & Wang, Z.: Properties of individual contrails: a compilation of observations and some comparisons. Atmos. Chem. Phys., 17, 403–438, doi:10.5194/acp-17-403-2017, 2017.

Schumann, U., Bugliaro, L., Dörnbrack, A., Baumann, R., & Voigt, C.: Aviation Contrail Cirrus and Radiative Forcing Over Europe During 6 Months of COVID-19. Geophys. Res. Lett., 48, doi:10.1029/2021GL096230, 2021.

Schumann, U., Penner, J. E., Chen, Y., Zhou, C., & Graf, K.: Dehydration effects from contrails in a coupled contrail-climate model. Atmos. Chem. Phys., 15, 11179–11199, doi:10.5194/acp-15-11179-2015, 2015.

Schumann, U., Ström, J., Busen, R., Baumann, R., Gierens, K., Krautstrunk, M., ... & Stingl, J.: In situ observations of particles in jet aircraft exhausts and contrails for different sulfur-containing fuels. J. Geophys. Res., 101, 6853–6870, doi:10.1029/95JD00240, 1996.

Schumann, U.: A contrail cirrus prediction model. Geosci. Model Dev., 5, 543–580, doi:10.5194/gmd-5-543-2012, 2012.

Schumann, U.: On conditions for contrail formation from aircraft exhausts. Meteorol. Z., 5, 4–23, doi:10.1127/metz/5/1996/4, 1996.

Schumann, U., Konopka, P., Baumann, R., Busen, B., Gerz, T., Schlager, H., ... & Volkert, H.: Estimate of diffusion parameters of aircraft exhaust plumes near the tropopause from nitric oxide and turbulence measurements. J. Geophys. Res., 100, 147–162, doi:10.1029/94JD01508, 1995.

Schumann, U., Schlager, H., Arnold, F., Baumann, R., Haschberger, P., and Klemm, O.: Dilution of aircraft exhaust plumes at cruise altitudes, Atmos. Environ., 32, 3097–3103, 1998.

Schumann, U., Jeßberger, P., and Voigt, C.: Contrail ice particles in aircraft wakes and their climatic importance, Geophys. Res. Lett., 40, 2867–2872, 2013.

Schumann, U.: Formation, properties and climatic effects of contrails, C. R. Phys., 6, 549–565, 2005.

Siddiqui, N.: Atmospheric Contrail Detection with a Deep Learning Algorithm, Scholarly Horizons: Univ. Minnesota Morris Undergraduate Journal, 7(1), Article 5, doi:10.26757/sh.v7i1.1334, 2020.

Spangenberg, D. A., Minnis, P., Bedka, S. T., Palikonda, R., Duda, D. P., & Rose, F. G.: Contrail radiative forcing over the Northern Hemisphere from 2006 Aqua MODIS data. Geophys. Res. Lett., 40, 595–600, doi:10.1002/grl.50119, 2013.

Spinhirne, J. D., Hart, W. D., & Duda, D. P.: Evolution of the morphology and microphysics of contrail cirrus from airborne remote sensing. Geophys. Res. Lett., 25, 1153–1156, doi:10.1029/97GL03477, 1998.

Sridhar, B., Ng, H. K., & Chen, N. Y.: Aircraft Trajectory Optimization and Contrails Avoidance in the Presence of Winds, in: 10th AIAA Aviation Technology, Integration and Operations Conference (ATIO), Fort Worth, TX, 2010.

Stenke, A., Grewe, V., & Pechtl, S.: Do supersonic aircraft avoid contrails?, Atmos. Chem. Phys., 8, 955–967, doi:10.5194/acp-8-955-2008, 2008.

Stier, P., Feichter, J., Kinne, S., Kloster, S., Vignati, E., Wilson, J., et al.: The aerosol-climate model ECHAM5-HAM. Atmos. Chem. Phys., 5(4), 1125–1156, 2005.

Stocker, T.F., Qin, D., Plattner, G.K., Tignor, M., Allen, S.K., Boschung, J., ... & Midgley, P. M. (Eds.): Climate Change 2013: the Physical Science Basis, Contribution of Working Group I to the Fifth Assessment Report of the Intergovernmental Panel on Climate Change. Cambridge University Press, Cambridge, United Kingdom and New York, NY, USA, 2013.

Stuber, N., Sausen, R., & Ponater, M.: Stratosphere adjusted radiative forcing calculations in a comprehensive climate model. Theor. Appl. Climatol., 68(3–4), 125–135, doi:10.1007/s007040170048, 2001.

Sun, J., & Roosenbrand, E.: Flight Contrail Segmentation via Augmented Transfer Learning with Novel SR Loss Function in Hough Space. arXiv preprint arXiv:2307.12032, 2023 Jul 22.

Taylor, K. E., Williamson, D., & Zwiers, F.: The sea surface temperature and sea-ice concentration boundary conditions for AMIP II simulations, PCMDI report no. 60, program for climate model diagnostics and intercomparison. The University of California, Lawrence Livermore National Laboratory, 2000.

Teoh, R., Schumann, U., Majumdar, A., & Stettler, M.E.: Mitigating the climate forcing of aircraft contrails by small-scale diversions and technology adoption. Environ. Sci. Technol., 54(5), 2941–2950, doi:10.1021/acs.est.9b07102, 2020.

Teoh, R., Engberg, Z., Shapiro, M., Dray, L., & Stettler, M. E. J.: The high-resolution Global Aviation emissions Inventory based on ADS-B (GAIA) for 2019–2021, Atmos. Chem. Phys., 24, 725–744, doi:10.5194/acp-24-725-2024, 2024.

Tesche, M., Achtert, P., Glantz, P., & Noone, K. J.: Aviation effects on already-existing cirrus clouds. Nat. Commun., 7(1), 12016, doi:10.1038/ncomms12016, 2016.

Testa, B., Durdina, L., Edebeli, J., Spirig, C., & Kanji, Z. A.: Contrail processed aviation soot aerosol are poor ice nucleating particles at cirrus temperatures [Preprint]. EGUsphere, doi:10.5194/egusphere-2024-151, 2024.

Unterstrasser, S.: Properties of young contrails-A parametrization based on large-eddy simulations. Atmos. Chem. Phys., 16(4), 2059–2082, doi:10.5194/acp-16-2059-2016, 2016.

Unterstrasser, S., & Sölch, I.: Numerical modeling of contrail cluster formation. Proc. Third Int. Conf. on Transport, Atmosphere and Climate (TAC-3). Prien am Chiemsee, Germany, DLR, 114–119, 2012.

Unterstrasser, S., & Görsch, N.: Aircraft-type dependency of contrail evolution. J. Geophys. Res.-Atmos., 119, 14 015–14 027, doi:10.1002/2014JD022083, 2014.

2493 Unterstrasser, S., Gierens, K., Sölch, I., & Wirth, M.: Numerical simulations of homogeneously
2494   nucleated natural cirrus and contrail-cirrus. Part 2: Interaction on a local scale. Meteorol. Z.,
2495   26, 643–661, doi:10.1127/metz/2017/0844, 2017.
2496 Vazquez-Navarro, M., Mannstein, H., & Kox, S.: Contrail life cycle and properties from 1 year of
2497   MSG and SEVIRI rapid scan images. Atmos. Chem. Phys., 15(15), 8739–8749,
2498   doi:10.5194/acp-15-8739-2015, 2015.
2499 Vázquez-Navarro, M., Mannstein, H., & Mayer, B.: An automatic contrail tracking algorithm.
2500   Atmos. Meas. Tech., 3, 1089–1101, doi:10.5194/amt-3-1089-2010, 2010.
2501 Vazquez-Navarro, M., Mayer, B., & Mannstein, H.: A fast method for the retrieval of integrated
2502   longwave and shortwave top-of-atmosphere upwelling irradiances from MSG and SEVIRI
2503   (RRUMS). Atmos. Meas. Tech., 6(10), 2627–2640, doi:10.5194/acp-6-2627-2013, 2013.
2504 Verma, P., & Burkhardt, U.: Contrail formation within cirrus: ICON-LEM simulations of the
2505   impact of cirrus cloud properties on contrail formation. Atmos. Chem. Phys., 22(13), 8819–
2506   8842, doi:10.5194/acp-22-8819-2022, 2022.
2507 Voigt, C., Schumann, U., Jessberger, P., Jurkat, T., Petzold, A., Gayet, J.-F., ... & Fahey, D. W.:
2508   Extinction and optical depth of contrails. Geophys. Res. Lett., 38, L11806,
2509   doi:10.1029/2011GL047189, 2011.
2510 Voigt, C., Schumann, U., Minikin, A., Abdelmonem, A., Afchine, A., Borrmann, S., ... & Curtius,
2511   J.: ML-CIRRUS: The airborne experiment on natural cirrus and contrail cirrus with the high-
2512   altitude long-range research aircraft HALO. Bull. Am. Meteorol. Soc., 98, 271–288,
2513   doi:10.1175/BAMS-D-14-00193.1, 2017.
2514 Wang, Z., Bugliaro, L., Jurkat-Witschas, T., Heller, R., Burkhardt, U., Ziereis, H., Dekoutsidis,
2515   G., Wirth, M., Groß, S., Kirschler, S., and Kaufmann, S.: Observations of microphysical
2516   properties and radiative effects of a contrail cirrus outbreak over the North Atlantic, Atmos.
2517   Chem. Phys., 23, 1941–1961, 2023.
2518 Weickmann, H.: Formen und Bildung atmosphärischer Eiskristalle. Beitr. Phys. freien Atmos., 28,
2519   33, 1945.
2520 Wilkerson, J. T., Jacobson, M. Z., Malwitz, A., Balasubramanian, S., Wayson, R., Fleming, G., ...
2521   & Lele, S.: Analysis of emission data from global commercial aviation: 2004 and 2006. Atmos.
2522   Chem. Phys., 10(13), 6391–6408, doi:10.5194/acp-10-6391-2010, 2010.
2523 Wolf, K., Bellouin, N., & Boucher, O.: Sensitivity of cirrus and contrail radiative effect on cloud
2524   microphysical and environmental parameters. Atmos. Chem. Phys., 9(21), 14003-14037,
2525   doi:10.5194/acp-9-14003-2009, 2009.
2526 Wuebbles, D., Gupta, M., & Ko, M.: Evaluating the impacts of aviation on climate change. Eos,
2527   Trans. AGU, 88(14), 157-160, doi:10.1029/2007EO140001, 2007.
2528 Wuebbles, D., Forster, P., Rogers, H., & Herman, R.: Issues and uncertainties affecting metrics
2529   for aviation impacts on climate. Bull. Amer. Meteor. Soc., 91(4), 491-496,
2530   doi:10.1175/2009BAMS2835.1, 2010.
2531 Xie, Y., Yang, P., Liou, K.N., Minnis, P., & Duda, D. P.: Parameterization of contrail radiative
2532   properties for climate studies. Geophys. Res. Lett., 39, L00F02, doi:10.1029/2011GL050205,
2533   2012.
2534 Yi, B., Yang, P., Liou, K.N., Minnis, P., & Penner, J. E.: Simulation of the global contrail radiative
2535   forcing: A sensitivity analysis. Geophys. Res. Lett., 39, L00F03, doi:10.1029/2011GL050207,
2536   2012.

2537   Yun, Y., Penner, J. E., & Popovicheva, O.: The effects of hygroscopicity on ice nucleation of fossil
2538   fuel combustion aerosols in mixed-phase clouds. Atmos. Chem. Phys., 13, 4339–4348,
2539   doi:10.5194/acp-13-4339-2013, 2013.
2540   Zängl, G., Reinert, D., Rípodas, P., & Baldauf, M.: The ICON (ICOsahedral Non-hydrostatic)
2541   modelling framework of DWD and MPI-M: Description of the non-hydrostatic dynamical
2542   core. Q. J. R. Meteorol. Soc., 141(687), 563-579, doi:10.1002/qj.2378, 2015.
2543   Zhou, C., & Penner, J. E.: Aircraft soot indirect effect on large-scale cirrus clouds: Is the indirect
2544   forcing by aircraft soot positive or negative? J. Geophys. Res.: Atmos., 119, 11 303–11 320,
2545   doi:10.1002/2014JD021821, 2014.
2546
2547